Function of MicroRNA-146a and NF-κB in Physiologic and Pathologic Hematopoiesis

Thesis by

Jimmy Liu Zhao

In Partial Fulfillment of the Requirements for the Degree of

Doctor of Philosophy

CALIFORNIA INSTITUTE OF TECHNOLOGY

Pasadena, California

2013

Defended February 5, 2013

ACKNOWLEDGEMENTS

I want to thank Professor David Baltimore for providing great mentorship and training over the years. I also want to thank Dr. Dinesh Rao for excellent mentorship and Drs. Ryan O'Connell, Alejandro Balazs, Devdoot Majumdar, Parameswaran Ramakrishnanand, Lili Yang, Shengli Hao, Aadel Chaudhuri, Arnav Mehta, Yvette Garcia, and other members of the Baltimore Lab for tremendous help and stimulating discussion over the years. I also want to thank members of my thesis committee, Paul Patterson, Sarkis Mazmanian, David Baltimore and Dinesh Rao, as well as UCLA MSTP directors, Steve Smale and Kelsey Martin, for guidance and mentorship. Lastly, I'd like to acknowledge the staff at the California Institute of Technology animal facility, FACS Core sorting facility and genomic core facility for excellent technical support. NFκB-GFP reporter mice were a generous gift of Dr. Christian Jobin at the University of North Carolina, Chapel Hill. My training experience and research work were significantly enriched and enhanced by wonderful collaborations with Chao Ma of the Heath Lab and Beverly Lu of the Tirrell Lab at Caltech, and many external collaborators from other institutions. The work was supported by research grant R01AI079243 (D.B.), National Research Service Award F30HL110691 and the UCLA/Caltech Joint Medical Scientist Training Program (J.L.Z.), from the National Institute of Health.

ABSTRACT

During inflammation and infection, hematopoietic stem and progenitor cells (HSPCs) are stimulated to proliferate and differentiate into mature immune cells, especially of the myeloid lineage. MicroRNA-146a (miR-146a) is a critical negative regulator of inflammation. Deletion of the gene encoding miR-146a—expressed in all blood cell types—produces effects that appear as dysregulated inflammatory hematopoiesis, leading to a decline in the number and quality of hematopoietic stem cells (HSCs), excessive myeloproliferation, and, ultimately, to exhaustion of the HSCs and hematopoietic neoplasms. Six-week-old deleted mice are normal, with no effect on cell numbers, but by 4 months bone marrow hypercellularity can be seen, and by 8 months marrow exhaustion is becoming evident. The ability of HSCs to replenish the entire hematopoietic repertoire in a myelo-ablated mouse also declines precipitously as miR-146a-deficient mice age. In the absence of miR-146a, LPS-mediated serial inflammatory stimulation accelerates the effects of aging. This chronic inflammatory stress on HSCs in deleted mice involves a molecular axis consisting of upregulation of the signaling protein TRAF6 leading to excessive activity of the transcription factor NF-κB and overproduction of the cytokine IL-6. At the cellular level, transplant studies show that the defects are attributable to both an intrinsic problem in the miR-146a-deficient HSCs and extrinsic effects of miR-146a-deficient lymphocytes and non-hematopoietic cells. This study has identified a microRNA, miR-146a, to be a critical regulator of HSC homeostasis during chronic inflammatory challenge in mice and has provided a molecular connection between chronic inflammation and the development of bone marrow failure and myeloproliferative neoplasms. This may have implications for human hematopoietic malignancies, such as myelodysplastic syndrome, which frequently displays downregulated miR-146a expression.

TABLE OF CONTENTS

OVERVIEW and SCIENTIFIC BACKGROUND

MicroRNA

Initially discovered by the Ambros and Ruvkun labs in the early 1990s, microRNAs (miRNAs) have emerged as important regulators of gene expression [1-2]. In the past several years, significant advances have been made with regards to understanding their integration into molecular networks that control cellular development and function. In the hematopoietic system, several individual miRNAs have emerged as important regulators of physiological and pathologic myeloid development and function. MiRNAs are encoded within exons of unique non-coding genes, or sometimes within introns of protein-coding genes, and are most often transcribed from the genome by RNA polymerase II. Some miRNAs exist as clusters and are encoded on the same primary transcript. The primary transcript (pri-miRNA) is processed by the ribonuclease Drosha/DGCR8 in the nucleus and then transported into the cytoplasm as a pre-miRNA, which contains the miRNA stem-loop structure. For most miRNAs, this serves as a substrate for the endoribonuclease Dicer, which creates a double-stranded short RNA that is unwound and then loaded into the RNA-induced silencing complex (RISC) (reviewed in [3-4]). This "classical" description of miRNA biogenesis was true for all known miRNA until mid-2010, when two seminal papers reported that Dicer independent production of miRNAs could occur via the "slicer" RNAse function of Argonaute 2 (Ago2), a component of the RNA induced silencing complex (RISC)[5-6]. The mature miRNA is loaded onto the RISC, a multi-protein complex that includes members of the Argonaute protein family [7]. Once in the RISC, the mature miRNA interacts with a target mRNA via the latter's 3'UTR. Structural, biochemical and bioinformatics analyses indicate that a 6-nucleotide seed sequence at the 5' end of the miRNA is important in mediating the interaction with its target [8]. In most cases, miRNAs repress their targets and this change is detectable at the RNA level, and it is now thought that this represents the majority of the change induced by miRNAs [9-10]. It should be noted that

there are scattered reports of miRNAs that interact with their targets in a non-3'UTR-dependent or non-seed-dependent fashion, and miRNAs that cause upregulation of "targets" [11-12]. These studies suggest that there are aspects to miRNA function that remain elusive. Initial studies revealed the global importance of miRNAs in hematopoiesis. Dicer deletionin the hematopoietic lineage leads to marked defect in competitive repopulation assays and the deletion of Ago2 leads to severe problems with erythroid and B-cell development [13-14]. However, the main focus of research in the field has been on examining how individual miRNAs are integrated into various regulatory pathways in myelopoiesis. miRNAs are induced by transcription factors and other genes involved in myelopoiesis. For example, PU.1 induces expression of miR-223 and NF-kB induces expression of miR-155 and miR-146a. miRNAs, in turn, repress the expression of their targets, for example, miR-155 regulates PU.1 and C/EBP-β, thereby changing the transcriptional profile of the cell [15]. In this search for targets, global RNA expression profiling followed by correlation with algorithmic target prediction has been fruitful [15]. Confirmation of the targets on a case-by-case basis can then be followed by functional analyses of the regulated pathways.

MicroRNA-146a

MicroRNA-146a (miR-146a) along with miR-146b form a highly conserved two-member miRNA family. MiR-146a and miR-146b are located on chromosome 5 and 10, respectively, in the human genome and on chromosome 11 and 19, respectively, in the mouse genome. In 2006, miR-146a first came to our attention in a systemic microarray screen to identify miRNAs that are involved in innate immune activation [16]. Stimulating THP1 cells, a human monocytic cell line, with lipopolysaccharide (LPS) was found to selectively upregulate the expression of three miRNAs, miR-155, miR-146 and miR-132. Since then, we have been focused on investigating the function of miR-155 and miR-146 in

the immune system. In the hematopoietic system, the expression of miR-146a is relatively low in progenitor cells and increases modestly with maturation. However, in certain specialized cell types, such as Ly-6Clo monocytes and epidermal Langerhans cells, miR-146a is constitutively expressed at a high level ([17-18] and immunological genome project http://www.immgen.org/). In addition, miR-146a expression is up-regulated upon stimulation of myeloid cells with microbial components and pro-inflammatory cytokines. MiR-146a is also stimulated upon activation of T cells with T-cell receptor antigens [19-21]. Viral and fungal infection also induces miR-146a expression [22-24]. Basal and induced expression of miR-146a is regulated by several important transcription factors in immune cells. Our initial characterization of miR-146a promoter locus identified two consensus NF-κB binding sites that were shown to be important in transcriptional activation of miR-146a in myeloid cells in response to inflammatory stimulation; mutations of these consensus sequences abolished the promoter activity in a luciferase reporter system [16]. Subsequent studies showed that downregulation of NF-κB activity chemically or genetically inhibits basal and induced expression of miR-146a in macrophages and T cells, confirming the role of NF-κB in regulating miR-146a expression [20,22-23]. In addition to regulation by NF-κB, expression of miR-146a is also regulated by lineage-dependent transcription factors. During myeloid differentiation, PU.1 works together with NF-κB to control the basal expression of miR-146a through dynamic occupancy at the promoter region [18,25]. In lymphocytes, the lineage-specific regulation of miR-146a may be fulfilled by other transcriptional factors, such as c-ETS [24,26]. In addition to transcriptional activation, miR-146a expression may be repressed in a lineage specific manner. This was shown in the example of megakaryocyte differentiation, where PLZF upregulation interacts with the miR-146a promoter to inhibit its expression [27]. A more extreme case involves global miRNA repression, including miR-146a, by the myc oncogenic transcriptional factor during lymphomagenesis [28]. One interesting observation suggests estrogen can modestly downregulate miR-

146a, but not miR-146b, in mouse splenic lymphocytes. However, it is not clear from the study whether the effect of estrogen on miR-146a expression is direct [29]. Overall, basal miR-146a expression is regulated by a set of lineage-dependent transcription factors in a cell-lineage specific manner. This basal level can be further regulated in an activation-dependent manner by inducible transcription factors, such as NF-κB (Figure i). In comparison to miR-146a, the regulation of miR-146b expression is less understood. Some previous reports on miR-146b expression were performed primarily with hybridization-based methods, which may have not been specific enough to separate the mature sequences of miR-146a and miR-146b because they only differ by one nucleotide. Nevertheless, miR-146b seems also to be induced by pro-inflammatory cytokines and dysregulated miR-146b expression is associated with several human non-hematologic cancers [30-35]. In addition, in unpublished work, we have shown that miR-146b expression can be clearly detected by RT-qPCR in miR-146a-deficient bone marrow cells, indicating that it is not a pseudogene or undetectable in adult hematopoietic cells as previously suggested [19,36].

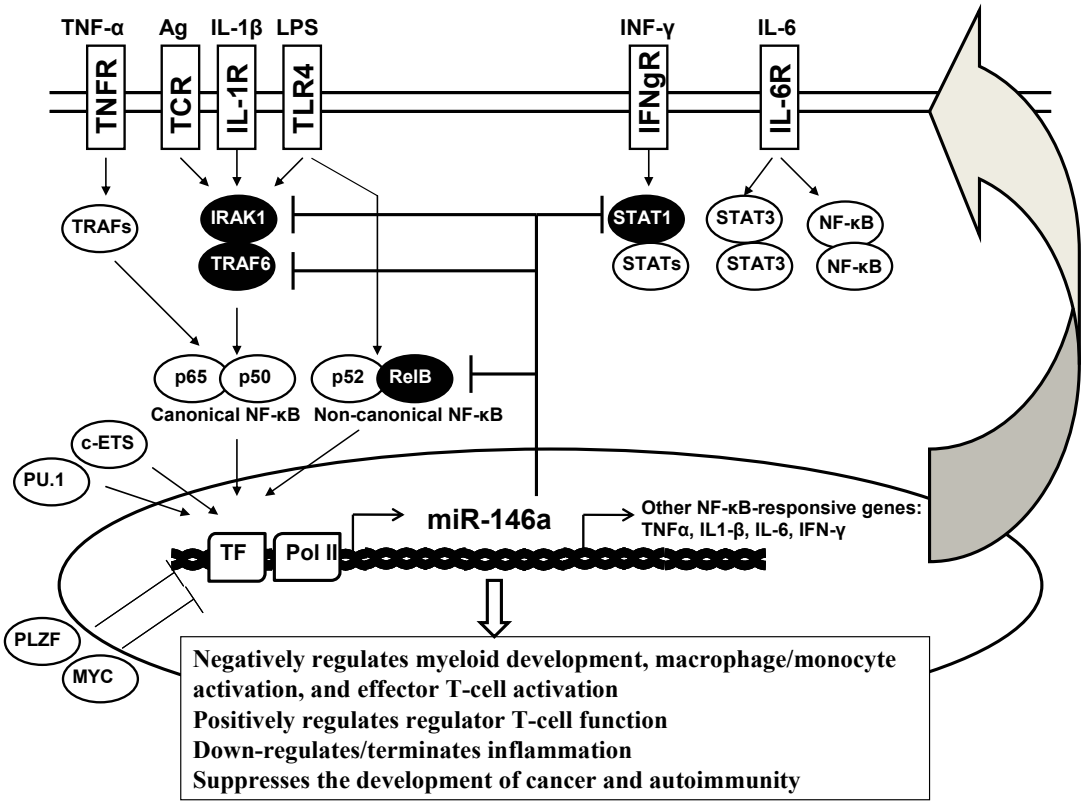

Figure i. Expression of miR-146a is regulated by a set of transcriptional factors in a cell-lineage specific manner, involving such factors as PU.1, c-ETS, and PLZF, and in an activation-dependent manner, involving such factors as NF-κB. Validated targets of miR-146a include Irak1, Traf6, Stat1 and RelB, which are all involved in the NF-κB and STAT pathways, highlighting the role of miR-146a as a critical negative regulator of inflammatory and interferon signaling.

MiR-146a Functions in Immunity

Our initial report showed that miR-146a is highly up-regulated in human monocytes in a NF-κB-dependent manner following toll-like receptor (TLR) stimulation [16]. Initial sequence complementation-based algorithms (e.g. TargetScan) identified TRAF6 and IRAK1 as targets of miR-146a. The regulation of these two proteins by miR-146a in monocyte/macrophages, T- and B- lymphocytes was then confirmed by 3'UTR luciferase reporter assays and gene expression analyses [16,19-20,22,37]. Because TRAF6 and IRAK1 are known feedback regulators of the NF-κB signal pathway, a molecular circuitry involving miR-146a, TRAF6/IRAK1 and NF-κB is proposed to be important in the regulation of both innate and adaptive immunity [38]. One of the first pieces of definitive evidence of this hypothesis came

from the study of miR-146a-deficient mice generated in our laboratory [19]. Consistent with the proposed hypothesis, miR-146a-/- mice were found to be hyper-responsive to LPS challenge. Stimulation with sublethal level of LPS in vivo induced a higher serum level of pro-inflammatory cytokines— including TNFα and IL-6 and IL-1β— in miR-146a-/- mice than in wild type mice. In addition, miR-146a-/- mice experienced a higher mortality rate in response to minimal lethal LPS challenge. The hyper-inflammatory response was also observed in bone marrow derived macrophages (BMDMs) from miR-146a-/- mice in vitro. To complement the study on miR-146a-/- mice, enforced overexpression of miR-146a in THP-1 cells resulted in an attenuated inflammatory response [19]. Work of others has confirmed these general observations. These studies provide further support that miR-146a is an important negative regulator of innate immune activation, potentially by targeting TRAF6 and IRAK1 and by orchestrating the silencing of TNFα gene in human monocytic cell lines in the context of endotoxin-induced tolerance [39-41]. In addition to regulating pro-inflammatory cytokine production, miR-146a negatively regulates type I interferon (IFN) production in vesicular stomatitis virus-infected mouse peritoneal macrophages by targeting TRAF6, IRAK1 and IRAK2 through a RIG-I/NF-κB-dependent but TLR4/MyD88-independent pathway [22]. A study in human peripheral blood mononuclear cells confirmed a role for miR-146a as a negative regulator of the type I IFN pathway [42]. In a more elaborate example of cell-type-specific regulation by miR-146a in the innate immune system, miR-146a specifically controls the Ly-6Chi, but not Ly-6Clo, monocyte response during inflammatory challenge [17]. The regulation by miR-146a in this context is cell-intrinsic, apparently through directly targeting Relb, thus also connecting miR-146a to the non-canonical pathway of NF-κB activation. This study further substantiates the role of miR-146a in innate immunity by controlling monocyte functional heterogeneity during an inflammatory response. Given the hyper-inflammation and the exaggerated immune response in the absence of miR-146a, we would expect miR-146a-/- mice to be more resistant

to bacterial infection than wild type animals. Indeed, miR-146a-/- mice displayed a lower bacterial load upon infection with Listeria monocytogenes [17]. The role of miR-146a in adaptive immunity is particularly well studied in T cells. Aging miR-146a-/- mice develop an autoimmune disorder with lymphadenopathy, lymphocyte infiltration in various organs and an activated T cell phenotype [19]. We carried out detailed analysis in a subsequent study to understand the physiological role of miR-146a in regulating the T cell response to antigen stimulation [20]. We showed that miR-146a-deficient CD4 and CD8 T cells are hyper-responsive following T-cell receptor (TCR) stimulation, as indicated by increased proliferation and survival, exaggerated activation phenotype and enhanced effector cytokine production. The regulation of cell-intrinsic T cell response upon TCR stimulation by miR-146a was shown to again be through the regulation of TRAF6/IRAK1 and NF-κB signaling. This study adds miR-146a to a list of well-known negative regulators of NF-κB, including IκBα and A20, acting following TCR activation and suggests that these feedback regulators function collaboratively to limit the extent and timing of activation, with each apparently fulfilling a crucial non-redundant role. These mice studies were supported by studies in human T cells showing that miR-146a overexpression impairs IL-2 production. However, contrary to our observation that TCR-induced apoptosis was reduced in miR-146a-deficient T cells and enhanced in T cells with miR-146a overexpression, activation-induced cell death seems to be inhibited by miR-146a overexpression in human Jurkat T cell cancer line [26]. The discrepancy may be due to the differences between mouse primary T cells and human cancer cell lines or the level of miR-146a overexpression achieved in the two experimental systems. In addition to functioning in effector T cells in a cell-intrinsic manner, miR-146a also controls the regulation of Th1 responses by affecting regulatory T cell (Treg)-function [43]. Treg cells maintain immune homeostasis by suppressing the inflammatory response and preventing an over-reaction. In Treg cells, expression of miR-146a, but not miR-146b, is much higher than that in naïve T cells. In

turn, miR-146a-deficient Treg cells are functionally defective in their ability to restrain effector T cells, leading to overproduction of IFNγ and autoimmunity. Stat1 appears to be a responsible target for miR-146a in regulating Treg cells. This study revealed an important regulatory function of miR-146a in Treg cells, suggesting upregulation of miR-146a is required for Treg cells to properly control the IFNγ-mediated Th1 response. The results imply an interesting phenomenon, which is that excessive effector cytokine signaling in Treg cells can lead to their failure to suppress the corresponding cytokine response in effector T cells. Further studies are required to elucidate the mechanistic implications behind this type of Treg cells/effector T cells regulation. Our knowledge of the function of miR-146a in B cells is limited. One study has provided evidence for miR-146a induction in a NF-κB-dependent manner by Epstein-Barr virus Latent Membrane Protein 1 (LMP1) in human B lymphocytes [24]. Study from miR-146a-deficient mice suggested that B cells in these mice are also hyper-activated and autoreactive, because we can detect anti-dsDNA antibodies in the serum and a small percentage of B-cell lymphomas in aging miR-146a-/- mice [19,44]. We have also seen de-repression of TRAF6 and IRAK1 by Western blot in splenic B cells from miR-146a-/- mice [19]. Further studies will be required to understand the function of miR-146a in B cells.

Functions of miR-146a in Hematopoiesis

In addition to the functional role of miR-146a within immune cells, miR-146a also is important for regulating the development of hematopoietic cells (Figure ii). Consistent with its expression pattern, miR-146a plays a role in the development of a wide spectrum of hematopoietic cells. An early in vitro study using human leukemic cell lines and CD34+ progenitor cell culture suggested a role for miR-146a in megakaryopoiesis, during which upregulation of the transcription factor PLZF represses miR-146a expression, which in turn leads to increased expression of a direct target of miR-146a, CXCR4.

In this study, overexpression of miR-146a led to impaired megakaryocytic proliferation, differentiation and maturation [27]. However, the cell-autonomous regulation of miR-146a in megakaryopoiesis is challenged by a later study, which showed no detectable changes in megakaryocyte development and platelet activation properties by overexpression of miR-146a in all hematopoietic cells in mice [45]. This discrepancy may be a consequence of differences between the two experimental systems, an in vitro study with human cells versus a mouse in vivo system. Nevertheless, the study done with an overexpression system does not exclude a role for miR-146a in megakaryopoiesis because miR-146a expression is upregulated during megakaryopoiesis and the endogenous level of miR-146a may be sufficient to downregulate the relevant target genes to ensure normal megakaryocyte development. On the other hand, knocking down miR-146a and miR-145 concurrently with a "sponge" in mouse hematopoietic stem and progenitor cells (HSPCs) leads to megakaryocyte expansion and thrombocytosis in vivo. However, this effect may be indirectly mediated by increased production of the positive acting cytokine IL-6 from miR-146a-deficient myeloid and lymphoid cells [37]. In contrast, significant reduction in platelet counts is frequently seen in aging, but not in young, miR-146-/- mice [19,44]. The observed thrombocytopenia in aging miR-146a-/- is a manifestation of bone marrow failure and fibrosis or chronic dysregulation of inflammatory cytokine production. Overall, miR-146a has a regulatory function in megakaryopoiesis in a cell-intrinsic manner and/or by controlling the inflammatory environment. The involvement of miR-146a in myeloid development is particularly interesting. Stable knock-down of both miR-145 and miR-146a concurrently in mouse HSPCs results in variable neutropenia and decreased colony-forming ability of bone marrow cells [37]. In support of miR-146a as the dominant miRNA in this effect, over-expression of TRAF6, a validated target of miR-146a, also leads to mild neutropenia, with a subset of mice progressing to marrow failure or acute myeloid leukemia [37]. More conclusive data came from the subsequent analysis of miR-146a-/- mice.

MiR-146a-/- mice are born at the expected Mendalian frequency and show no detectable phenotype during the first 2 months of their life in the absence of an inflammatory or infectious challenge. This suggests that miR-146a is not an essential gene for the proper development of blood lineages under steady state in young mice. However, with natural aging, miR-146a-/- mice develop a progressive myeloproliferative phenotype in both spleen and bone marrow. Specifically, there is a significant increase in the percentage of CD11b+ cells in their spleens and bone marrows. It can readily be detected by FACS analysis of 6-month-old miR-146a-/- mice. The myeloid expansion becomes progressively larger by 12 months, as indicated by more than a 3-fold increase in the CD11b+ percentage and more than a 10-fold increase in the total number of CD11b+ cells in spleens. Bone marrows of these mice are also dominated by myeloid cells, representing close to 80% of all bone marrow cells [19,44]. Bone marrow-derived macrophages (BMDM) developed from young knockout mice also proliferate faster in response to macrophage colony-stimulating factor (M-CSF). Consistent with this observation, increased surface expression of CSF1R, the receptor for M-CSF, is also detected in the knockout spleen, bone marrow and peripheral blood myeloid cells [19,44]. In addition, miR-146a-deficiency also confers a proliferative advantage on Ly-6Chi monocytes in bone marrow, spleen and the peritoneal cavity in inflammatory conditions [17]. Mechanistically, miR-146a-/- spleen and bone marrow cells exhibit increased transcription of NF-κB-responsive genes. Increased NF-κB p65 translocation to the nucleus is also evident in miR-146a-/- spleen cells. The increased myeloproliferation is dependent on the activation of NF-κB because genetic ablation of an important subunit of NF-κB, p50, suppresses myeloproliferation [44]. Study pursuing the mechanism of NF-κB-driven myeloproliferation will help shed further insight on the molecular link between chronic inflammation and hematopoietic malignancy. Enforced expression of miR-146a in bone marrow transplant studies in mice has produced inconsistent results. One study reported that overexpression of

miR-146a in 5-fluorouracil (5-FU) treated bone marrow cells results in a transient myeloid expansion that subsequently returns to normal [21]. Another report showed no detectable change in circulating granulocytes, T cells and B cells by overexpressing miR-146a in lineage negative bone marrow cells [45]. Lastly, one other group showed that ectopic expression of miR-146a in sorted LKS (Lineage-cKit+Sca1+) cells directs the selective differentiation of HSCs into peritoneal macrophages in mice. Surprisingly, other than the peritoneal cavity, this study failed to detect any transplanted miR-146a-expressing donor cells in the peripheral blood, spleen and bone marrow, precluding comparison in these hematopoietic compartments with the other overexpression studies. The same report also showed that inhibition of miR-146a impairs macrophage formation during early zebrafish development [25]. In addition to different investigators overexpressing miR-146a in different fractions of bone marrow cells, it is also unclear whether the levels of miR-146a overexpression achieved were comparable between these studies. Despite some inconsistent findings, it appears that enforced expression of miR-146a in mouse bone marrow cells has an overall minor effect on hematopoiesis, at least in the major hematopoietic organs under steady state.

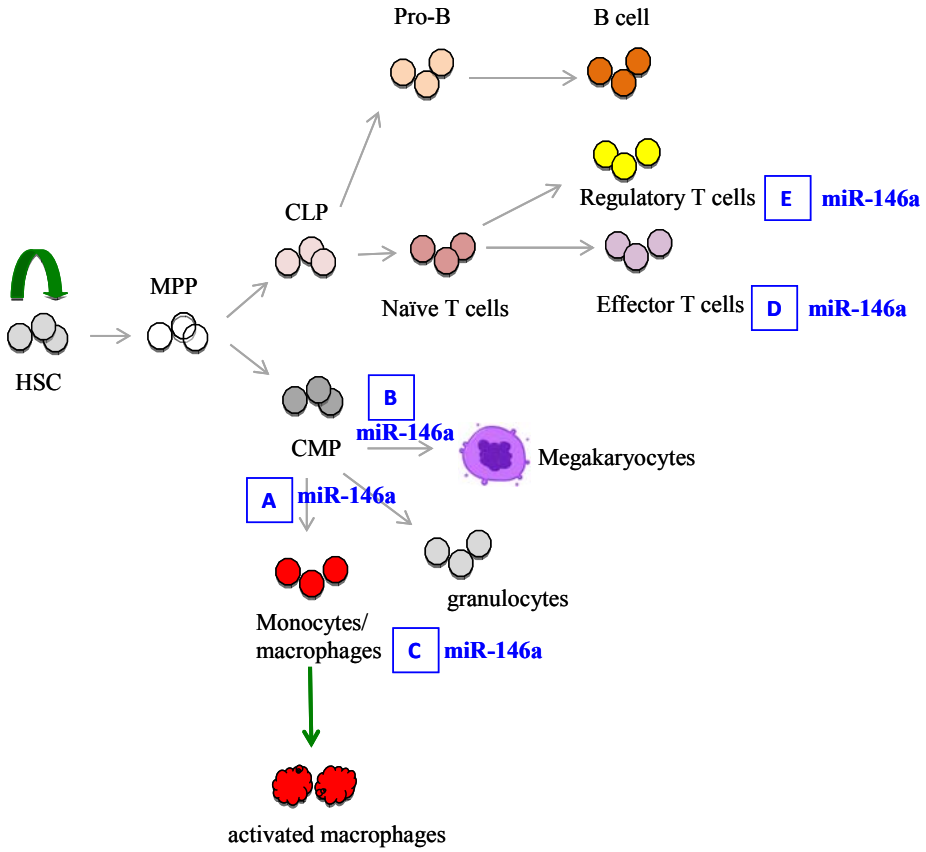

Figure ii. A simplified schematic depiction of hematopoietic tree highlighting the role of miR-146a in hematopoiesis and immune cell function. A. miR-146a negatively regulates myelopoiesis and myeloproliferation during inflammation and aging. In the absence of miR-146a, increased myeloprolifreation is observed. B. miR-146a negatively regulates megakaryopoiesis. Overexpression of miR-146a inhibits megakaryocyte proliferation and differentiation while down-regulation of miR-146a promotes megakaryocyte expansion and platelet production. However, in aging miR-146a-deficient mice with bone marrow fibrosis, thrombocytopenia is observed. MiR-146a is a negative regulator of monocyte and macrophage activation (C) and effector T cell activation (D). E. In regulatory T cells, miR-146a positively controls Treg functional competence. In the absence of miR-146a, Treg cells are defective in suppressing effector T cell activation.

Overview of MiRNA-146a in Pathology

The importance of miR-146a is further exemplified by its extensive involvement in immunological pathologies, including autoimmunity and hematologic malignancy. Loss-of-function studies in mice have provided some important insight in the role of miR-146a in the pathogenesis of autoimmunity. Genetic deletion of miR-146a in all the cells in mice leads to autoimmunity, indicated by

splenomegaly, lymphadenopathy, lymphocyte-infiltration in liver, kidney and lung, and the development anti-dsDNA antibodies [19]. The contribution of miR-146a to autoimmunity occurs in at least 3 separate ways: (1) regulation of miR-146a in effector T cells; (2) regulation of miR-146a in Treg cells; (3) regulation of myeloid cell-mediated inflammation. MiR-146a-deficient T effector cells contribute to autoimmunity in a cell-intrinsic manner. MiR-146a-deficeint T cells remain hyper-responsive to antigen stimulation when adoptively transferred into wild type mice and they induce a spontaneous autoimmune pathology when transferred into Rag1-/- mice. Mechanistically, the enhanced proliferation, impaired activation-induced apoptosis, and exaggerated effector cytokine production seen in miR-146a-deficient CD4 and CD8 T cells derive from uncontrolled NF-κB activation as a result of de-repressed TRAF6 and IRAK1 [20]. Whether the multi-organ autoimmune pathology is caused by a general over-activation of miR-146a-deficient T cells or by a more specific autoreactivity against a particular cell type or self-antigen remains an interesting unanswered question. In addition, miR-146a-deficient Treg cells are also functionally defective in suppressing excessive Th1 response. In the absence of miR-146a, upregulation of STAT1 in Treg cells is responsible for the failure to suppress wildtype effector T cells, leading to fatal IFNγ-mediated autoimmunity in a variety of organs [43]. The chronic inflammatory environment conditioned by miR-146a-deficient myeloid cells also contributes to autoimmune pathology by further stimulating T-cell and promoting tissue damage [19,44]. Lastly, anti-dsDNA antibodies are present in the serum of aging miR-146a-/- mice [19]. Future studies examining of the role of miR-146a in B cells may yield additional insight into the regulation of autoantibody production. Given the widespread expression of miR-146a outside of hematopoietic cells, miR-146a may exert protective function in non-hematopoietic tissues. Evidence supporting this comes from studies on lung epithelial cells and neonate guts [46-47]. Interestingly, during the dramatic transition from a sterile environment to a bacteria-colonized surface in neonate guts, sustained miR-

146a expression seems to be critical to mediate innate immune tolerance by repressing IRAK1 [46]. In light of this, we speculate that miR-146a-deficiency in intestinal epithelial cells may lead to intestinal inflammation, contributing to the overall autoimmune pathology in miR-146a-/- mice. Corroborating the in vivo studies in mice, miR-146a has been found to be extensively dysregulated in human patients with autoimmune diseases, including systemic lupus erythematosus (SLE) and rheumatoid arthritis (RA). In lupus patients, miR-146a expression is downregulated in peripheral blood mononuclear cells (PBMCs). In addition, the level of miR-146a expression is negatively correlated with disease severity, with lower expression correlating with more active disease and proteinuria symptoms [42]. Type I IFN is suggested to be the responsible pathway upregulated in lupus and additional targets of miR-146a, IRF5 and STAT1, have been identified based on 3'UTR luciferase reporter assay and Western blot analysis in 293T cells overexpressiing miR-146a. Interestingly, enforced expression of miR-146a in PBMCs of lupus patients can downregulate a subset of IFN-responsive genes [42]. Additional evidence comes from genome-wide association studies that identified SNPs (single-nucleotide polymorphism) in the regulatory region of miR-146a that are associated with lupus disease risk [48-49]. One such SNP (rs57095329) in the promoter region of miR-146a is associated with the binding strength of transcription factor Ets-1, another lupus-susceptibility gene. The risk-associated G allele in this SNP correlates with reduced Ets-1 binding and decreased miR-146a expression [49]. In contrast to SLE where miR-146a expression is shown to be down-regulated, over-expression of miR-146a is frequently detected in rheumatoid arthritis (RA) patients [50-52]. MiR-146a also seems to be highly expressed in osteoarthritis cartilage [53]. Despite that both SLE and RA are autoimmune diseases with some shared characteristics, the underlying etiologies may be distinct. For example, chronic inflammation is a shared pathology, but the dysregulated cytokine profiles are different between SLE and RA. The IFN pathway is intimately linked to the pathogenesis of SLE while increased TNFα, IL-1β, and IL-6

production are more prominent features of RA [50]. Because pro-inflammatory cytokines can significantly upregulate miR-146a expression in various cell types, increased miR-146a expression may simply reflect the hyper-inflammatory environment and may be a useful marker for disease severity in RA. On the other hand, miR-146a-deficiency may be causally related to the pathogenesis of SLE. It will be interesting to further investigate the involvement of miR-146a-deficiency in the development and progression of SLE and a number of other autoimmune diseases and whether upregulation of miR-146a may have therapeutic benefit in mouse models and human clinical samples. In the addition to the role of miR-146a in Th1 cells, Treg cells and monocyte/macrophages, understanding the function of miR-146a in T17 cells [54], a key cell type in a number of autoimmune diseases, may provide additional insight on this miRNA's involvement in autoimmunity. There is also some evidence suggesting a role of miR-146a in atherosclerosis, a less studied aspect of miR-146a biology. Two reports suggested that upregulation of miR-146a may inhibit atherosclerosis by suppressing TLR-4 and CD40L expression in low-density lipoprotein (LDL)-induced macrophages and dendritic cells [55-56].

MiRNA-146a in Hematologic Malignancy

Recent studies have also revealed an important role of miR-146a in hematologic pre-malignancy and malignancy, most notably myelodysplastic syndromes (MDS), myeloproliferative disease, myeloid cancer and bone marrow failure. MDS represent a heterogeneous group of clonal diseases of HSC origin characterized by ineffective hematopoietic differentiation, peripheral blood cytopenias, bone marrow dysplasia, and a propensity to progress to leukemia and bone marrow failure. Recent studies have made significant advances on the molecular pathogenesis of MDS, including dysregulated expression of miRNAs [57-58]. Starczynowski et al have shown that two miRNAs, miR-145 and miR-

146a, are located in or near the commonly deleted region of 5q- syndrome, a common subtype of MDS [37]. Accordingly, expression of these two miRNAs is reduced in patients of 5q- syndrome. The same study also showed that the stable knockdown of miR-145 and miR-146a concurrently in mouse HSPCs recapitulates many of the key features of human 5q- syndrome, including thrombocytosis, megakaryocytic dysplasia and mild neutropenia. In addition, overexpression of TRAF6, a target of miR-146a, was sufficient to phenocopy many of the features of knocking down miR-145 and miR-146a, suggesting that miR-146a may be a more dominant miRNA. Studies with miR-146a knockout mouse are reaffirming. With increasing age, miR-146a-/- mice develop myeloid expansion in spleen and bone marrow, pancytopenia in the periphery and a propensity to progress to bone marrow failure and myeloid cancer, a constellation of features reminiscent of a mixed myelodysplastic syndrome and myeloproliferative neoplasm (MDS/MPN) [19,44]. Mechanistically, increased NF-κB activation is a main driver of the myeloproliferative and bone marrow failure phenotype because ablation of the p50 subunit greatly reduces MDS/MPN symptoms. It is now increasingly appreciated that a distinct hematopoietic developmental program, termed inflammatory hematopoiesis, is activated in bone marrow during inflammation to promote myelopoiesis at the expense of lymphopoiesis and erythropoiesis [59]. We speculate that uncontrolled and persistent inflammatory hematopoiesis may promote pathological features of MDS and MPN, and over time, the pathologic hematopoietic program becomes permanent and irreversible through additional genetic mutations and/or epigenetic changes. Because chronic inflammation is a prominent feature of miR-146a-/- mice during stimulation and aging, it will be interesting to investigate whether miR-146a may serve as a molecular link between chronic inflammation and hematopoietic malignancy, such as MDS and MPN. In addition to myeloid cancers, about 15% of miR-146a-/- mice also develop B-cell or mixed B and T-cell lymphomas by 18 to 24 months [44]. It's not clear whether the mechanism underlying lymphoma development in miR-

146a-deficient mice is distinct from the one driving myeloid oncogenesis. Many groups have extensively profiled miRNA expression in human leukemia in an effort to identify microRNA signatures associated with leukemia diagnosis, prognosis, and pathogenesis. Reports from different groups have identified miR-146a downregulation in CD34+ cells or total bone marrow cells from patients with 5q- syndrome [37,58,60]. However, miR-146a downregulation is not consistently observed in leukemia studies. One expression profiling study showed that miR-146a is downregulated in bone marrow cells of AML patients compared to normal CD34+ cells [61]. However, in another study that compared miRNA expression between AML and ALL samples, increased expression of miR-146a in both ALL and AML was shown to correlate with poor survival [62]. MiR-146a was also shown to function as a tumor-suppressor in natural killer/T cell lymphoma and reduced expression of miR-146a was identified as a poor prognostic factor [63]. It seems miR-146a-downregulation is a consistent feature of 5q- syndrome or even all MDS and may be involved in the pathogenesis of MDS. The role of miR-146a in leukemia and lymphoma requires further clarification.

Relationship between MiR-146a and MiR-155

MicroRNA-155 (miR-155) is another miRNAs identified from our original screen for miRNAs induced upon NF-κB activation [16]. However, in contrast to miR-146a, miR-155 plays an almost exact opposite role in immunity and hematopoiesis. For more detailed reviews of miR-155 biology, we refer you to these recent reviews elsewhere [3,36,59,64-65]. Here we will only focus on the aspect of miR-155 function opposing that of miR-146a. NF-κB activates an elaborate and potent transcription program central to inflammation and immunity. Because of the potency of this pathway, proper regulation of the magnitude and duration of NF-κB activation is essential [36,66-68]. NF-κB-induced miRNAs, miR-146a and miR-155, may be two important regulators that balance the negative and positive effects

driven by NF-κB activation. The opposing roles of miR-146a and miR-155 have been most clearly demonstrated in the function and development of myeloid cells. While basal expression of miR-155 is low in myeloid cells, many of the inflammatory stimuli that can induce miR-146a expression, including TLR ligands and pro-inflammatory cytokines, also upregulate miR-155 expression significantly [15,69]. In regulating the functional capacity of myeloid cells, upon induction miR-155 promotes expression of pro-inflammatory cytokines and the IFN response. This regulation is most likely through repression of SOCS1 and SHIP1, both negative regulators of the pro-inflammatory pathways [70-71]. Consistent with this, inhibition of miR-155 in macrophages confers tolerance to endotoxin shock in mice while mice with miR-155 overexpression become hypersensitive [71-72]. The exactly opposite effect has been observed with miR-146a inhibition and overexpression [19]. In addition to pro-inflammatory cytokine production, miR-146a and miR-155 also regulate immunity in the opposite manner. In general, mice with targeted miR-155 deletion are immuno-compromised as indicated by attenuated immune response to immunization and infection [73-74]. On the other hand, inhibiting miR-146a may result in a heightened immune response as shown by enhanced protection against Listeria infection [17]. MiR-146a and miR-155 also have an opposite effect in regulating certain aspects of T cell function. As discussed above, miR-146a-deficient CD4 T cells display a hyper-activated response upon TCR stimulation while miR-155-deficient CD4 T cells are attenuated in IL-2 and IFNγ cytokine production upon TCR stimulation [20,73]. Similarly, miR-155 and miR-146a also function in an opposite direction in autoimmunity. Contrary to miR-146a-/- mice that are prone to developing autoimmune disease, miR-155-/- mice were shown to be significantly resistant to an induced model of experimental autoimmune encephalomyelitis (EAE) because of a deficit in inflammatory T-cell development and, to a lesser extent, a defect in myeloid dendritic cell function [75]. In a recent effort to directly study the opposing function of miR-146a and miR-155, mice deficient of

miR-146a, miR-155, or both miRNAs were implanted with subcutaneous solid tumors and were shown to have differential ability to control tumor growth [76]. This study showed again that in the context of antitumor immunity, miR-146a and miR-155 play opposing roles with miR-155 promotes, while miR-146a represses antitumor immunity, correlating their functions to regulate IFNγ-producing CD4+ T cells development. As described above, miR-146a and miR-155 are concurrently up-regulated in response to pro-inflammatory cues. Data suggest that miR-146a and miR-155 may counterbalance each other during inflammatory hematopoiesis. Sustained expression of miR-155 in mouse HSPCs results in a myeloproliferative disorder, characterized by profound myeloproliferation with dysplastic changes in the bone marrow, splenomegaly as a result of extramedullary hematopoiesis, peripheral anemia, lymphopenia, and thrombocytopenia with increased myeloid cells [15]. The constellation of hematologic abnormalities seen in miR-155-overexpressing mice is strikingly similar to the one observed in aging miR-146a-deficient mice [44]. MiR-155-induced myeloproliferative disorder is thought to be primarily through repressing SHIP1 [70]. In addition, over-expression of miR-155 in a B-cell-specific manner in a transgenic mouse model with E(mu)-promoter-driven miR-155 expression results in B-cell leukemia and lymphoma [77]. Similar B-cell lymphoma pathology has also been observed in a subset of aging miR-146a-/- mice [44]. Given the above evidence, it is tempting to speculate that miR-146a and miR-155 are evolutionarily selected to function in a tug-of-war manner to properly control the magnitude and duration of NF-κB activation. Balanced level and proper timing of miR-146a and miR-155 expression represents one critical layer of regulation to ensure that NF-κB is activated in a controlled manner.

CHAPTER ONE

NF-κB Dysregulation in MicroRNA-146a-deficient Mice Drives the Development of Myeloid Malignancies

INTRODUCTION

MicroRNAs (miRNA) are a group of ~19-23 nucleotide-long non-coding RNAs that repress target gene expression by a combination of mRNA degradation and translation inhibition [8]. Recent studies have revealed important physiological roles of miRNAs in many aspects of mammalian hematopoiesis and immune cell function, and their altered expression has been linked to pathological conditions of the immune system, such as hematologic cancers and autoimmunity [3,78-79].

Chronic inflammation contributes to cancer initiation and progression. Among a myriad of proposed mechanisms linking inflammation to cancer, NF-κB has been identified as a key mediator of inflammation-induced carcinogenesis [80]. Moreover, constitutive NF-κB activation is frequently detected in many types of lymphoid and myeloid malignancies [81-82]. Hence understanding how NF-κB activity is downregulated has been a focus of study with important advances in recent years [67]. In particular, NF-κB regulation by non-coding RNAs has recently begun to be characterized. A few years ago, we carried out a microarray screen to identify miRNAs induced by NF-κB activation and miR-146a was discovered to be one of the miRNAs induced by lipopolysacharide (LPS) in a human monocytic cell line. The induction of miR-146a was shown to be NF-κB-dependent, and upon induction, miR-146a functioned to directly down-regulate TNF receptor-associated factor 6 (TRAF6) and Interleukin-1 receptor-associated kinase 1 (IRAK1), two of the signal transducers in the NF-κB activation pathway [16]. Based on this study and others [22,83], we hypothesized that miR-146a, by repressing TRAF6 and IRAK1, may have an effect on NF-κB activation, dampening and/or

terminating an inflammatory response via a negative feedback loop. To definitively characterize the function of miR-146a *in vivo* and directly test the hypothesis that miR-146a is a negative regulator of the NF-κB pathway, we generated two independent mouse strains with a targeted germline deletion of miR-146a, one on the mixed C57BL/6x129/sv background and one on the pure C57BL/6 background. Initial study done primarily with the mixed background miR-146a-/- mice showed that miR-146a-/- mice were hypersensitive to LPS challenge, and aging miR-146a-/- mice developed autoimmune-like disease, myeloid proliferation in their spleens, and hematopoietic tumors [84]. However, the cellular lineage of the tumors and the mechanistic basis of miR-146a-deficiency mediated myeloproliferation remained important unanswered questions. In addition, the relationship of the tumor phenotype in miR-146a-/- mice and NF-κB dysregulation was uncertain due to the multiple potential targets of miR-146a in different molecular pathways. Here, we focus on characterizing the incidence, cellular lineage, and transplantability of the tumors and to understand the molecular basis of oncogenesis.

We have found that when they are allowed to age naturally, miR-146a-/- mice on a pure C57BL/6 background develop a chronic inflammatory phenotype with progressive myeloproliferation involving both the spleen and the bone marrow, which eventually progresses to splenic myeloid sarcoma and bone marrow failure at about 18 months of age. Lymphomas of either a B-cell lineage or a mixed T-and-B-cell lineage are also observed in older miR-146a-/- mice at a much higher frequency than in wild-type animals. Myeloproliferation in miR-146a-deficient mice are driven primarily by the action of NF-κB because reduction in the NF-κB level by deletion of the NF-κB subunit p50 effectively suppresses the pathology. Thus, we have provided genetic evidence that miR-146a functions as a tumor suppressor in both myeloid and lymphoid cells and that chronic NF-κB activation as a result of miR-146a-deficiency is responsible for driving the myeloproliferative disease, which can progress to malignant myeloid sarcoma.

RESULTS

miR-146a knockout mice develop myeloid and lymphoid malignancies.

The miR-146a-deficient pure C57BL/6 mouse was made by deleting about 300 base pairs of genomic DNA fragment containing the miR-146a precursor [84]. The miR-146a-deficient mice (homozygous knockouts, designated as miR-146a KO) were born at the expected Mendelian frequency and appeared to be normal at birth. But starting at about 5-6 month of age, they developed progressively enlarged spleens. By 18-22 months of age, 80% of the KO mice were moribund and were culled for analysis. However, the entire cohort of age-matched littermate C57BL/6 (WT) control mice, except for one case of thymoma and one case of seizure, were still alive and healthy (Figure S1A). On necropsy, KO mice demonstrated various degrees of splenomegaly, with KO spleens on average weighing 6-7 times more than WT spleens (Figure S1B and S1C). By FACS analysis, splenomegaly was correlated with a massive expansion of the CD11b+ myeloid population (Figure S1D, S1E, and S1F). Expanded splenic hematopoiesis was also noted based on the increased Ter119+ erythroid precursor population in the spleen. About 40% of the mice demonstrated distinct splenic tumors (Figure 1A and 1B). The majority of these tumors displayed the histologic appearance of a myeloid sarcoma (Figure 1B) [85]. FACS analysis of carefully dissected tumors showed that the cells derived from these tumors expressed the pan-myeloid antigen, CD11b (Figure 1B). Occasionally, liver and kidney were also heavily infiltrated by myeloid sarcoma (Figure S2A and S2B). A general role of miR-146a as a tumor-suppressor miRNA in the hematolymphoid system was demonstrated by the development of lymphomas of a B-cell or a mixed T-and-B cell lineage in cervical lymph node, gastrointestinal tract, liver, and kidney, in about 20% of the KO mice (Figure 1A). Similar lymphoid tumors were not identified in wild-type mice. The lineage of these tumors was confirmed by FACS as well as immunohistochemical stains (Figure 1C and 1D and Figure S2C, and S2D). Histological analysis revealed that the lymphomas

ranged from low-grade follicular lymphoma (Figure S2C) to high-grade diffuse large B-cell lymphoma with apoptotic bodies and atypical mitosis (Figure 1C and Figure S2D).

Myeloid tumors are transplantable into immunocompromised recipient mice.

The ability of a mass of cells to form tumors upon transplantation to a secondary mouse can distinguish a malignant growth from a reactive inflammatory process. KO splenic tumor cells dissected from the tumor nodules in the spleen and wild-type (WT) control spleen cells were transplanted into immunocompromised Rag2-/-γC-/- Balb/c recipient mice intravenously (i.v.), with or without transduction by a retrovirus expressing enhanced green fluorescence protein (eGFP) and luciferase protein. For experiments with retroviral transduction, bioluminescent imaging was utilized as a sensitive method to track luciferase expression by the transplanted cells *in vivo* in recipient mice. Starting one to two weeks after intravenous injection, KO splenocytes showed markedly increased proliferation compared to wild-type splenocytes in recipient mice (Figure 2A). When whole body bioluminiscence intensity was quantified over the course of eight weeks, mice receiving KO splenocytes showed a progressive increase in signal culminating in an approximately 10-20-fold higher signal, indicating a proliferation of the transplanted cells, while WT cells did not (Fig 2B). Interestingly, recipient spleens, kidneys, and livers showed the strongest biolumniscence signal, indicating the proclivity of transplanted splenic tumor cells to localize to the same organs where the most significant myeloid tumor pathology was observed in the original KO mice. By two months following transplantation, most KO recipient mice became cachectic and moribund, while WT recipient mice showed some mild weight loss. In mice receiving KO spleen cells, but not in those receiving WT spleen cells, necropsy revealed significant myeloid pathologies, including enlarged spleens and massive infiltration of kidneys and livers by neoplastic myeloid cells (Figure 2C to F).

Interestingly, not every KO spleen was transplantable. Transplantation of age-matched KO splenocytes from mice without overt myeloid sarcoma did not result in significant myeloid pathology in recipient mice, suggesting there is a qualitative difference (e.g. additional mutations) between KO spleens with myeloproliferation and those with overt myeloid sarcoma.

Chronic myeloproliferation and myelofibrosis in miR-146a deficient bone marrow.

In addition to splenic myeloproliferation and/or myeloid sarcoma, the bone marrow of miR-146a KO mice showed significant myeloproliferative disease. By 18-22 months of age, the CD11b+ population accounted for 80% of all nucleated bone marrow cells, while the percentages of CD19+ B cell dropped to below 10% in miR-146a KO mice (Figure 3A and 3B). In line with the myeloid-dominated bone marrow, peripheral blood showed significant lymphopenia, anemia, and thrombocytopenia, but preserved granulocyte numbers (Figure 3C and S3A). In addition, the expanded CD11b+ population in both bone marrow and spleen was also predominantly Gr1+. An increased expression of macrophage colony stimulating factor receptor (CSF1R) was also noted in the myeloid population in both spleen and peripheral blood (Figure S3B). By 18-22 months of age, WT bone marrow showed partial replacement of bone marrow cells by adipose tissue as a result of aging, while KO bone marrow showed end-stage fibrosis or a hypercellular bone marrow. The end-stage KO bone marrow was markedly pale by gross analysis, and histologic sections demonstrated paucicellular marrow with thickened bone and fibrosis (Figure 3D and S3C). This chronic myeloproliferation resembles in some ways human myeloproliferative diseases that result in an end stage of marrow fibrosis.

Spleen and bone marrow cells from miR-146a-deficient mice show increased activation of NF-κB-mediated transcription.

We and others have previously identified TRAF6 and IRAK1 as targets of miR-146a in various cell types, including monocytes and macrophages [16,22]. Because TRAF6 and IRAK1 are signal transducers upstream of NF-κB activation, their de-repression in miR-146a deficient mice could result in increased activation of NF-κB. In fact, we have recently demonstrated that TRAF6 and IRAK1 are derepressed in miR-146a KO mice [84]. Therefore, we investigated whether increased NF-κB activation might be a feature of the myeloproliferation and/or myeloid sarcoma in the miR-146a-deficient mice. We extracted RNA from total nucleated spleen cells and total nucleated bone marrow cells and examined RNA expression levels for some genes well-known to be NF-κB-responsive, including interleukin-6 (IL-6), tumor-necrosis factor α (Tnfα), monocyte-chemotatic protein 1 (Mcp1), A20, and the NF-κB subunit p50 (Nfkb1). In the absence of *ex vivo* stimulation, KO splenocytes and bone marrow cells showed basally up-regulated expression of a subset of NF-κB-responsive genes compared to the WT control, suggesting the presence of constitutively activated NF-κB (Figure 4A and 4B). For some of the genes, such as Tnfα and Mcp1, the expression was even higher in tumor cells isolated from the KO spleen (Figure 4A). To exclude the possibility that a different cellular composition is responsible for the difference, especially in spleens where KO spleens showed a 3-fold increase in CD11b+ myeloid population, we purified the CD11b+ population from WT and KO spleens by magnetic bead labeled cell separation (MACS). When the enriched CD11b+ splenocyte population was subjected to the same gene expression analysis, NF-κB-activated genes, including Tnfα and Mcp1, were still up-regulated in the KO population compared to the WT control (Figure 4C). To further confirm the status of NF-κB activation, we assessed the level of nuclear translocation of the NF-κB subunit, RelA (p65), by western blot analysis of the nuclear protein extract from total nucleated splenocytes. KO splenocytes showed a 1.5- to 2-fold higher level of nuclear p65 than WT splenocytes, confirming the activated status of NF-κB (Figure 4D). It is important to note that not every KO spleen showed constitutively higher level of

nuclear p65 protein. Increased nuclear p65 correlated well with the presence of myeloid sarcoma (Figure S4), suggesting that the activation of the NF-κB becomes constitutive only when the KO spleen progresses from myeloproliferation to myeloid sarcoma.

Reduction in the NF-κB level rescues the myeloproliferation in spleen and bone marrow.

Both gene expression and nuclear protein analysis indicated that the KO spleen and bone marrow cells showed increased NF-κB activation. To investigate whether activated NF-κB is a causal factor in the observed myeloproliferation, we bred the miR-146a KO strain with an Nfkb1 (p50) KO strain to generate the double transgenic strain with homozygous deletion in both miR-146a and the p50 subunit. p50-/- mice show no developmental abnormality in the immune system and elsewhere but display defective B cell proliferation and specific antibody production. Cytokine production, including IL-6, TNFα, and IL-1α, from LPS-stimulated macrophage is also impaired [86-87]. When we intercrossed double heterozygotes for the two knockout genes, the various genotypes were born at the expected Mendelian frequency (Figure S5A) and showed no overt abnormalities. Littermates from different genotype groups, miR-146a+/+ p50+/+ (WT), miR-146a-/- p50+/+ (miRKO), miR-146a-/- p50+/- (miRKO p50HET), and miR-146a-/- p50-/- (DKO), were aged to 6-7 month-old and then were sacrificed for analysis for the development of myeloproliferation in spleen and bone marrow. As expected, by 6-7 months of age, miR-146a KO mice started to develop splenomegaly and myeloproliferation. Importantly, splenomegaly and myeloproliferative disease were significantly reduced in the miR-146a-/- p50+/- group, with the exception of a few outliers. The rescue from the myeloproliferative phenotype was more consistent in the miR-146a-/- p50-/- double knockout (DKO) group, as indicated by the reduction in spleen weight and the lack of myeloid cell expansion in the spleen and bone marrow (Figure 5A and 5B). In contrast to the pale, fibrotic bone marrow observed in

miRKO femurs, the bone marrow in DKO mice was a vibrant red color, similar to what was observed routinely in WT mice (Figure S5B). In the spleens of DKO mice, there was also significant reduction in Ter119+ cells relative to miRKO mice, suggesting that expanded splenic hematopoiesis was also rescued by the deletion of p50 in DKO mice (Figure 5B). We conclude that activated NF-κB as a result of miR-146a deletion is the primary factor driving myeloproliferation in miR-146a-deficient mice, because reduction in the NF-κB level by deleting the NF-κB subunit p50 effectively rescues the myeloproliferative phenotype.

FIGURE

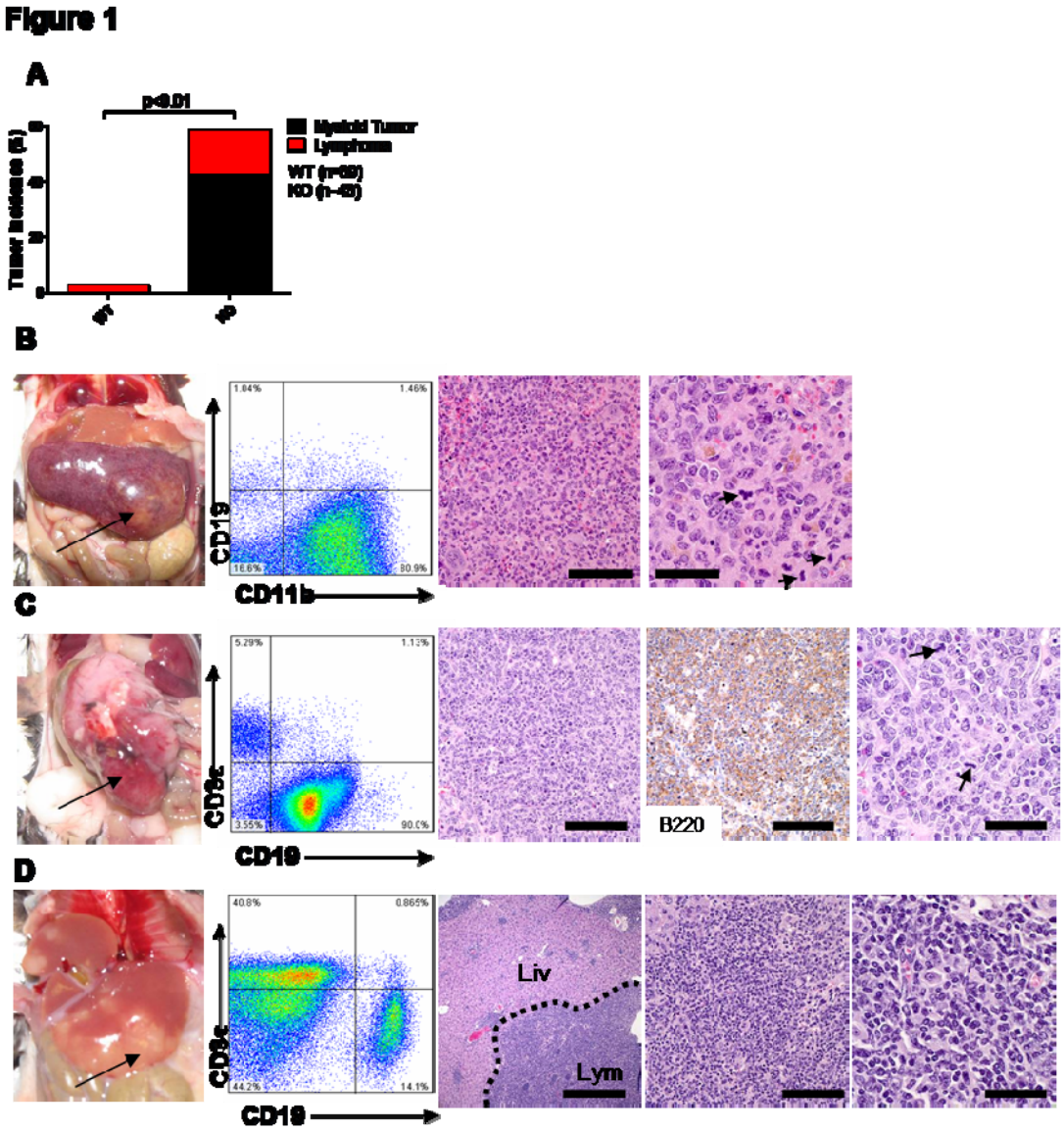

Figure 1. miR-146a-deficient mice develop myeloid and lymphoid malignancies. Mice were18-22 month-old miR-146a-/- mice (KO) and sex and age-matched C57BL/6 control mice (WT).

(A) Incidences of myeloid and lymphoid malignancies observed in WT (n=39) and KO (n=43) mice.

(B) Photograph, FACS plot, and histological analysis of a representative myeloid tumor from a KO spleen. Panel 3 and 4, Hematoxylin and eosin (H&E) stained spleen section. Left scale bar, 100 microns; right scale bar, 40 microns. Arrows, mitotic figures.

(C) Photograph, FACS plot, and histological analysis of a representative B-cell lymphoma from a KO gastrointestinal tract. Panel 3 and 5, Hematoxylin and eosin (H&E) stained tumor section; Panel 4: Positive immunohistochemical staining (IHC) for B220. L to R scale bars are 100 microns in Panel 3, 4 and 40 microns in Panel 5.

(D) Photograph, FACS plot, and histological analysis of a representative mixed T-and-B-cell lymphoma from a KO liver. Panel 3,4, and 5, Hematoxylin and eosin (H&E) stained liver section; L to R, scale bars are 400 microns, 100 microns, 40 microns. Lym, Lymphoma; Liv, relatively uninvolved liver.

Figure 2

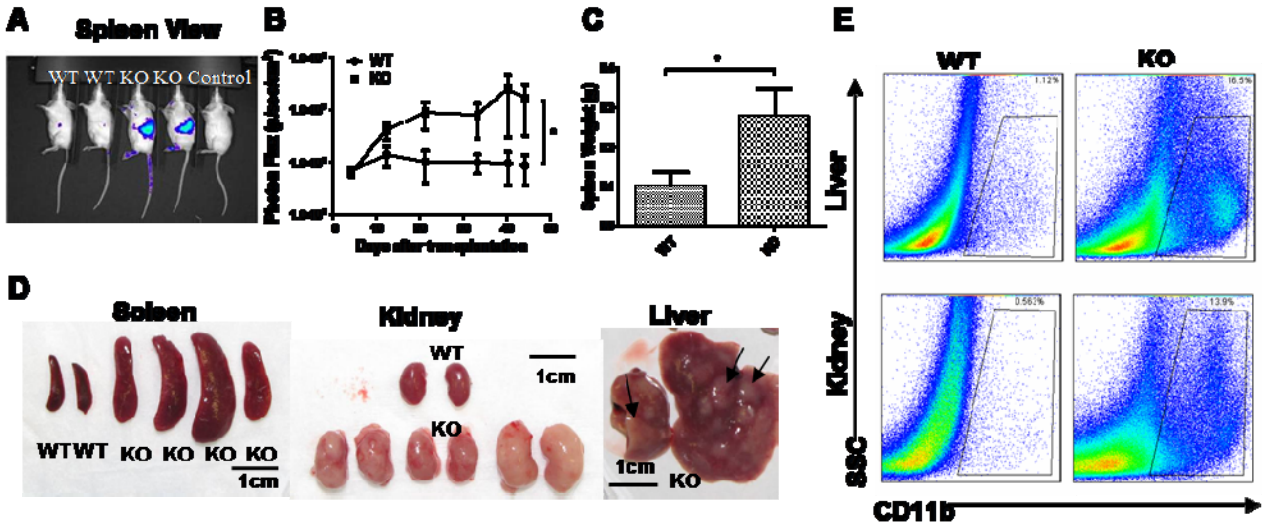

Figure 2. Myeloid sarcoma is transplantable into immunocompromised Rag2-/-γC-/- recipient mice, causing lethal myeloid pathology. WT designates Rag2-/-γC-/- mice transplanted with WT splenocytes; KO designates Rag2-/-γC-/- mice transplanted with miR-146a KO splenocytes. (n=4 for WT and n=4 for KO; data are representative of three independent experiments. Student t-test, * designates $p < 0.05$)

(A) Representative bioluminiscence images of Rag2-/-γC-/- recipient mice splenic side view.

(B) Quantification of whole body bioluminiscence intensity from splenic side view of one representative experiment. Vertical axis is in logarithmic scale. Transduction efficiency is determined by flow cytometric analysis of GFP+ cells prior to injection. The bioluminescence intensity is normalized to the percentage of initially transduced cells.

(C) Spleen weight of Rag2-/-γC-/- recipient mice.

(D) Photographs of spleens, kidneys, and livers from representative Rag2-/-γC-/- recipient mice.

(E) Flow cytometric analysis of myeloid cells (defined as CD11b+) in representative recipient kidneys and livers. SSC, side scatter.

(F) Histological analysis (H&E staining) of livers and kidneys from Rag2-/-γC-/- recipient mice. Arrows, myeloid tumor cells infiltrating recipient liver and kidney.

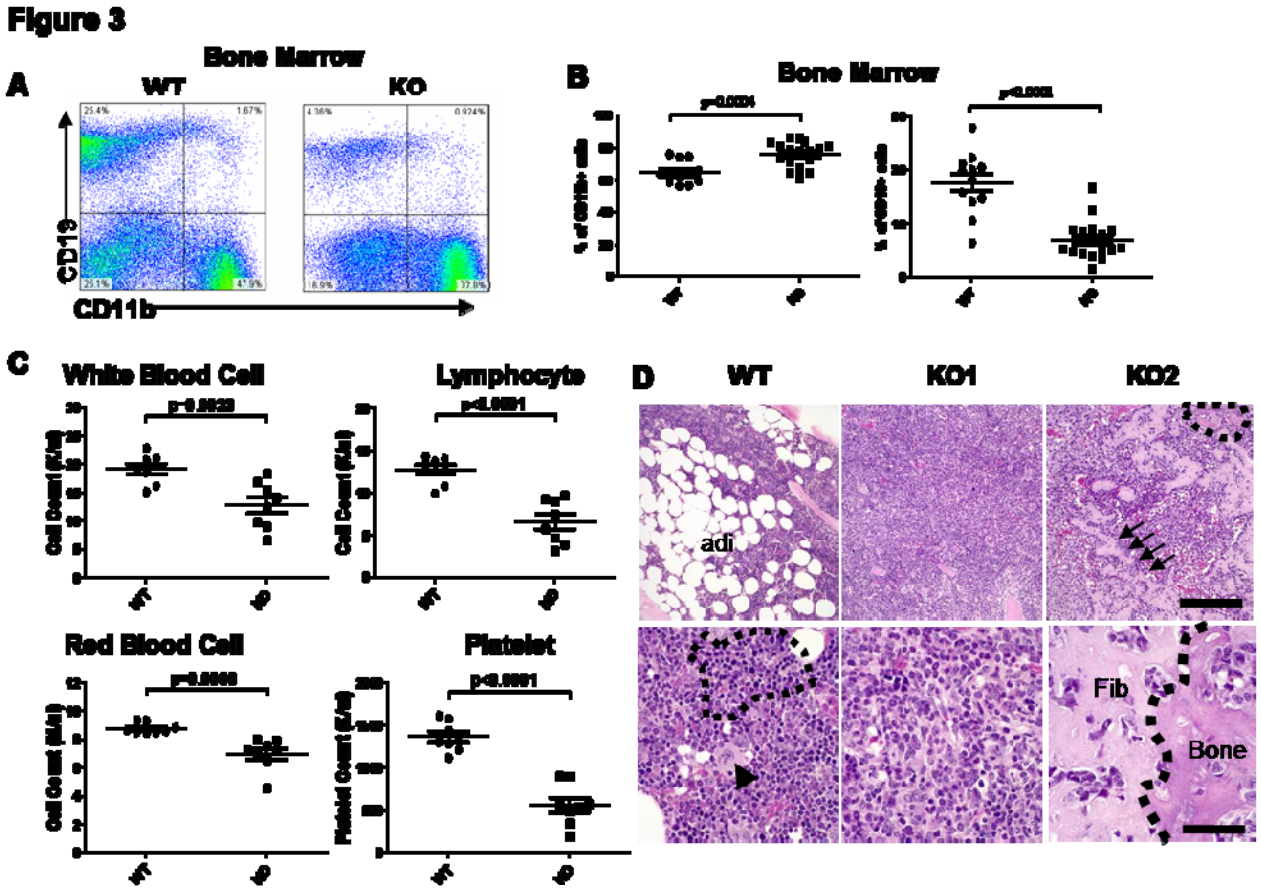

Figure 3. Chronic myeloproliferation and myelofibrosis occur in miR-146a-deficient bone marrow. Mice were 18-22 month-old miR-146a-/- mice (KO) and sex and age-matched wild type control mice (WT). Data are shown as Mean +/- SEM. Each individual dot represents one individual mouse.

(A) Flow cytometric analysis of nucleated bone marrow cells from one representative WT mouse and one representative KO mouse for B cells (defined as CD19+) and myeloid cells (defined as CD11b+).

(B) Percentage of B cells (defined as CD19+) and myeloid cells (defined as CD11b+) in nucleated bone marrow cells by flow cytometric analysis (n=12 for WT and n=17 for KO from at least three independent experiments).

(C) Absolute numbers of total white blood cells, lymphocytes, red blood cells, and platelets by complete blood count (CBC) analysis (n=8 for WT and n=8 for KO).

(D) Representative hematoxylin and eosin (H&E) stained tibia sections from KO mice showing myelofibrosis and WT control. WT: WT bone marrow; adi, adipose tissue. KO1: markedly hypercellular KO bone marrow that contains virtually no megakaryocytres (arrowhead, lower left panel) or erythroid islands (outlined by dashed line, lower left panel). KO2: fibrotic KO bone marrow; arrows in the upper right panel, a broad band of fibrosis, of which there are many in this field; within the dotted line, an area of new bone formation that may represent end-stage fibrosis; the lower right panel, the interface between an area of fibrosis (fib) with entrapped myeloid cells and new bone formation (bone). Scale bars, top row, 200 microns; bottom row, 40 microns.

Figure 4

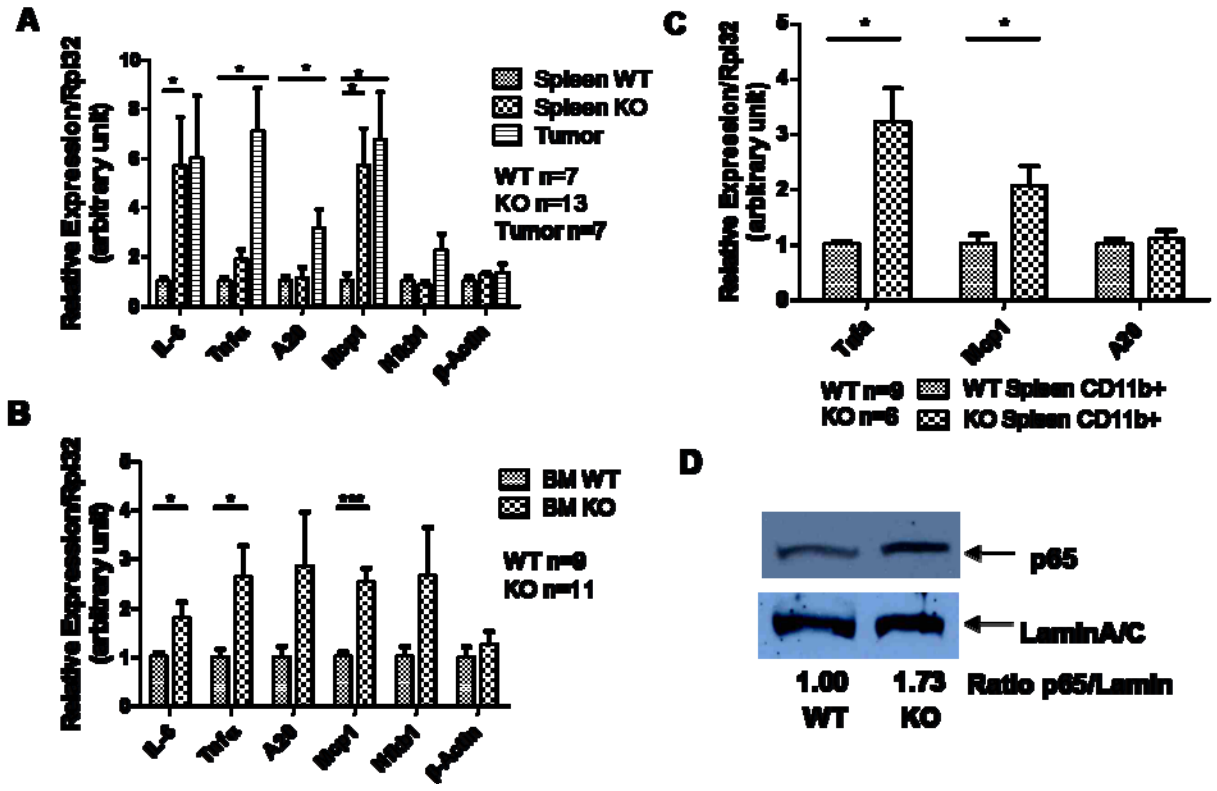

Figure 4. Spleen and bone marrow cells from miR-146a-deficient mice (KO) show increased activation of the NF-κB-mediated transcription. Mice were 18-22 month-old miR-146a-/- mice (KO) and sex and age-matched wild type control mice (WT). Data are shown as Mean +/- SEM. n equals to the number of mice analyzed from at least two independent experiments. Student t-test, * designates $p<0.05$, *** designates $p<0.005$.

(A) Gene expression analysis of NF-κB-responsive genes in WT (n=7) nucleated splenocytes, KO (n=13) nucleated splenocytes, and myeloid tumor cells (Tumor, n=7) isolated from KO spleen by gross dissection.

(B) Gene expression analysis of NF-κB-responsive genes in WT (n=9) and KO (n=11) bone marrow cells.

(C) Gene expression analysis of NF-κB-responsive genes in CD11b+ population purified with MACS beads (WT n=9 and KO n=6).

(D) Western blot analysis of the nuclear protein extracts from WT or KO spleen. Data are representative of three independent experiments.

Figure 5

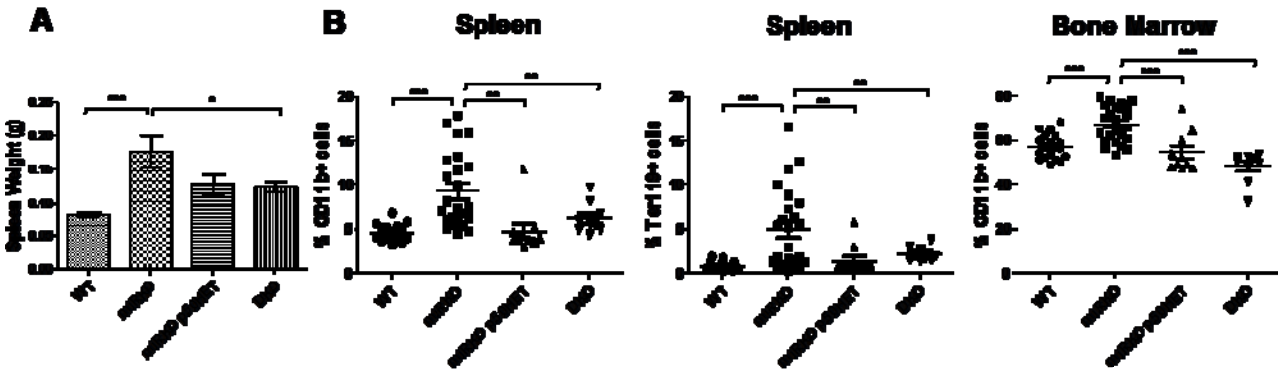

Figure 5. Reduction in the NF-κB level by deleting the p50 subunit of NF-κB effectively rescues the myeloproliferative phenotype in miR-146a-deficient mice. All mice were 6-7 month-old miR-146a+/+, p50+/+ (WT), miR-146a-/-, p50+/+ (miRKO), miR-146a-/-, p50+/- (miRKO p50HET), or miR-146a-/-, p50-/- (DKO) mice (n=17 for WT, n=24 miRKO, n=10 for miRKO p50HET, and n=9 for DKO. Data are shown as Mean +/- SEM from at least three independent experiments. Student t-test, * designates $p<0.05$, ** designates $p<0.01$, and *** designates $p<0.005$.)

(A) Spleen weight of WT, miRKO, miRKO p50HET, and DKO mice.

(B) Percentage of T cells (defined as CD3ε+), B cells (defined as CD19+, myeloid cells (defined as CD11b+), and erythroid cells (defined as Ter119+) in nucleated spleen and bone marrow cells from WT, miRKO, miRKO p50HET, and DKO mice by flow cytometric analysis.

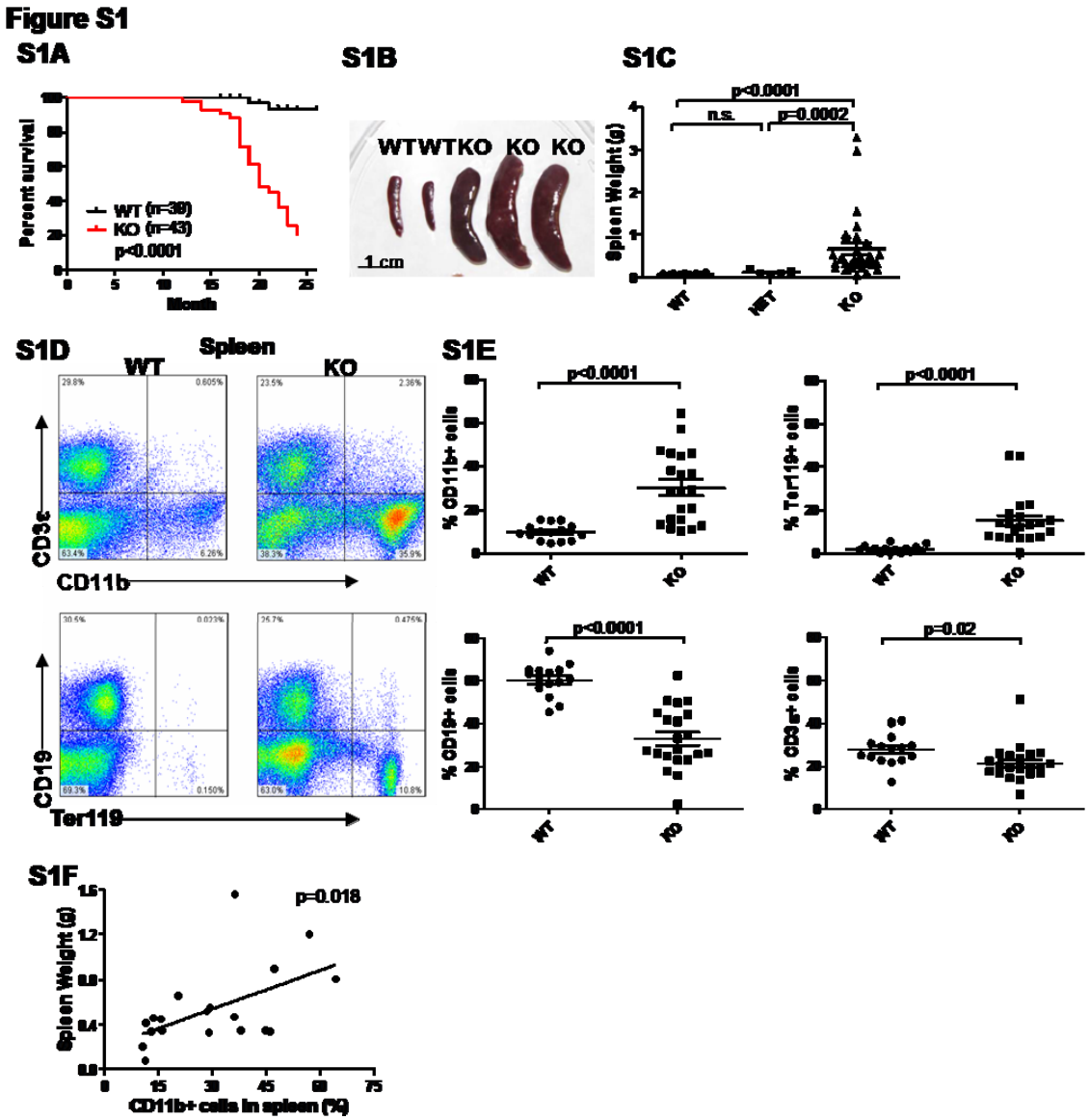

Figure S1. miR-146a-deficient mice develop myeloproliferation in spleens. Mice were 18-22 month-old miR-146a-/- mice (KO), miR-146a+/- mice (HET), and sex and age-matched C57BL/6 control mice (WT). Data are shown as Mean +/- SEM. Each individual dot represents one individual mouse. At least 3 independent experiments were performed.

(A) Kaplan-Meier survival curve of aging miR-146a KO and WT mice starting at 1 year of age (n=39 for WT and n=43 for KO).

(B) Photographs of spleens isolated from KO and WT mice.

(C) Weight of spleens isolated from KO, HET, and WT mice (n=26 for WT, n=5 for HET, and n=33 for KO).

(D) Flow cytometric analysis of nucleated splenocytes from one representative KO mouse and one representative WT mouse for T cells (defined as CD3ε+), B cells (defined as CD19+), myeloid cells (defined as CD11b+), and erythroid cells (defined as Ter119+).

(E) Percentage of T cells, B cells, myeloid cells, and erythroid cells, as defined above, in nucleated splenocytes in KO and WT mice by flow cytometry (n=15 for WT and n=21 for KO from at least three independent experiments).

(F) Correlation between spleen weight and percentage CD11b+ cells in spleen from 18-22 month-old miR-146a-deficient mice (n=19).

Figure S2

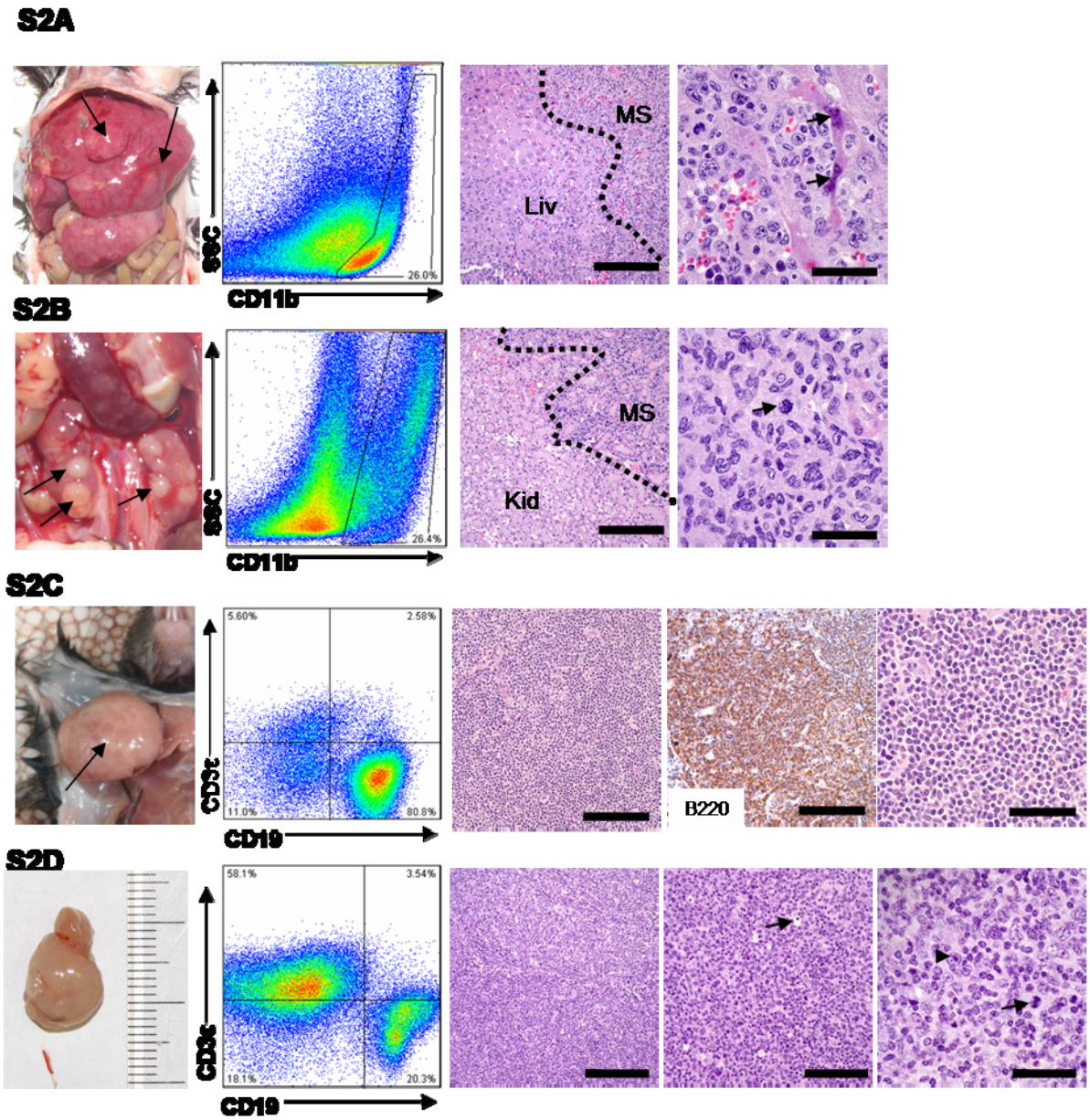

Figure S2. Additional examples of myeloid and lymphoid malignancies in miR-146a-deficient mice.

(A) Photograph, FACS plot, and histological analysis of a representative myeloid tumor infiltrating a KO liver. Panel 3 and 4, Hematoxylin and eosin (H&E) stained liver section. Liv, residual liver, MS, myeloid sarcoma infiltration. Scale bar on Panel 3, 200 microns and on Panel 4, 40 microns. Arrows, apoptotic hepatocytes at the edge of the infiltrate.

(B) Photograph, FACS plot, and histological analysis of a representative myeloid tumor infiltrating a KO kidney. Panel 3 and 4, Hematoxylin and eosin (H&E) stained kidney section. Kid, residual uninvolved kidney; MS, myeloid sarcoma infiltration. Scale bar on Panel 3, 200 microns and on Panel 4, 40 microns. Arrow, markedly atypical mitotic figure.

(C) Photograph, FACS plot, and histological analysis of a representative B-cell lymphoma from a KO cervical lymph node. Panel 3 and 5, Hematoxylin and eosin (H&E) stained spleen section; Panel 4: Positive immunohistochemical staining (IHC) for B220. Scale bars are 100 microns in Panel 3, 4 and 40 microns in Panel 5.

(D) Photograph, FACS plot, and histological analysis of a representative mixed T-and-B-cell lymphoma from a KO gastrointestinal tract. Panel 3, 4, and 5, Hematoxylin and eosin (H&E) stained tumor section. Scale bars are 200 microns, 100 microns, 40 microns from left to right. Arrow on Panel 4, apoptotic body ("starry sky appearance"), arrowhead on Panel 5, large immunoblastic cell (there are many more in this field); arrow on Panel 5, atypical mitotic figure.

Figure S3

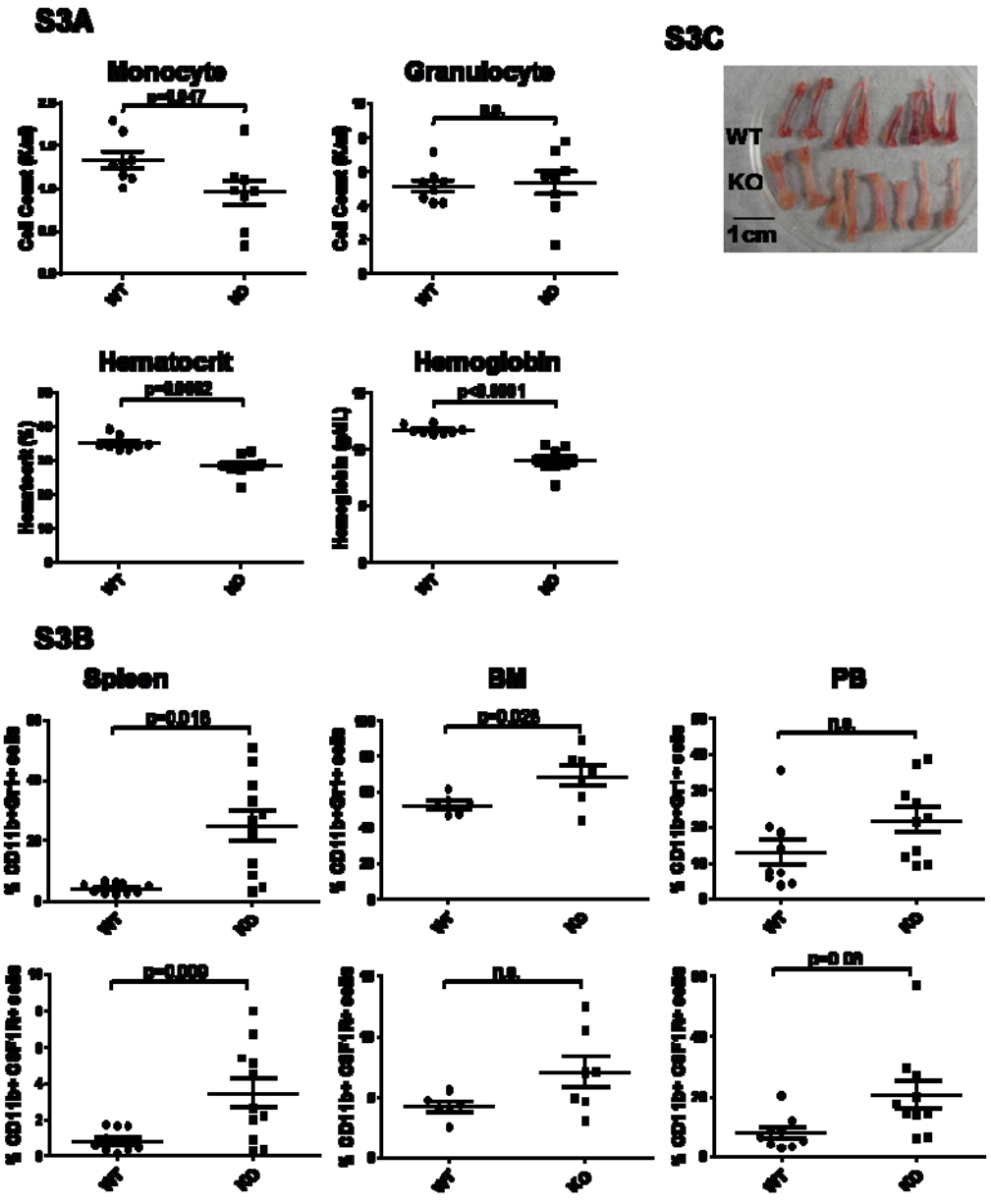

Figure S3. Cell count and flow cytometric analysis of peripheral blood, spleen, and bone marrow.

(A) Complete blood count (CBC) of peripheral blood from 18-22 month-old miR-146a-/- mice (KO, n=8) and sex and age-matched wild type control mice (WT, n=8). Data are shown as Mean +/- SEM. Each individual dot represents one individual mouse. n.s., not significant.
(B) Percentage of CD11b/Gr1 double positive cells and CD11b/CSF1R double positive cells in spleen, bone marrow (BM), and peripheral blood (PB) of 18-22 month-old miR-146a-/- mice (KO) and sex and age-matched wild type control mice (WT). Data are shown as Mean +/- SEM. Each individual dot represents one individual mouse. Total number of mice ranges from 6 to 11 from 3 independent experiments. n.s., not significant.
(C) Photograph of representative tibias and fibulas isolated from WT or KO mice.

Figure S4

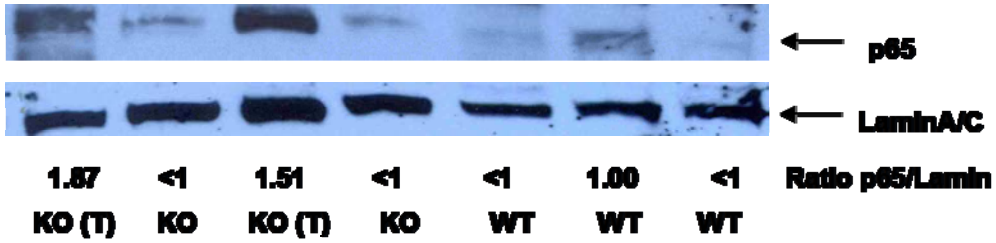

Figure S4. Western blot analysis of the nuclear protein extracts from spleens of 18-22 month-old miR-146a-/- mice (KO) and sex and age-matched wild type control. KO (T), KO spleen with myeloid sarcoma; KO, KO spleen without myeloid sarcoma.

Figure S5

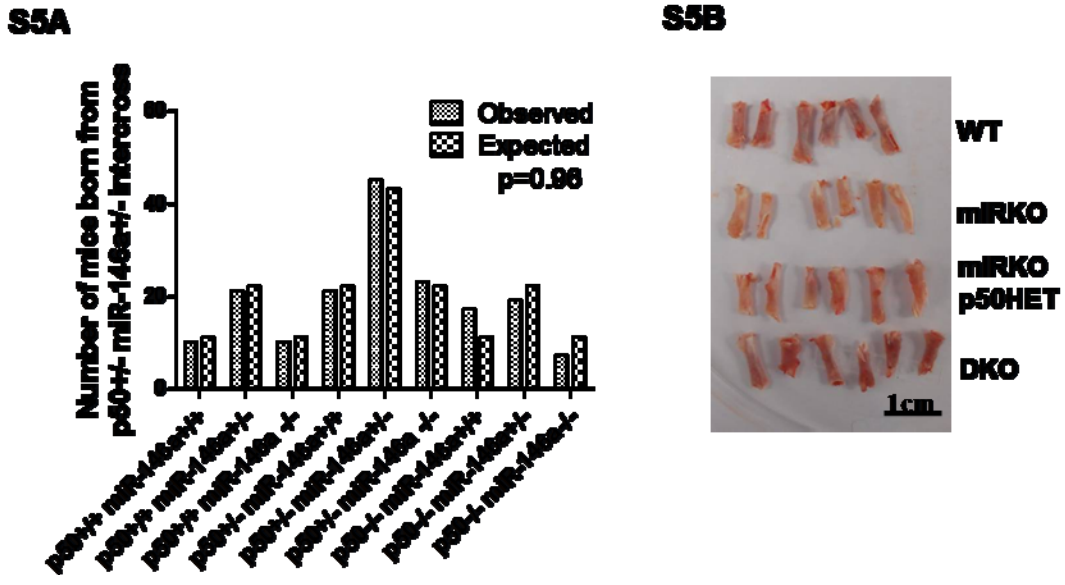

Figure S5.
(A) Number of offspring (n=173) produced from p50+/- miR-146a+/- double heterozygote intercross.
(B) Photograph of tibias from WT, miRKO, miRKO p50HET, and DKO mice.

DISCUSSION

These results and our previous paper [84] demonstrate that miR-146a plays an important role as a tumor suppressor miRNA in hematopoietic lineages because chronic miR-146a-deficiency in mice leads to myeloid sarcomas in spleens and lymphomas in various organs. miR-146a controls myeloproliferation in both the spleen and bone marrow compartments primarily through negatively regulating NF-κB. NF-κB is known to activate many genes involved in inflammation so that this study provides direct evidence correlating the chronic inflammation caused by activated NF-κB and the development of progressive myeloproliferative disease.

Consistent with the initial observation of miR-146a KO mice on the mixed C57BL/6x129/sv genetic background [84], miR-146a KO mice on the pure C57BL/6 background developed progressive myeloproliferation in their spleens, although the onset was delayed compared with the mixed background mice. miR-146a KO on the pure C57BL/6 background also developed significant myeloproliferative disease in the bone marrow, which was not observed in the mixed background strain. Moreover, miR-146a KO mice on the pure C57BL/6 background displayed less severe autoimmune-like disease but developed a higher incidence of tumor later on in life. All these indicate that the genetic background can significantly influence the phenotypic manifestation of deleting the miR-146a KO gene.

It is interesting that miR-146a-deficient mice showed no obvious abnormality early on when left unchallenged but gradually developed myeloproliferation in both spleen and bone marrow compartments starting at about 5-6 months of age. Eventually, more than 50% of the mice developed myeloid sarcomas and lymphomas at about 18-22 months of age. miR-146a normally down-regulates TRAF6 and IRAK1, and in the miR-146a-deficient mice, derepression of these important signal transducers may increase signaling to the NF-κB pathway. It should be noted that overexpression of

TRAF6 or IRAK1 in the 293 human embryonic kidney cell line is able to activate NF-κB [88-89], suggesting a possibility of cell-intrinsic activation of NF-κB when TRAF6 or IRAK1 is overexpressed at a high level. However, this is unlikely to be the case in miR-146a KO mice. We believe that the NF-κB activation in miR-146a KO mice likely involves external stimulation from other cells (autoimmune stimuli) or from environmental pathogens/commensal bacteria for TRAF6/IRAK1 to amplify the signal and that the mechanism of myeloproliferation and oncogenesis requires repeated episodes of activation of NF-κB due to external stimulation. In support of this notion, our previous paper reports an increased expression of both TRAF6 and IRAK1 at the protein level in bone marrow-derived macrophages (BMDM) from young miR-146a KO mice. But there was no difference in the serum levels of TNFα and IL-6 inflammatory cytokine between young WT and KO mice without LPS challenge [84]. In addition, constitutive NF-κB activity detected by conventional biochemical methods was only consistently noted in spleens with overt myeloid sarcoma (Figure S4). Based on this evidence, we suggest that the activation of the NF-κB may only become constitutive and significant when KO spleens transition from the pre-malignant myeloproliferative state to malignant myeloid tumor. Given the long latency and the partial penetrance of the tumor phenotype, there are likely secondary mutations cooperating in the oncogenesis, either complementing the NF-κB activity or amplifying it, resulting in malignant tumors. It will be interesting to identify secondary mutations driving this progression and malignant transformation.

NF-κB family transcription factors are homo-or heterodimers of 5 subunits, RelA (p65), Nfkb1 (p50), Nfkb2 (p52), RelB, and c-Rel. Among them, p65 and p50 are thought to play an important role in the induction of many of the inflammatory genes [90]. In addition, nfkb1$^{\Delta CT/\Delta CT}$ mice, with elevated p50 activity as a result of targeted deletion of the C-terminal ankyrin repeats, display phenotypes similar to those of miR-146a-/- mice, namely chronic inflammation with splenomegaly and enlarged

lymph nodes [91]. Moreover, deletion of p50 is able to partially rescue IkBα-deficienct mice, which display constitutive NF-κB activation, increased granulopoiesis, and neonatal lethality [92]. Given the importance of the p50 subunit to NF-κB-driven inflammation, we bred miR-146a-/- mice with p50-/- mice to investigate the role of NF-κB activation in the pathogenesis of myeloproliferation in miR-146a-deficient mice. We showed that p50-deficiency effectively rescued myeloproliferation in miR-146a-deficient mice. The rescue seen in miRKO p50HET mice was not consistent and complete, but merely a delay of symptoms, because by about one-year-old, mice in the mIRKO p50HET group started to show increased myeloid cells while the DKO mice continued to show consistent rescue of the myeloproliferative phenotype. The 50% increase in spleen weight and the marginal increase in CD11b+ and Ter119+ cells in the spleen of DKO mice, compared to WT (Figure 5B and 5C), suggest that the other pathways and factors other than p50 may also be involved. In addition, p50-deficiency may not rescue all the phenotypes in miR-146a KO mice, such as autoimmunity as a result of defective regulatory T-cells and/or activated effector T-cells, which has been shown to be due to a different pathway, the Signal Transducer and Activator of Transcription 1 (STAT1)/interferon pathway [43]. Autoimmune inflammation may contribute to the modestly increased spleen weight in the DKO mice.

Constitutive NF-κB activation is a well recognized phenomenon in lymphoid and plasma cell malignancies, but the status of NF-κB activation in myeloid malignancies is less well characterized. Some recent studies have demonstrated constitutive NF-κB activity in cells from high-risk MDS, some AML cases, and CML with blast crisis, suggesting that constitutive NF-κB activation may be associated with more advanced myeloid malignancies [81,93-94]. In many of these cases, the mechanisms for constitutive NF-κB activation remain to be established. It is likely that some of these myeloid malignancies with intrinsic NF-κB activity may have down-regulated miR-146a expression. Indeed,

reduced miR-146a has been found in MDS with chromosome 5q deletion and a subset of AML cases [37,61].

Based on this work and the work of others, it seems apparent that miR-146a is an important component of immune cell gene regulation and that its main function is to negatively regulate NF-κB. We demonstrate pathologic states as a consequence of miR-146a deficiency, corroborating work from other groups showing deregulation of this miRNA in human diseases. Further work is required to better understand the pathogenesis of miR-146a deficient diseases in humans and to develop methods to deliver miR-146a to immune cells in order to reduce NF-κB activation.

EXPERIMENTAL PROCEDURES

Mice

For a description of the miR-146a-/- generation and genotyping, see Supplemental Information and reference [84]. All experiments with miR-146a-/- and p50-/- [87] mice were approved by the institutional Animal Care and Use Committee (IACUC) of the California Institute of Technology.

Survival and Tumor Incidence Study

Survival and tumor incidence studies were done by following a cohort of about 40 miR-146a-/- and 40 littermate wild-type control mice for up to 24 months. Mice were carefully monitored for the development of diseases and were sacrificed when visibly ill. Tumor diagnosis was based on a combination of gross examination, histological analysis, immunohistochemistry, and flow cytometric analysis.

Quantitative RT-PCR

Total RNA was extracted with Trizol reagent (Invitrogen) from total nucleated splenocytes, bone marrow cells, CD11b+ enriched splenocytes after RBC lysis (Biolegend). CD11b+ enriched

splenocytes were purified by CD11b antibody-conjugated MACS beads (Miltenyi Biotec) according to manufacturer's instructions. Complementary DNA was synthesized using iScript cDNA synthesis kit (Bio-Rad) followed by SYBR Green-based quantitative PCR (Applied Biosystem) as previously described [15]. Rpl32 level was used as the normalization.

Western Blot Analysis

Nuclear protein lysates were extracted using nuclear extraction kit (Sigma) according to manufacturer's instruction. Antibodies against p65 (sc-8008 and sc-372), laminA/C (sc-20681), and HRP-conjugated secondary antibody (sc-2031 and sc-2004 all from Santa Cruz Biotechnology) were used for detection.

Flow Cytometry

Cells were harvested, homogenized, and RBC lysed with RBC lysis buffer (Biolegend). Fluorophore-conjugated antibodies against CD3ε, CD11b, CD19, Ter119, Gr1 (all from Biolegend) and CSF1R (Ebioscience) were used for staining. Cells were analyzed on a FACSCalibur (BD Bioscience) machine and data analysis was performed with FloJo software (Tree Star).

Tumor Transplantation Experiments

Tumor was grossly dissected out from miR-146a-/- mice. 1 X 10^6 splenic tumor cells or equal number of wild-type splenocytes were injected into 8-12 week-old Rag2-/-γC-/- recipients via retro-orbital vein. For experiments with retro-viral transduction, MIG-Luc (MSCV-IRES-GFP vector expressing firefly luciferase) retroviruses were prepared and used to infect murine cells as previously described [95]. Flow cytometry was used to quantify the percentage of infected cells (GFP+) prior to injection and bioluminescence imaging (Xenogen) was used to monitor *in vivo* cell growth in Rag2-/-γC-/- recipients weekly for up to 2 months. Bioluminescence intensity was quantified with Living Image® 2.50.1 (Xenogen).

CHAPTER TWO

MicroRNA-146a is a Critical Guardian of the Quality and Longevity of Hematopoietic Stem Cells

INTRODUCTION

Hematopoietic stem cells (HSCs) have the ability to self-renew and replenish the entire hematopoieic repertoire during the lifetime of an organism. Balanced self-renewal versus differentiation of HSCs is intricately regulated to ensure the long-term maintenance of HSCs and the hematopoietic system [96]. Under stressed conditions, such as inflammation and infection, the balance is shifted in favor of hematpoietic stem and progenitor cell (HSPC) proliferation and differentiation to produce more mature immune cells [97]. Following the discovery that HSCs express TLRs and may sense and respond to infection and inflammatory signals directly [98], there has been an increasingly appreciation of the role of pro-inflammatory cytokines and infection in the modulation of HSC activity. Numerous recent studies have shown that TLR activation or interferon stimulation leads to proliferation, skewed myeloid differentiation and impaired engraftment and self-renewal of HSCs [99-101]. Since its discovery over 25 years ago, NF-κB has been shown to be active in a wide variety of innate and adaptive immune cells as well as non-hematopoietic cells and to function as an essential player in orchestrating inflammation and immune cell functions [66]. However, the function of NF-κB in HSCs remains relatively unexplored. Under stress-free conditions, NF-κB is not essential for HSC function, because mice genetically deleted for NF-κB subunits, such as NF-κB1 (known as p50) and c-Rel, have no apparent developmental abnormality in the hematopoietic system. Mice engrafted with $p50^{-/-}$ or $c\text{-}Rel^{-/-}$ HSCs or $RelA^{-/-}$ fetal HSCs also develop relatively normal immune system under stress-free conditions [102]. On the other hand, mice with activated NF-κB signaling, as a consequence of deleting IκBα, A20 (as

known as TNFAIP3), or the inhibitory domain of NF-κB1 (p50) or NF-κB2 (p52), display severe inflammation, early lethality, and complex phenotypes, making studies of HSCs difficult to perform and interpret [86,103]. In recent years, microRNAs (miRNAs) have emerged as a class of small non-coding RNAs involved in the regulation of NF-κB [36]. Among them, miR-146a has been shown to be a particularly important negative regulator of NF-κB by targeting two upstream signal transducers, TRAF6 and IRAK1. Mice with targeted miR-146a deletion represent one of the first genetic mouse models with NF-κB-driven chronic and low-grade inflammation that develops spontaneously with aging and can be accelerated by repeated stimulation, allowing investigation of the the long-term effects of chronic inflammation and NF-κB activation on HSCs and oncogenic processes [19,44]. Given this background, we have used miR-146a-deficient mice to examine the function of NF-κB and miR-146a in HSCs during chronic inflammation and to directly test a long-standing hypothesis that chronic inflammation promotes excessive HSC proliferation and differentiation and can lead to eventual HSC exhaustion and pathological myelopoiesis. Here we demonstrate that this single miRNA, miR-146a, functions as a critical regulator of HSC homeostasis during chronic inflammatory stress in mice. In the absence of miR-146a, HSC homeostasis is disrupted under physiological stresses such as aging and periodic bacterial encounters, as indicated by declines of HSC number and quality and accelerated HSC proliferation and differentiation. Chronically, these nominal stressors can lead to severe pathologies, such as HSC exhaustion, bone marrow failure and development of myeloproliferative disease, produced by chronic NF-κB hyperactivation and IL-6 overproduction. This study speaks to a molecular pathway involving miR-146a/TRAF6/NF-κB/IL-6 that links chronic inflammatory stresses to the functional decline and depletion of HSCs and the development of myeloproliferative diseases.

RESULTS

MiR-146a regulates HSC numbers during chronic inflammatory stress

To examine the role of miR-146a we first assessed the pattern of expression of it and its related family member, miR-146b, during hematopoietic differentiation. We purified by FACS various types of hematopoietic stem and progenitor cell (HSPC) populations from young wild type (WT) mice. We found that miR-146a and miR-146b were expressed at variable levels throughout hematopoietic development. The expression of miR-146a increased by 2-fold as long-term HSCs (defined as Lineage$^-$ Sca1$^+$cKit$^+$ CD150$^+$CD48$^-$) differentiated into a mixed pool of short-term HSCs and multpotent progenitor cells (MPPs) (defined by Lineage$^-$Sca1$^+$cKit$^+$, referred to as LSK cells). The lowest expression of miR-146a was detected in myeloid progenitor cells (defined by Lineage$^-$Sca1$^-$cKit$^+$, referred to as L$^-$S$^-$K$^+$ cells) (Fig. 1A). In comparison, miR-146b expression was more uniform throughout hematopoietic development (Fig. 1A). This expression pattern suggests that miR-146a and miR-146b could be functional in cells as primitive as the long-term HSCs and throughout hematopoietic development.

To characterize the physiological function of miR-146a in HSCs, we examined the consequences of miR-146a deficiency on various hematopoietic cells using mice with a targeted deletion of the *miR-146a* gene [19,44]. We found identical numbers of phenotypically defined subsets and equal colony-forming ability *in vitro* in WT and miR-146a$^{-/-}$ (miR-146a KO) 6-week-old mice (Fig. S1A-C). These data indicate that deleting miR-146a has no detectable effect on hematopoiesis early on in life in a standard pathogen-free environment.

We have previously shown that miR-146a KO mice develop spontaneous inflammation as they age [19,44]. To characterize the role of miR-146a in HSCs during chronic low level inflammation, we allowed age-and-sex-matched WT and miR-146a KO mice to age over a year. By 4 months, miR-146a

KO mice developed a mildly hypercellular bone marrow indicated by an increase in total bone marrow $CD45^+$ cells, LSK cells and long-term HSCs, with unaltered percentages of $CD19^+$, $CD11b^+$ and $CD3\varepsilon^+$ cells (Fig. S1D). However, the increase in bone marrow HSPCs and mature cells was not sustained. By 8 months of age, miR-146a KO mice showed a significant decrease in the number of total bone marrow cells and phenotypically defined HSPCs, including LSK cells and $CD150^+CD48^-$ or $EPCR^+$ long-term HSCs (Fig 1B, C). The depletion became progressively more severe by 12 months of age when the majority of miR-146a KO mice showed only a residual number of $CD45^+$ bone marrow cells and nearly complete exhaustion of HSCs (Fig 1D). To understand the cellular process leading to a transient hypercellular marrow and eventual HSC exhaustion, we analyzed bone marrow and spleen of aging miR-146a KO mice. Accelerated hematopoietic differentiation from long-term HSCs to LSK cells and mature myeloid cells was evident in 8-month-old mice, as shown by an increased percent of LSK cells within the total bone marrow but a significantly decreased fraction of long-term HSCs among the LSK cells, (Fig 1E). By this age, miR-146a KO mice have already developed a prominent myeloproliferative phenotype in the spleen [44]. In addition, miR-146a KO mice also showed a significant increase in the number of LSK cells and long-term HSCs in their spleens, suggesting either HSPC mobilization from bone marrow to spleen or *de novo* splenic HSPC proliferation in response to bone marrow failure (Fig. 1F). Thus, although miR-146a KO mice contain normal levels of HSPCs when they are young, as they age, they go through a hypercellular stage and then eventually start to lose bone marrow HSCs and differentiated cells, leading to HSC exhaustion and bone marrow failure. This is likely due to accelerated HSC differentiation into progenitor and mature cells, especially of the myeloid lineage. It is accompanied by an increased appearance of HSCs in the spleen, probably as a form of homeostatic compensation.

Importantly, we found that chronic inflammatory stimulation with bacterial components in young miR-146a KO mice was sufficient to accelerate the development of the same hematopoietic defects seen during aging of these mice. We stimulated 8-week-old WT and miR-146a KO mice with LPS repeatedly for a month and observed an accelerated differentiation of long-term HSCs towards LSK cells and myeloid cells in miR-146a KO mice, compared to WT mice, a phenotype similar to the one that spontaneously occurs during aging of the KO mice (Fig 1G-I and S1E). Thus, miR-146a is needed to maintain HSC homeostasis in response to chronic inflammation. This suggests that the stress of chronic inflammation may be the physiologically relevant stimulator of HSC deficiency and myeloproliferative disease in the miR-146a KO mice. Perhaps this becomes evident in aging miR-146a KO mice not subjected to experimental inflammatory stimulation because of a low level continual exposure to bacterial materials even in our relatively clean conditions of animal husbandry. Whether true pathogens or commensals might be the inducing agents will require further investigation.

MiR-146a-defciency results in progressive decline in the quality of HSCs

In addition to the progressive loss of phenotypically defined HSCs in aging miR-146a KO bone marrow, we found that the functional quality of HSCs deteriorates in mice lacking miR-146a. To assess HSC function, we compared WT and miR-146a KO bone marrow HSCs in their ability to generate the entire hematopoietic repertoire competitively *in vivo*. Total bone marrow cells from either 6-week-old WT or miR-146a KO mice, both which were $CD45.2^+$, were transplanted along with an equal number of $CD45.1^+$ WT bone marrow cells, into lethally irradiated $CD45.1^+$ WT recipient mice (Fig 2A). Six months after transplant, $CD45.2^+$ and $CD45.1^+$ cells in both the CD45.2 WT/CD45.1 WT and CD45.2 KO/CD45.1 WT mice contributed identical proportions of cells in nearly all mature hematopoietic lineages and HSPCs (Fig 2B). Furthermore, when we purified long-term HSCs (defined

by LSK $CD150^{+}CD48^{-}$) from WT or miR-146a KO bone marrow for competitive repopulation assay, we again observed a similar contribution of WT or miR-146a KO HSCs to total white blood cells and HSPCs 6-month post transplantation (Fig S2A). However, when we extended the experiment past 10 months, we began to observe a decreased contribution of miR-146a KO cells to long-term HSCs and LSK cells, but no reduction in $CD45^{+}$ cells, in the bone marrow of CD45.2 KO/CD45.1 WT mice (Fig 2C-E). These data indicate that miR-146a-deficient long-term HSCs from young mice have an intrinsic functional defect, when competed against WT cells, for the generation of the hematopoietic repertoire in the WT environment; however, the intrinsic defect of miR-146a KO HSCs takes 10 months to become apparent in this transplant setting.

To investigate how age affects the quality of miR-146a KO HSCs, we used 4-month-old, instead of 6-week-old, miR-146a KO and WT mice for competitive repopulation assay. At 4 months of age, miR-146a KO mice display a modestly hypercellular bone marrow and mildly increased phenotypically defined HSCs, but no disease phenotype (Fig S1D). Surprisingly, miR-146a KO cells were out-competed by their WT counterparts as early as the first month after the transplant, and there was a steady decline in their percentage over a period of 6 months (Fig 2G, H). Six months after transplant, neither group of mice showed signs of pathology and they had identical levels of total mature hematopoietic cells and HSPCs (Fig S2B-E). However, when comparing the contribution of $CD45.1^{+}$ cells versus $CD45.2^{+}$ cells to the total pool, we observed a significant disadvantage of miR-146a KO HSPCs and mature lineages (Fig 2I). Similar to the progressive decline of HSC number, the functional quality of HSCs became more and more compromised as miR-146a KO mice aged. When the competitive repopulation experiment was carried out with 6-month-old WT and miR-146a KO bone marrow cells, at which time increased myeloid and LSK cells and decreased long-term HSCs were already evident (Fig S2F), we observed that miR-146a KO cells were completely overwhelmed by

their WT counterparts in the recipient mice, with ratios of about one miR-146a KO cell to ten WT cells for nearly all mature lineages and HSPCs (Fig S2G). The defective repopulating ability observed in all mature and HSPC lineages, including the long-term HSCs, in all three major hematopoietic compartments strongly suggests that the defect must originate in the most primitive HSCs. These data indicate that miR-146a-deficiency has a detrimental effect on the quality of HSCs under chronic inflammatory stress. The functional decline of HSCs in the competitive repopulation setting is evident in healthy 8-week-old miR-146a KO mice and becomes significant in 4-month-old mice in the absence of any observable pathology, indicating the physiological importance of miR-146a as a guardian of HSC quality and longevity.

Hematopoetic-intrinsic and -extrinsic contributions to HSC defects and pathological hematopoiesis

To directly examine both hematopoietic-intrinsic defects and extrinsic factors on hematopoiesis in the absence of miR-146a, we performed reciprocal bone marrow transplants, transferring WT bone marrow cells into miR-146a KO recipient mice (WT to KO) and KO bone marrow cells into WT recipient mice (KO to WT). WT to WT transplant and KO to KO transplant mice were included as controls. After 5 months, we harvested all groups for analysis. Interestingly, mice of the WT to WT and WT to KO groups had identical levels of HSPCs in their bone marrows and spleens, suggesting that the miR-146a-deficient environment is not sufficient to induce significant HSC abnormalities in WT cells during this time (Fig 3A-G). In comparison, mice in the KO to WT and KO to KO groups both showed 2-3 fold reductions in bone marrow HSCs and myeloid progenitor cells, but not in LSK cells (Fig 3A-C), and about a 10-fold increase in spleen HSPCs (Fig 3D-G). As in the miR-146a germline KO mice, an increased percentage of LSK cells and a decreased representation of long-term

HSCs within the LSK fraction was also observed in these transplantation groups, indicating an accelerated process of HSC differentiation (Fig 3H-J). In addition to the HSPC abnormality, mice of the KO to WT and KO to KO groups also developed pathological features recapitulating those seen in aged miR-146a germline KO mice [19,44]. By 5 months post-transplant, 2 out of 8 mice in the KO to KO transplant group had succumbed to tumor pathology, including one case of $CD4^+$ T-cell lymphoma in the thymus and one case of kidney tumor, with no tumors observed in any of the other groups (Fig S3A, B). Necropsy also showed splenomegaly and pale bone marrows in the KO to WT and the KO to KO groups (Fig S3C, D). Myeloproliferation was a prominent feature in mice of the KO to WT and the KO to KO groups, which showed an increase of spleen weight, number of white blood cells, B cells, T cells, and, most dramatically, in the number of $CD11b^+$ or $Gr1^+$ myeloid cells in their spleens, compared to the WT to WT and the WT to KO groups (Fig S3E-L). Increased myeloproliferation/myelopoiesis was also observed in the bone marrow and peripheral blood (Fig S3M, N). Moreover, in line with HSC exhaustion and bone marrow failure, mice of the KO to WT and KO to KO groups exhibited hypocellular bone marrow and peripheral cytopenia (Fig S3O-U).

Overall, these data indicate that it is the miR-146a deficiency in hematopoietic cells that plays the dominant role in determining the phenotype of the miR-146a knockout mouse, because transferring miR-146a-deficient bone marrow cells into WT environment, but not the reciprocal transfer, is sufficient to yield a majority of the phenotypes seen in mice with miR-146a deleted in both hematopoietic and non-hematopoietic cells. However, the miR-146a-deficient environment has a contributory role to the overall enhanced myelopoiesis because WT bone marrow cells in the KO environment gave rise to a mild but significant increase in the number of $CD45^+$ and $CD11b^+$ marrow cells and the percentage of $CD11b^+$ and $Gr1^+$ cells in their spleens, compared to the WT to WT mice (Fig S3K, L, O, P). More indicative is that when WT bone marrow cells that were transiently

transplanted into miR-146a KO environment for 2 months were competed against WT control bone marrow cells (Fig 3K), they showed a modest advantage in generating myeloid and lymphoid lineages in their spleens, peripheral blood and to a lesser extent bone marrows, while bone marrow HSPCs remained unaffected (Fig 3L-O). Overall, these data suggest that it is a hematopoietic-intrinsic deficiency of miR-146a that plays the dominant role in driving the HSC defects and pathologic myeloproliferation, while the miR-146a deficient environment contributes to the overall phenotype by promoting hematopoietic differentiation. In the absence of the driving force from the miR-146a deficient environment, lethal tumor pathology and HSC functional decline are attenuated or delayed.

Lymphocytes contribute to the progressive loss of HSCs and myeloproliferative disease

Although hematopoietic-intrinsic factors play the predominant role in the dysregulated hematopoiesis of miR-146a deficient mice, this does not tell us which cell type(s) in the hematopoietic compartment might influence aspects of hematopoiesis either through direct interaction or secretion of soluble factors. Because miR-146a-deficient lymphocytes display a hyper-activated phenotype with dysregulated cytokine production [20], we first determined whether dysregulation of miR-146a-deficient lymphocytes might contribute to HSC depletion in miR-146a KO mice. To this end, we crossed mice with a targeted deletion of the *Rag1* gene, which is required for lymphocyte maturation, with miR-146a KO mice to generate miR-146a$^{-/-}$Rag1$^{-/-}$ double knockout mice (miR/Rag1 DKO). When WT, miR-146a$^{-/-}$ (miR KO), Rag1$^{-/-}$ (Rag1 KO), and miR/Rag DKO mice were allowed to age for 10 months, the miR KO mice showed significant depletion of HSPCs (Fig 4A-D), a finding consistent with what we have observed previously in an independent examination of WT and miR-146a KO mice (Fig 1). Specifically, long-term HSCs and LSK cells in the miR KO marrow were reduced to only 3% and 15% of the respective WT levels. In comparison, depletion of HSPCs in miR/Rag1 DKO bone

marrow was significantly attenuated. LSK and myeloid progenitor cells in miR/Rag1 DKO bone marrow were at levels comparable to those of WT and Rag1 KO mice and long-term HSCs were about half of normal (Fig 4A-D). These data indicate that miR-146a-deficient lymphocytes contribute substantially to the overall HSPC exhaustion. In addition, miR-146a-deficient lymphocytes were shown to be a major driver of the development of bone marrow failure and myeloproliferative disease, because miR/Rag1 DKO mice showed normal bone marrow cellularity and an attenuated splenomegaly and myeloproliferative phenotype (Fig 4E-L). However, the rescue was not complete because miR/Rag1 DKO mice still had mildly enlarged spleens and a 2-3 fold increase in the number of total white blood cells and myeloid cells compared to Rag1 KO mice, indicating that miR-146a deficiency in myeloid lineages has an intrinsic effect on the development of myeloproliferation (Fig 4M). It is worth noting that this effect may either be in cis or trans: it could be the proliferating cells responding to a changed intracellular milieu or to factors secreted by myeloid cells acting in an autocrine or paracrine manner.

NF-κB regulates HSC homeostasis under chronic inflammatory stress

To understand the molecular mechanism responsible for the stress-induced hematopoiesis, we focused on the main pathway known to be regulated by miR-146a, the NF-κB pathway. We have previously shown that aging miR-146a KO mice display hyper-activated NF-κB activity that is responsible for the development of myeloid malignancy [44]. To study whether NF-κB may also regulate HSC homeostasis under inflammatory stress, we utilized a transgenic NF-κB-GFP reporter mouse to monitor NF-κB activity quantitatively and efficiently in various cell types by measuring GFP fluorescence [104-105]. We first tested whether NF-κB can be activated in LSK cells and HSCs in 2-month-old WT NF-κB-GFP (WT-GFP) reporter mouse under steady state and after LPS stimulation. We found that about 6-7% of

WT LSK cells and HSCs had basally activated NF-κB activity, as measured by GFP expression. Six hours after LPS challenge *in vivo*, the percentage of LSK cells and HSCs with activated NF-κB increased to more than 25% (Fig S4A). Interestingly, 8-month-old WT-GFP mice also showed an increased percentage of LSK cells and HSCs with basal NF-κB activation, compared to 2-month-old mice (Fig S4A). These data suggest that both LSK cells and HSCs have functional NF-κB-mediated transcription that can be augmented by LPS stimulation and aging. To analyze whether hyper-activated NF-κB activity is a feature in miR-146a KO HSPCs, we bred NF-κB-GFP reporter mice with miR-146a$^{-/-}$ mice to generate NF-κB-GFP^{+} miR-146a$^{+/+}$ (WT-GFP), NF-κB-GFP^{+} miR-146a$^{+/-}$ (miRHET-GFP), and NF-κB-GFP^{+} miR-146a$^{-/-}$ (miRKO-GFP) mice. Unperturbed 8-week-old mice of WT-GFP, miRHET-GFP, and miRKO-GFP genotypes showed identical levels of basal NF-κB activity (Fig S4B-D). After repeated LPS stimulation, miRKO-GFP mice, in comparison to WT-GFP and miRHET-GFP mice, showed increased percentages of GFP^{+} cells in various HSPCs (Fig 5A-C) and mature cells in their bone marrows, spleens and peripheral blood (Fig S5A-C), demonstrating that chronic inflammatory stimulation with bacterial components leads to hyperactivated NF-κB activity in young miR-146a-deficient mice.

To further investigate whether the increased NF-κB activity is responsible for driving HSC depletion in bone marrow, we deleted a main subunit of NF-κB, p50, to determine whether reduced NF-κB activity in miR-146a$^{-/-}$p50$^{-/-}$ (miR/p50 DKO) mice might rescue the HSC exhaustion. By 8-9 months of age, miR/p50 DKO mice still exhibited levels of white blood cells and long-term HSCs comparable to that of WT mice, indicating a rescue of the HSC defects (Fig 5D, E). We have previously shown that p50 deletion rescues the myeloproliferative disease in 6-month-old miR-146a KO mice [44]. To determine whether myeloid cancer can also be reversed in miR/p50 DKO mice, we aged a cohort of WT, miR KO, p50 KO and miR/p50 DKO mice to about one-and-half years, by

which time about 50% of miR-146a KO mice will have developed myeloid cancer. Interestingly, miR/p50 DKO mice still showed reduced spleen weight and prolonged survival (Fig S5D, E). The incidence of tumors was also significantly reduced in miR/p50 DKO mice, compared to miRKO mice (Fig S5F). However, there were two cases of splenic myeloid tumors from a total of 46 miR/p50 DKO mice analyzed. Histological analysis of spleens revealed that the majority of miR/p50 DKO spleens, in contrast to the miR KO spleens with frequent myeloid sarcoma, showed preserved lymphoid follicular structures (Fig S5G). Transplantation of miR/p50 DKO spleen cells into $Rag2^{-/-}\gamma C^{-/-}$ mice did not result in splenomegaly or myeloid pathology, although transplanting miRKO splenic tumor cells did (Fig S5H and [44]. Together, these data show that p50-deficiency significantly ameliorates the myeloproliferative and myeloid cancer phenotype in aging miR-146a$^{-/-}$ mice. These findings highlight the importance of the NF-κB pathway, particularly the p50 subunit, as the primary mediator of miR-146a-deficiency-driven myeloproliferation and myeloid tumorigenesis. However, the modest but significant increase in spleen weight and the occasional occurrence of myeloid tumors in aging miR/p50 DKO mice suggest that other NF-κB subunits or other pathways regulated by miR-146a may also be able to mediate the disease phenotype. Overall, we have shown that chronic inflammation-induced or aging-associated NF-κB activation is responsible for driving HSC exhaustion, myeloproliferative disease and myeloid cancer.

To explore whether the increased proliferation and cycling of miR-146a-deficient HSCs is an underlying cause of accelerated HSC depletion under chronic inflammation, we measured BrdU incorporation and Ki-67 expression in HSCs after LPS stimulation. Surprisingly, examining 2-month-old WT and miR-146a KO mice, we did not observe a significant difference in the percentage of $BrdU^+$ bone marrow LSK cells and HSCs whether the mice were unperturbed or studied 12 hours after a single LPS injection (Fig S5I). However, after repeated LPS stimulation for 3 days, there were

significantly higher percentages of $BrdU^+$ and $Ki\text{-}67^+$ miR-146a KO LSK cells and HSCs, compared to the WT cells, indicating an increased proliferation (Fig 5F, G). Consistent with increased HSC cycling and myeloid differentiation, miR-146a KO mice started to show a small but statistically significant increase in $CD11b^+$ myeloid cells in their spleens and bone marrows after 3 days of LPS stimulation (Fig 5J). It is also interesting to note that identically gated LSK cells and HSCs in spleen seemed to be less quiescent than their bone marrow counterparts, as indicated by a higher level of Ki-67 expression after LPS stimulation, suggesting that the bone marrow milieu may be a better environment for maintaining HSC quiescence during inflammation (Fig 5H). These data show that chronic inflammation induces increased HSC proliferation and cycling in miR-146a KO mice and underscores the particular importance of miR-146a in modulating HSC activity during chronic inflammation, as opposed to in an acute setting. Taken together, these data demonstrate that NF-κB regulates HSC activity by promoting HSC proliferation and myeloid differentiation during inflammation; in the absence of miR-146a, chronic dysregulated NF-κB activity leads to pathological HSC exhaustion, bone marrow failure and myeloid malignancies.

Pro-inflammatory cytokine IL-6 is a culprit NF-κB-responsive gene mediating HSC depletion and myeloproliferation

Pro-inflammatory cytokines, such as IL-6 and TNFα, both of which are highly upregulated upon NF-κB activation, can be potent oncogenic factors, especially in epithelial cancers [106]. More importantly, over-expression of IL-6 in bone marrow cells in mice results in myeloproliferative or lymphoproliferative disease [107-108]. Because we have shown the importance of NF-κB signaling in regulating HSC activity and in promoting HSC depletion and myeloproliferation in miR-146a-deficient mice, we wanted to determine whether this involves many NF-κB-activated genes acting

together or if there are key culprit genes. Because of the overwhelmingly large list of NF-κB-responsive genes, we focused on the pro-inflammatory cytokines that were overproduced in miR-146a$^{-/-}$ mice, believing that miR-146a-deficient mice likely suffer from a chronic inflammation-driven process.

IL-6 and TNFα are both upregulated in aging mR-146a $^{-/-}$ mice [19,44]. However, upregulation of TNFα was only prominent in miR-146a$^{-/-}$ spleens that have developed myeloid sarcomas, but not in ones without overt tumors, suggesting that TNFα upregulation may be a quite late event in oncogenesis. To evaluate the temporal relationship between the increase in inflammatory cytokines and the onset of HSC exhaustion and myeloproliferation, we examined younger, 6-10 month-old, mice. At this time, the HSC depletion and myeloproliferative phenotype start to become prominent but no overt splenic tumors have developed. Similar to what was observed in 18-month-old mice, IL-6 expression was upregulated in both spleen and bone marrow cells of miR KO mice, compared to WT mice. Importantly, miR/p50 DKO mice showed a level of IL-6 comparable to that of WT mice (Fig. 6A, B). However, the same trend was not observed for TNFα expression at this age (Fig. S6A). Furthermore, when bone-marrow-derived macrophages (BMMs) from 8-week-old mice were stimulated with LPS *in vitro*, IL-6, but not TNFα, showed consistently increased induction in miR KO BMMs compared to WT BMMs. Interestingly, the exaggerated IL-6 induction in miRKO BMMs was significantly more prominent with re-stimulation at a time when WT BMMs showed resistance to endotoxin re-stimulation (Fig. 6C) [109]. This again suggests that miR-146a may be particularly important during chronic and repeated inflammatory challenge. In addition, induction of IL-6, but not TNFα, in BMMs was highly dependent on p50. In p50$^{-/-}$ BMMs, IL-6 induction was almost completely abolished (Fig. 6C and S6B). These data suggest that IL-6 upregulation is an early feature in miR-

146a-deficiency-driven HSC depletion and myeloproliferation and reduction in the IL-6 level may be an important factor underlying the reduced pathology when p50 is deleted.

Because we have also shown that miR-146a-deficient lymphocytes are involved in the development of the HSC defect and myeloproliferation (Fig 4), we asked whether overproduction of IL-6 by miR-146a-deficient lymphocytes represents one potential contributing mechanism. When we stimulated splenocytes from WT or miR-146a KO mice *in vitro* with either LPS to activate both T and B cells or a combination of anti-CD3 and anti-CD28 to activate T cells specifically, we observed increased production of IL-6 by miR-146a KO splenocytes in both conditions (Fig 6D, E). Moreover, when we stimulated WT, miR KO, Rag1 KO and miR/Rag1 DKO mice with LPS *in vivo*, we found an exaggerated IL-6 production in the serum of miR KO mice, compared to that of WT mice. In comparison, the serum IL-6 level in miR/Rag1 DKO mice was only modestly increased in a non-statistically significant manner, compared to that of Rag1 KO mice (Fig 6F). However, miR/Rag1 DKO mice had a higher serum level of IL-6 than WT mice after LPS challenge. Because miR/Rag1 DKO mice show an attenuated HSC depletion and myeloproliferation, these data suggest that IL-6 is only one of the contributing factors and overproduction of IL-6 alone is not sufficient to induce the full range of pathologies in miR/Rag1 DKO mice.

Despite IL-6 overproduction not being sufficient to reproduce the full-blown phenotype of HSC depletion and myeloproliferative disease, we examined if exaggerated IL-6 production is a required element. To study this, we bred miR-146a$^{-/-}$ mice with mice knocked out for the *Il-6* gene. MiR-146a$^{-/-}$ IL-6$^{-/-}$ (miR/IL6 DKO) mice were born at the expected Mendelian frequency and appeared normal. Unperturbed, young wildtype (WT), miR-146a$^{-/-}$ (miR KO), IL-6$^{-/-}$ (IL6 KO) and miR-146a$^{-/-}$ IL-6$^{-/-}$ (miR/IL6 DKO) mice showed similar levels of CD11b^{+} and Gr1^{+} myeloid cells in peripheral blood, while B cells were slightly reduced in miR/IL6 DKO mice (Fig S6C). When LPS was

repeatedly administered in young WT, miR KO and miR/IL6 DKO mice, an accelerated myeloproliferative phenotype was observed in miR KO mice that was largely absent in miR/IL6 DKO mice. Specifically, the significantly increased spleen weight, total white blood cells, myeloid cells, and erythroid precursor cells present in miR KO were all reduced in miR/IL6 DKO mice to levels comparable to those of WT mice (Fig. 6G). The same trend was also observed in the peripheral blood (Fig. S6D). In the bone marrow, repeated LPS stimulation of WT and miR/IL6 DKO mice induced variable hypocellularity. However, the depletion was more severe and consistent in miR KO bone marrow (Fig. S6E). Furthermore, when WT, miR KO, IL6 KO and miR/IL6 DKO mice were allowed to age to 6-7 months of age, splenomegaly and myeloproliferation observed in miR KO mice were also significantly reduced in miR/IL6 DKO mice (Fig 6H and S6F). More interestingly, the accelerated differentiation of bone marrow HSCs into LSK cells and myeloid cells and expansion of splenic HSPCs seen in miR KO mice were also partially normalized in miR/IL-6 DKO mice (Fig 6I, J). These data show that in the absence of IL-6, miR-146a$^{-/-}$ mice display a partially reduced HSC defect and less myeloproliferative disease, indicating that upregulation of the NF-κB-responsive pro-inflammatory cytokine IL-6 is an important, yet by itself insufficient, driver of the accelerated HSC differentiation and myeloproliferative disease in miR-146a$^{-/-}$ mice under chronic inflammatory stress induced by aging or repeated bacterial stimulation.

Upregulation of the miR-146a target, TRAF6, results in bone marrow failure

Two of the best-validated miR-146a targets, TRAF6 and IRAK1, are signal transduction proteins upstream of NF-κB activation. To determine whether increased expression of TRAF6 and/or IRAK1 is responsible for the observed HSC exhaustion in the absence of miR-146a, we first measured whether their expression was de-repressed in miR-146a-deficient bone marrow cells. BMMs from miR-146a

KO and WT mice were stimulated with LPS for 48 hours and then re-stimulated with a second dose. The transcript level of TRAF6 showed consistent de-repression in miR-146a KO BMMs throughout stimulation, while the transcript level of IRAK1 showed perhaps an oscillating pattern but was not consistently higher than that of WT BMMs (Fig 7A, B). Furthermore, when various HSPCs from young WT and miR-146a KO mice were subjected to RT-qPCR analysis, de-repression of TRAF6 and IRAK1 were quite modest in bulk bone marrow cells but were highest in long-term HSCs, suggesting that miR-146a may play a particularly important repressive role in HSCs, acting on TRAF6 and IRAK1 (Fig 7C).

To determine the functional consequences of upregulating TRAF6 and IRAK1, we used a GFP-expressing retroviral vector to overexpress TRAF6 (pMIG-TRAF6) or IRAK1 (pMIG-IRAK1) in bone marrow cells enriched for HSPCs by 5-fluorouracil (5-FU) treatment. A vector expressing an irrelevant protein, luciferase, (pMIG-Luc) was used as the control. These vectors can consistently overexpress TRAF6 and IRAK1 by 10-fold and 100-fold, respectively, in bone marrow HSPCs (with about 50% transduction efficiency) (Fig S7A). After transplantation, we followed the mice for 9 months. Interestingly, the percent of GFP^+ cells in nucleated peripheral blood cells transduced with either pMIG-Luc or pMIG-IRAK1 remained stable or was slightly increased, while the GFP percentage in the pMIG-TRAF6 group declined from over 40% initially to less than 10% by the end of 9 months (Fig 7D). Histological analysis of harvested femur bones revealed that TRAF6-expressing mice had reduced bone marrow cellularity, compared to the control mice (Fig 7E). Given the lack of apparent phenotype in IRAK1-overexpressing mice, we further pursued TRAF6 as the more relevant target of miR-146a in the context of HSC biology. When we repeated the bone marrow transplant with 100% transduced bone marrow cells by sorting the GFP^+ cells, mice receiving TRAF6-overexpressing bone marrow cells rapidly succumbed to bone marrow failure (Fig 7F). The mice showed severe

anemia and reduced numbers of GFP^+ white blood cells in their peripheral blood, compared to the pMIG-Luc control group (Fig 7G-I). These data indicate that upregulation of TRAF6 in HSPCs results in bone marrow failure in mice, thus emphasizing the importance of tightly regulating TRAF6 level in HSPCs. This result suggests that derepression of TRAF6 in miR-146a-deficient HSPCs could be primarily responsible for driving HSC depletion and bone marrow failure.

Downregulation of miR-146a in human MDS samples

Myelodysplastic syndromes (MDS) represent a group of human hematopoietic malignancies that are thought to originate from HSCs [110]. HSCs in MDS patients have a defect in the ability to differentiate into mature cells, leading to peripheral cytopenia. MDS also have a predilection to progress to bone marrow failure or acute myelogenous leukemia (AML). MiR-146a KO mice recapitulate several key characteristics of MDS, including the decline in function of HSCs, peripheral cytopenia, and the propensity to progress to bone marrow failure and myeloid malignancy. To assess whether miR-146a-deficiency might represent a pathogenic feature of MDS, we analyzed the expression of miR-146a in bone marrow samples from healthy donors, MDS and AML patients. The cohort of unselected MDS, but not AML, samples showed a 4-fold reduction in the level of miR-146a (Fig 7J), suggesting that miR-146a-deficiency may be involved in MDS pathogenesis [37,58].

FIGURES

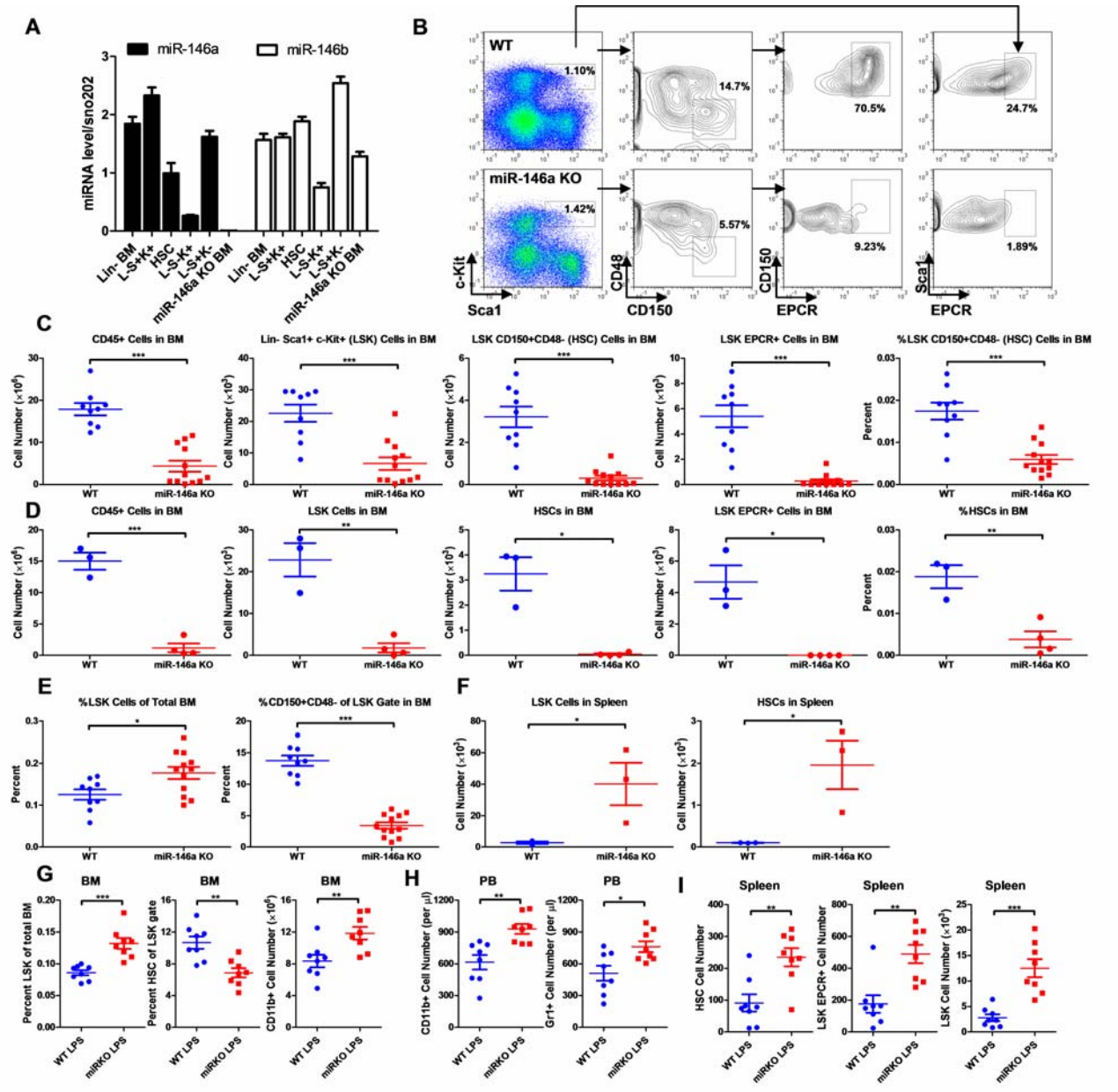

Figure 1. Accelerated HSC decline and myeloproliferation in miR-146a-deficient mice during chronic inflammation.
A. MiR-146a and miR-146b expression in FACS-sorted HSPC populations by Taqman RT-qPCR. Lin- BM, lineage negative bone marrow cells; L-S+K+ (LSK), Lin-Sca1+cKit+; HSC, LSK CD150+CD48-; L-S-K+, Lin-Sca1-cKit+; L-S+K-, Lin-Sca1+cKit-; miR-146a KO BM, total bone marrow cells from miR-146a-/- mice. B. Representative FACS plots of LSK cells and CD150+CD48- or EPCR+ HSCs from BM of 8-month-old wildtype (WT) and miR-146a-/- (miR-146a KO) mice. Quantification of number of BM CD45+ cells, LSK cells, LSK CD150+CD48- HSCs, LSK EPCR+ HSCs and percent of LSK CD150+CD48- HSCs of total BM from 8-month-old (C) and 12-month-old (D) WT and miR-146a KO mice by FACS. Quantification of percent of LSK cells of total BM (E) and percent of HSCs of LSK gate (F) from BM of 8-month-old WT and miR-146a KO mice by FACS. F. Quantification of number of LSK cells and LSK CD150+CD48- HSCs from spleen of 8-month-old WT and miR-146a KO mice by FACS.
G-I. 8-week-old WT and miR-146a KO (miR KO) mice were subjected to repeated low-dose of intraperitoneal LPS stimulation (1mg LPS/kg of body weight for 8 times) spread over a month. At the end the month, both groups of mice (WT LPS and miR KO LPS) were harvested for FACS analysis. G. Quantification of percent of LSK cells of total BM, CD150+CD48- HSCs of LSK gate, and number of CD11b+ myeloid cells in BM. H. Number of myeloid cells (CD11b+ or Gr1+) in peripheral blood. I. Quantification of total number of LSK CD150+CD48- HSCs, LSK EPCR+ HSCs and LSK cells in spleen.

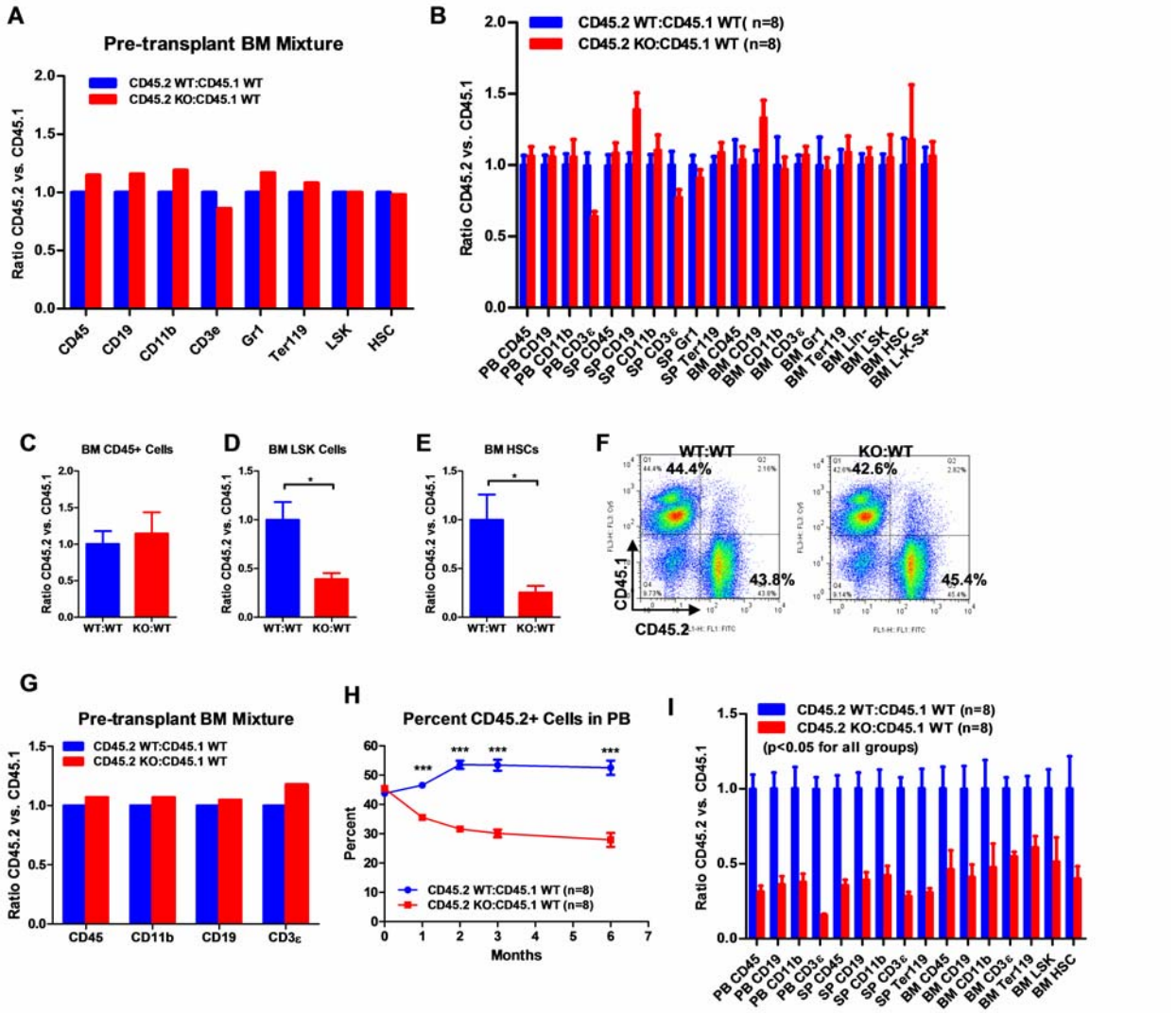

Figure 2. Progressive functional decline of miR-146a-deficient HSCs.

A. Ratio of CD45.2+ over CD45.1+ cells of various lineages in pre-transplanted bone marrow (BM) mixtures consisted of equal numbers of CD45.2+ WT and CD45.1+ WT total BM cells (blue bar, CD45.2 WT:CD45.1 WT) or equal numbers of CD45.2+ miR-146a KO and CD45.1+ WT total BM cells (red bar, CD45.2 KO:CD45.1 WT). FACS analysis was performed on the BM mixtures before transplantation to determine the starting ratios of various lineages. B. Ratio of CD45.2+ over CD45.1+ cells of various lineages in peripheral blood (PB), spleen (SP) and BM 6 months after transplantation. Blue bar, CD45.2 WT:CD45.1 WT, represents mice received CD45.2 WT:CD45.1 WT BM cells; red bar, CD45.2 KO:CD45.1 WT, represents mice received CD45.2 KO:CD45.1 WT BM cells. All donor mice were 6-week-old female and recipient mice were 2-month-old CD45.1+ WT female. Ratio of CD45.2+ over CD45.1+ of BM white blood (CD45+) cells (C), LSK cells (D) and HSCs (E)10-month after transplantation. WT:WT, CD45.2 WT:CD45.1 WT; KO:WT, CD45.2 KO:CD45.1 WT. n=8 for each group.

F-I. A repeat of the above experiment with age-and-sex-matched 4-month-old WT and miR-146a KO female mice. F. Representative FACS plots of BM mixtures before transplantation showing CD45.2/CD45.1 ratio close to 1 for both WT:WT and KO:WT BM mixtures. G. Ratio of CD45.2+ over CD45.1+ cells of various lineages before transplantation. H. Percentage of CD45.2+ cells of CD45+ peripheral blood nucleated cells at 1, 2, 3 and 6 months. I. Ratio of CD45.2+ over CD45.1+ cells of various lineages in PB, SP and BM 6 months after transplantation. All ratios of CD45.2 WT:CD45.1 WT are normalized to 1. LSK, Lin-cKit+Sca1+; HSC, LSK CD150+CD48-; L-K+S-, Lin-cKit+Sca1-.

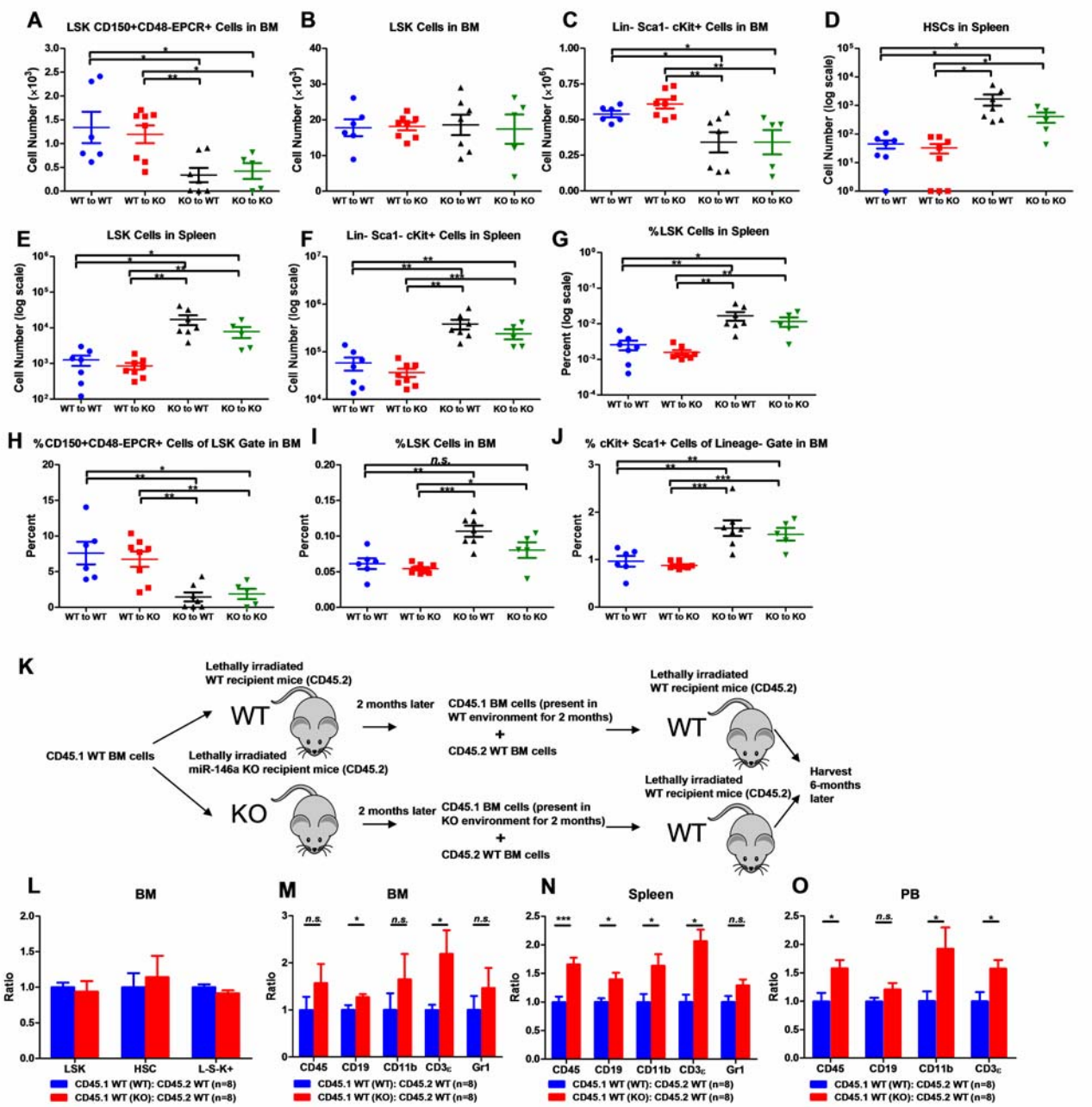

Figure 3. Hematopoetic-intrinsic and –extrinsic contribution to hematopoietic defects.

A-J. Reciprocal bone marrow (BM) transplant performed by transferring WT donor BM cells to WT recipient mice (WT to WT), WT donor BM cells to miR-146a KO recipient mice (WT to KO), miR-146a KO donor BM cells to WT recipient mice (KO to WT), and miR-146a KO donor BM cells to miR-146a KO recipient mice (KO to KO). All donor and recipient mice are 8-week-old female mice. Mice were harvested for analysis at the end of 5 months. Quantification of total number of HSPCs in spleen and BM, including LSK CD150+CD48-EPCR+ HSCs (A), LSK (Lin-cKit+Sca1+) cells (B), Lin-cKit+Sca1- cells (C) in BM, and LSK CD150+CD48- HSCs (D), LSK cells (E), Lin-cKit+Sca1- cells (F) in spleen. Quantification of percent of HSPCs in spleen and BM, including percent LSK cells in spleen (G), percent of CD150+CD48-EPCR+ HSCs in LSK gate in BM (H), percent of LSK cells in total BM (I) and percent of cKit+Sca1+ in Lin- gate in BM (J). K-O. Serial BM transplant performed by first transplanting CD45.1+ WT BM cells into either CD45.2+ WT or miR-146a KO recipient mice for 2 months, which were then harvested and mixed with CD45.2+ WT BM cells for second transplantation into CD45.2+ WT recipient mice. Mice received CD45.1 WT (WT):CD45.2 WT or CD45.1 WT (KO):CD45.2 WT cells were harvested 6 months later for FACS analysis. K. Schematic diagram of the experimental setup. L. Ratio of CD45.1+ over CD45.2+ cells of BM HSPCs, including LSK cells, LSK CD150+CD48- HSCs and L-K+S- cells. Ratio of CD45.1+ over CD45.2+ cells of various lineages in BM (M), spleen (N) and PB (O), including CD45+, CD19+, CD11b+, CD3ε+ and Gr1+ cells.

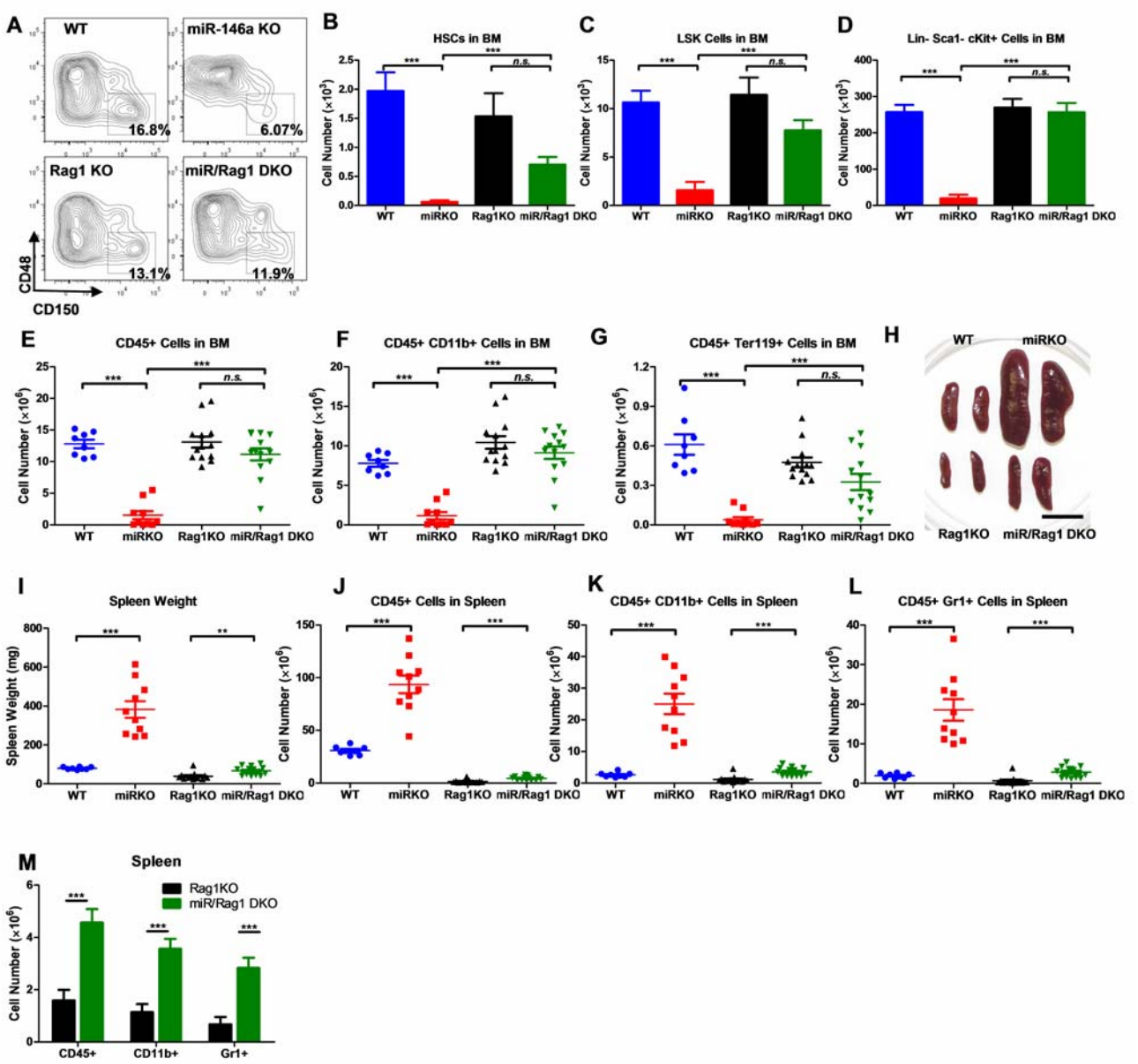

Figure 4. MiR-146a-deficient lymphocytes contribute to the HSC defect and myeloproliferation.
A-M. Age-and-sex-matched WT, miR-146a KO (miR KO), Rag1 KO and miR-146a/Rag1 double KO (miR/Rag1 DKO) mice were allowed to age to 10-month-old before harvested for analysis. A. Representative FACS plots of CD150+CD48- HSCs of the LSK gate. Quantification of total number of HSCs (B), LSK cells (C), Lin-cKit+Sca1- myeloid progenitor cells (D) in BM. Quantification of total number of CD45+ (E), CD11b+ (F) and Ter119+ (G) cells in BM. H. Representative photograph of spleens. Spleen weight (I) and total number of CD45+ (J), CD11b+ (K) and Gr1+ (L) cells in spleen. For comparison, various cell lineages in spleen of Rag1 KO and miR/Rag1 DKO mice were re-graphed (M).

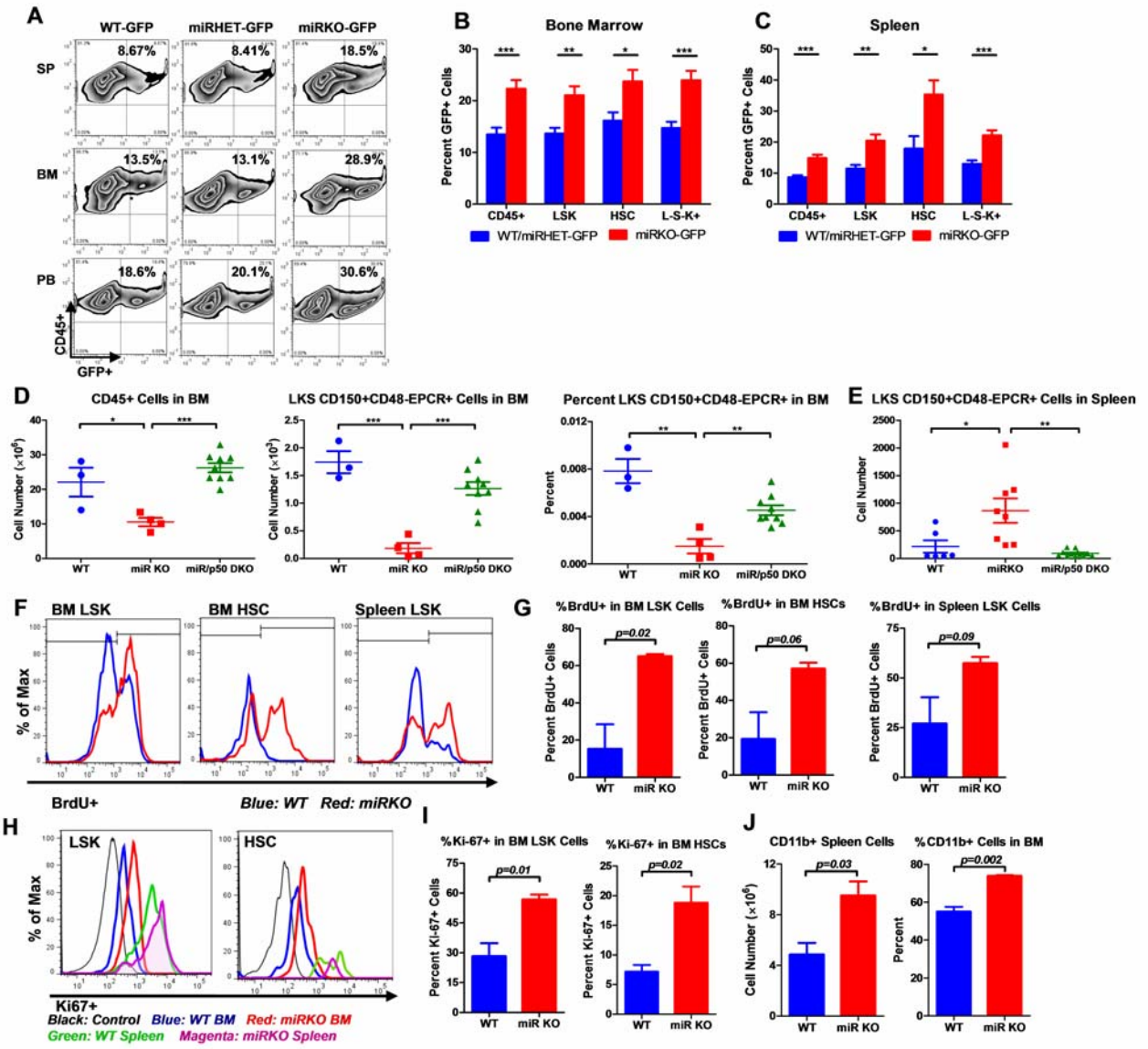

Figure 5. NF-κB regulates HSC proliferation and differentiation during chronic inflammation.

A-C. 8-week-old WT (WT-GFP), miR-146a+/- (miRHET-GFP), and miR-146a-/- (miRKO-GFP) NF-κB-GFP reporter mice were subjected to repeated intraperitoneal LPS stimulation (3mg LPS/kg of body weight every other day) for one week. Percent of GFP+ cells in various lineages were quantified by FACS. A. Representative FACS plots of GFP+ white blood cells (CD45+) in spleen (SP), bone marrow (BM) and peripheral blood (PB). Quantification of percent GFP+ cells of HSPCs in bone marrow (B) and spleen (C), including CD45+, LSK cells, HSCs (LSK CD150+CD48-) and L-S-K+ myeloid progenitor cells.

D-E. Age-and-sex-matched WT, miR-146a KO (miR KO) and miR-146a-/-p50-/- (miR/p50 DKO) mice were allowed to age to 8-9 months before harvested for analysis. Quantification of total number of CD45+, LSK CD150+CD48-EPCR+ HSCs in BM, percent of LSK CD150+CD48-EPCR+ HSCs of total BM (D), and total number of LSK CD150+CD48-EPCR+ HSCs in spleen (E) by FACS.

F-J. 8-week-old WT and miR-146a KO (miR KO) mice were subjected to repeated low-dose of intraperitoneal LPS stimulation (1mg LPS/kg of body weight) daily for 3 days. 1 mg of BrdU was injected intraperitoneally daily. BrdU+ and Ki-67+ HSPCs were quantified by FACS.

F. Representative FACS histograms of BrdU+ LSK cells and HSCs in BM and BrdU+ LSK cells in spleen. Blue, WT mice; red, miR KO mice. G. Quantification of percent of BrdU+ cells in BM LSK cells, HSCs and spleen LSK cells. H. Representative FACS histograms of Ki-67+ LSK and HSCs in BM and spleen. Black, negative control; blue, WT BM; red, miR KO BM; green, WT spleen; magenta, miR KO spleen. Quantification of Ki-67+ cells in BM LSK cells and HSCs (I). Quantification of number and percent of CD11b+ myeloid cells in spleen and BM (J).

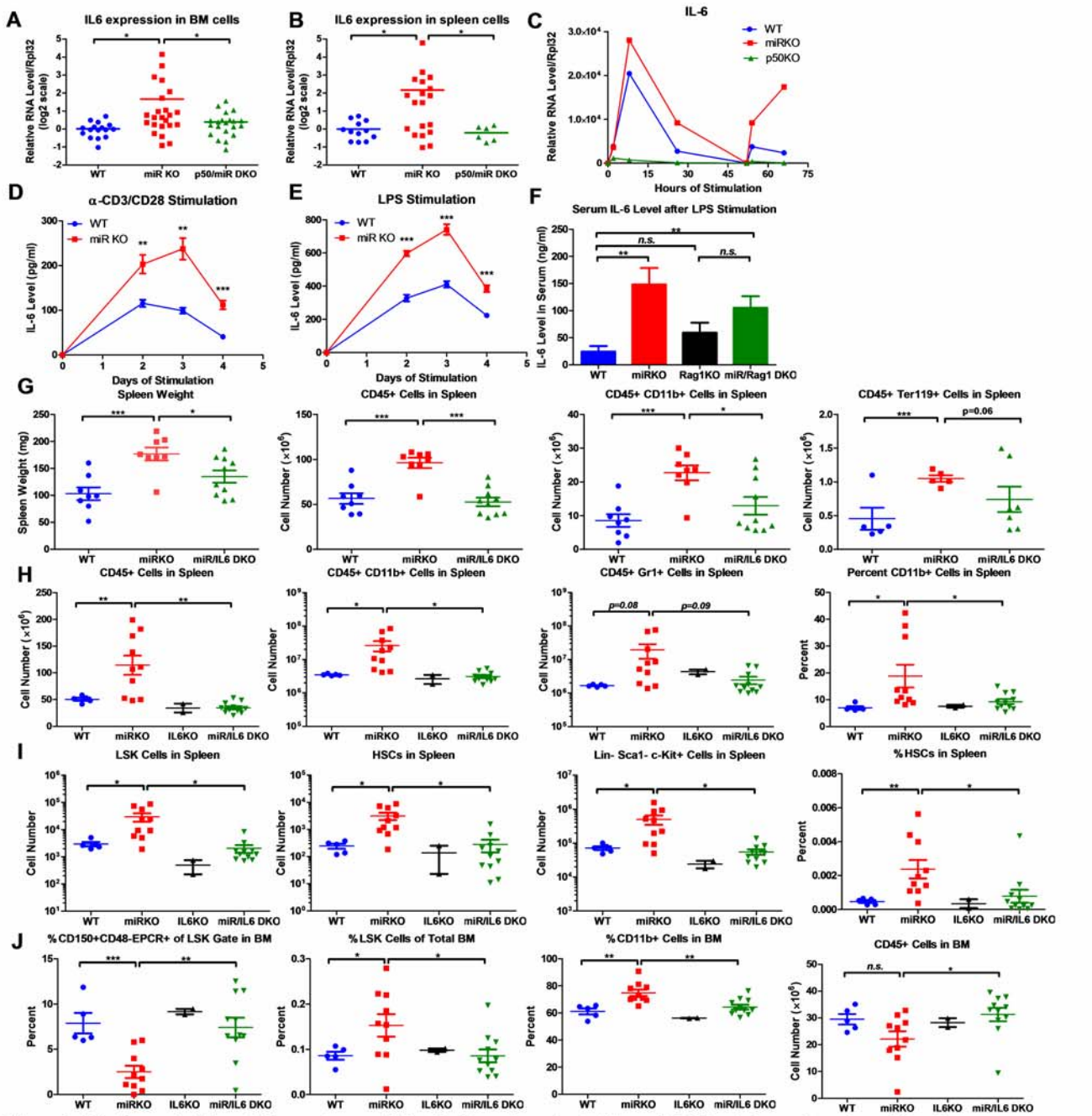

Figure 6. NF-κB-regulated pro-inflammatory cytokine IL-6 is an important driver of HSC depletion and myeloproliferation.
Gene expression of IL-6 in bone marrow cells (BM) (A) and spleen cells (B) of aging wildtype (WT), miR-146a-/- (miR KO), and miR-146a-/- p50-/- (miR/p50 DKO) mice measured by RT-qPCR. All mice are age-and-sex matched 6-10 month-old female mice. Gene expression of IL-6 (C) in bone marrow-derived macrophages (BMMs) stimulated *in vitro* with LPS (100 ng/ml) measured by RT-qPCR. First stimulation with LPS was given at 0 hour and re-stimulation at 48 hours. BMMs are generated from 8-week-old WT, miR KO, and p50 KO mice. IL-6 concentration in the culture medium of splenocytes stimulated *in vitro* with LPS (10 μg/ml) (D) or anti-CD3 (1 μg/ml)/anti-CD28 (0.5 μg/ml) antibodies (E) for 4 days measured by ELISA. Serum level of IL-6 in 2-month-old WT, miR KO, Rag1 KO and miR/Rag1 DKO mice stimulated *in vivo* with LPS (1 mg LPS /kg body weight) for 6 hours measured by ELISA. G. 2-month-old WT, miR KO, and miR/IL6 DKO mice after repeated intraperitoneal injection of LPS (3mg LPS/kg body weight on Day 1, 3, 5 and 7) and mice were harvested on Day 8. Spleen weight and total number of CD45+, CD45+CD11b+, and CD45+ Ter119+ cells in spleen were shown. H-J. Age-and-sex-matched WT, miR KO, IL6 KO and miR/IL6 DKO mice were allowed to age to 6-7 months before harvested for FACS analysis. H. Quantification of number of CD45+, CD45+CD11b+, CD45+Gr1+, and percent of CD11b+ cells in spleen. I. Quantification of number of HSPCs, including LSK cells, LSK CD150+CD48- HSCs and Lin-cKit+Sca1- myeloid progenitor cells, in spleen and percent of HSCs in spleen. J. Quantification of percent of CD150+CD48-EPCR+ HSCs of LSK gate, LSK cells of total BM, and CD11b+ cells of total BM and total number of CD45+ cells in BM.

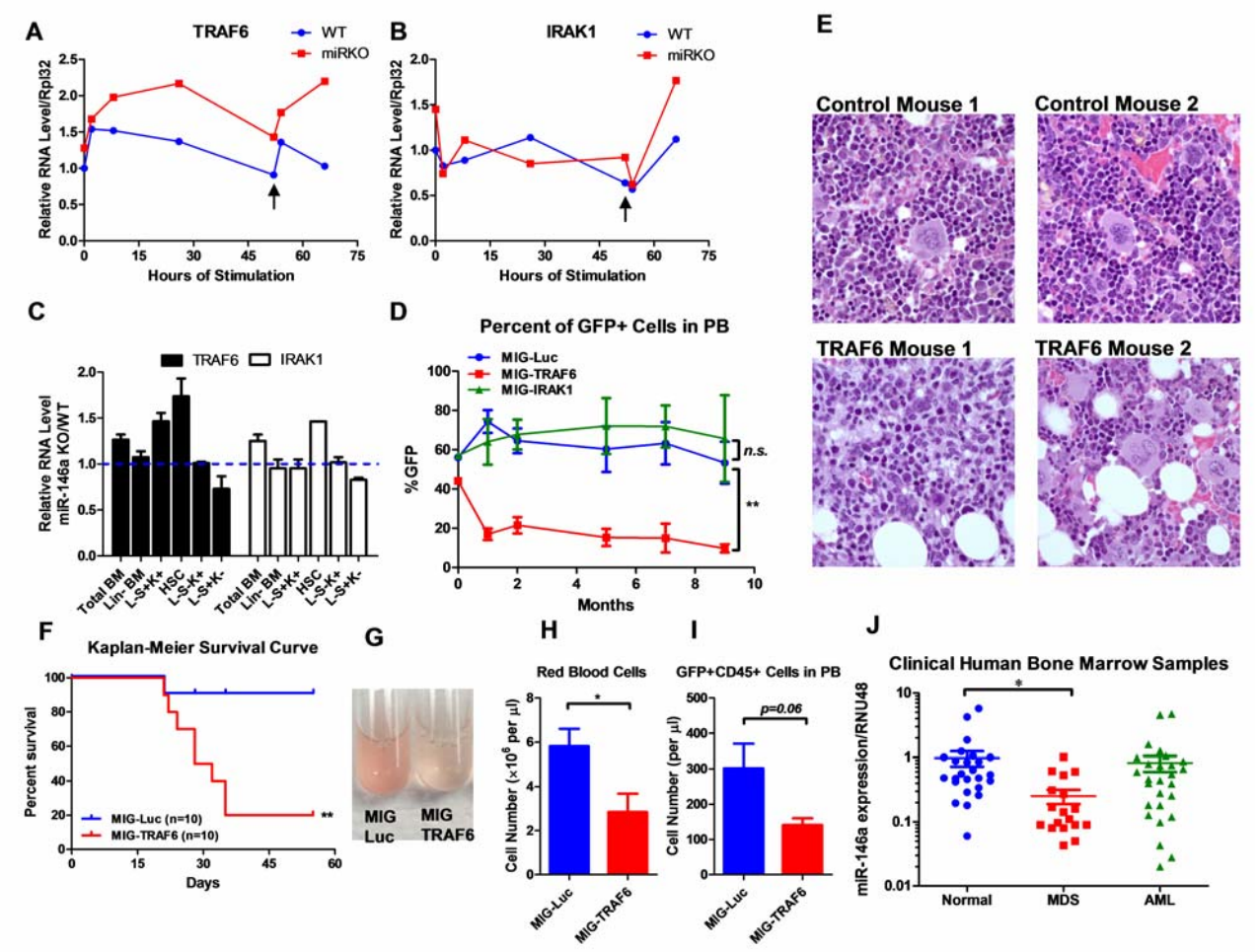

Figure 7. Derepression of TRAF6, a miR-146a target, is responsible for bone marrow failure.
Transcript levels of TRAF6 (A) and IRAK1 (B) in WT and miR-146a KO (miR KO) bone marrow derived macrophages (BMMs) stimulated with LPS, which was added to the culture medium at 0 hour and 48 hours (black arrow).
C. Transcript levels of TRAF6 and IRAK1 in total BM, Lin- BM, and FACS sorted LSK cells, LSK CD150+CD48- HSCs, L-K+S- cells and L-K-S+ cells from 8-week-old WT and miR-146a KO mice. Fold change of miR-146a KO over WT cells was graphed.
D-E. BM HSPCs overexpressing luciferase (MIG-Luc), TRAF6 (MIG-TRAF6), or IRAK1 (MIG-IRAK1) were transplanted into lethally irradiated WT recipient mice. Transduction efficiency was about 50% in all groups as measured by FACS before transplantation. D. Percent of GFP+ cells in transduced HSPCs before transplantation and in peripheral blood of reconstituted mice at month 1, 2, 5, 7 and 9 were analyzed by FACS. E. Representative photographs of histological analysis (H&E stain) of femur bones of MIG-Luc control and MIG-TRAF6 mice harvested 9-month after transplantation.
F-I. BM HSPCs overexpressing luciferase (MIG-Luc) or TRAF6 (MIG-TRAF6) were transplanted into lethally irradiated WT recipient mice. Transduced HSPCs were sorted for GFP expression to ensure the transplanted HSPCs were 100% GFP+. F. Kaplan-Meier survival curve of WT recipient mice reconstituted with BM HSPCs overexpressing luciferase (MIG-Luc) or TRAF6 (MIG-TRAF6). Peripheral blood (PB) analysis of MIG-Luc and MIG-TRAF6 mice at 1 month after transplantation. G. Representative photograph of 1:1000 diluted PB in phosphate-buffered saline (PBS). Red blood cells in PB were counted with hemocytometer (H) and total number of GFP+CD45+ cells in PB (I) were measured by FACS.
J. Downregulation of miR-146a in human myelodysplastic syndromes (MDS) samples. Expression level of miR-146a in bone marrow samples from healthy donors (Normal), MDS and acute myelogenous leukemia (AML) patients by Taqman RT-qPCR. RNU48 was used as the normalization gene.

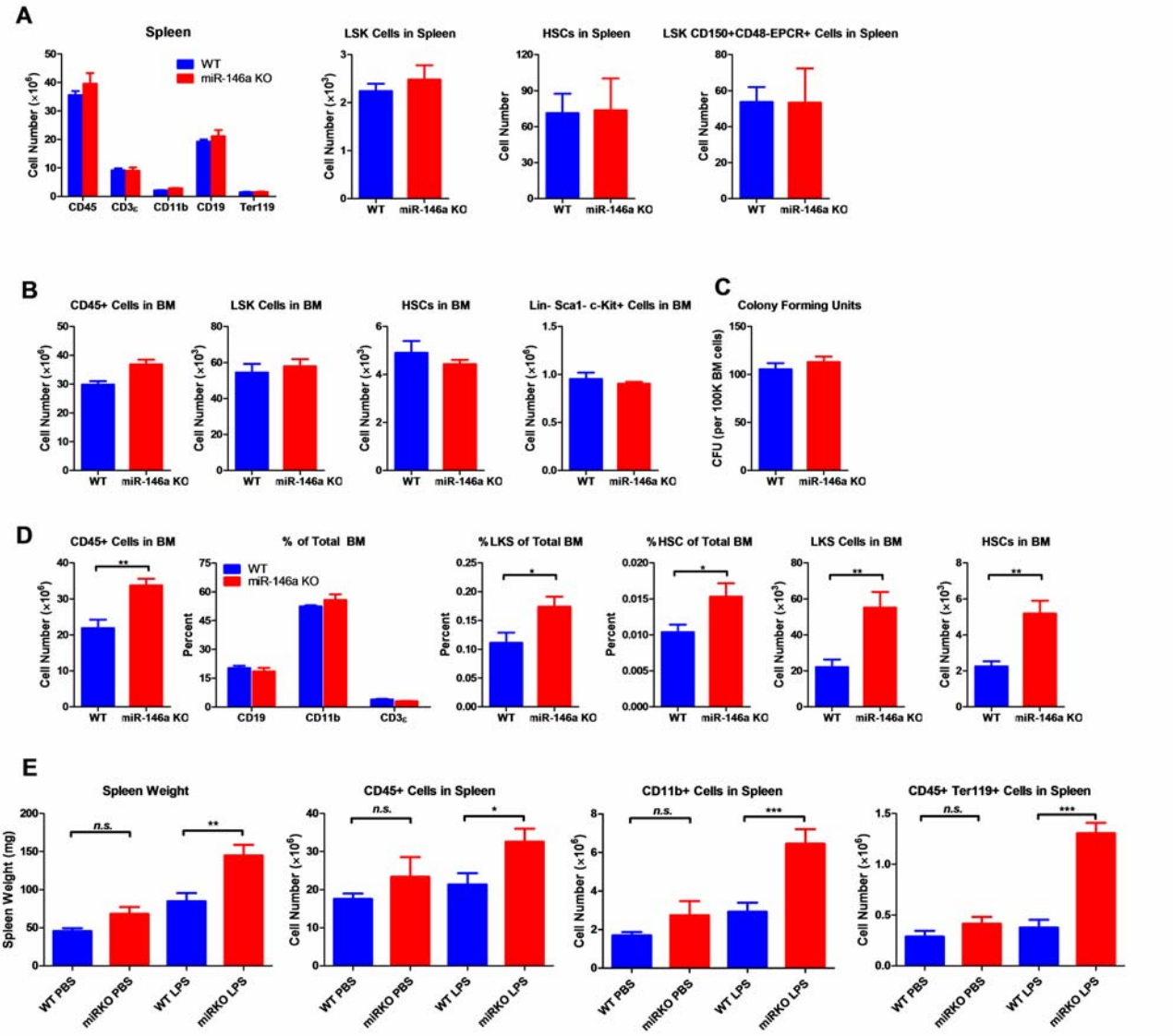

Figure S1. HSPC FACS analysis and colony-forming ability in 6-week-old and 4-month-old WT and miR-146a KO mice (Related to Figure 1).

A. Quantification of number of white blood cells (CD45), T cells (CD3ε), myeloid cells (CD11b), B cells (CD19), nucleated erythrocytes (Ter119), LSK cells, LSK CD150+CD48- HSCs and LSK CD150+CD48-EPCR+ HSCs from spleen of 6-week-old WT and miR-146a KO mice by FACS. B. Quantification of number of white blood cells (CD45), LSK cells, LSK CD150+CD48- HSCs, Lin-cKit+Sca1- myeloid progenitors from BM of 6-week-old WT and miR-146a KO mice by FACS. C. Colony forming units (CFU) *in vitro* in methycelluose medium per 100,000 total BM cells from 6-week-old WT and miR-146a KO mice. D. Quantification of number or percent of white blood cells (CD45), T cells (CD3ε), myeloid cells (CD11b), B cells (CD19), LSK cells and LSK CD150+CD48- HSCs from BM of 4-month-old WT and miR-146a KO mice by FACS.

E (related to Figure 1G-I). 8-week-old WT and miR-146a KO (miR KO) mice were subjected to repeated low-dose of intraperitoneal LPS stimulation (1mg LPS/kg of body weight for 8 times) spread over a month. WT and miR KO mice receiving phosphate-buffered saline (PBS) injection were included as controls. At the end the month, four groups of mice (WT PBS, miR KO PBS, WT LPS and miR KO LPS) were harvested for FACS analysis. Spleen weight, number of CD45+, CD11b+ and Ter119+ cells in spleen were shown.

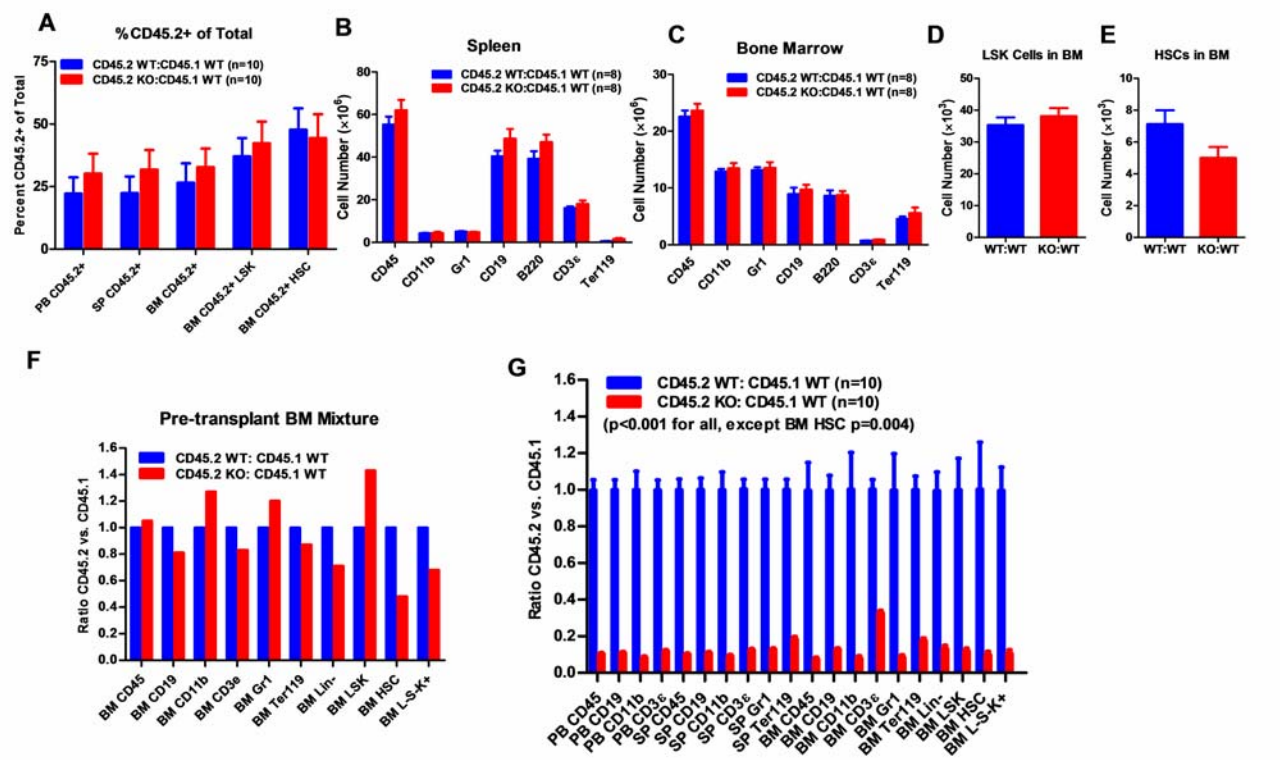

Figure S2. Functional decline of miR-146a-deficient HSCs (related to Figure 2).

A. Equal numbers of BM HSCs (LSK CD150+CD48-) were sorted from 8-week-old CD45.2+ WT and CD45.2+ miR-146a KO mice. 50 WT or KO HSCs were mixed with 500,000 CD45.1+ WT total BM cells and transplanted into a CD45.1+ WT recipient mouse. Percentage of CD45.2+ cells in various lineages in peripheral blood (PB), spleen (SP) and bone marrow (BM) was analyzed by FACS 8 months after transplantation.

B-E. Related to Figure 2A. Quantification of total number of cells (including both CD45.2+ and CD45.1+ cells) in various lineages in SP and BM of CD45.2 WT:CD45.1 WT and CD45.2 KO:CD45.1 WT recipient mice 6 months after transplantation.

F-G. A repeat of the experiment described in Figure 2A with sex-and-age-matched 6-month-old WT and miR-146a KO female mice. F. Ratio of CD45.2+ over CD45.1+ cells of various lineages in BM mixtures before transplantation. G. Ratio of CD45.2+ over CD45.1+ cells of various lineages in PB, SP and BM 3 months after transplantation. All ratios of CD45.2 WT:CD45.1 WT are normalized to 1. LSK, Lin-cKit+Sca1+; HSC, LSK CD150+CD48-; L-K+S-, Lin-cKit+Sca1-.

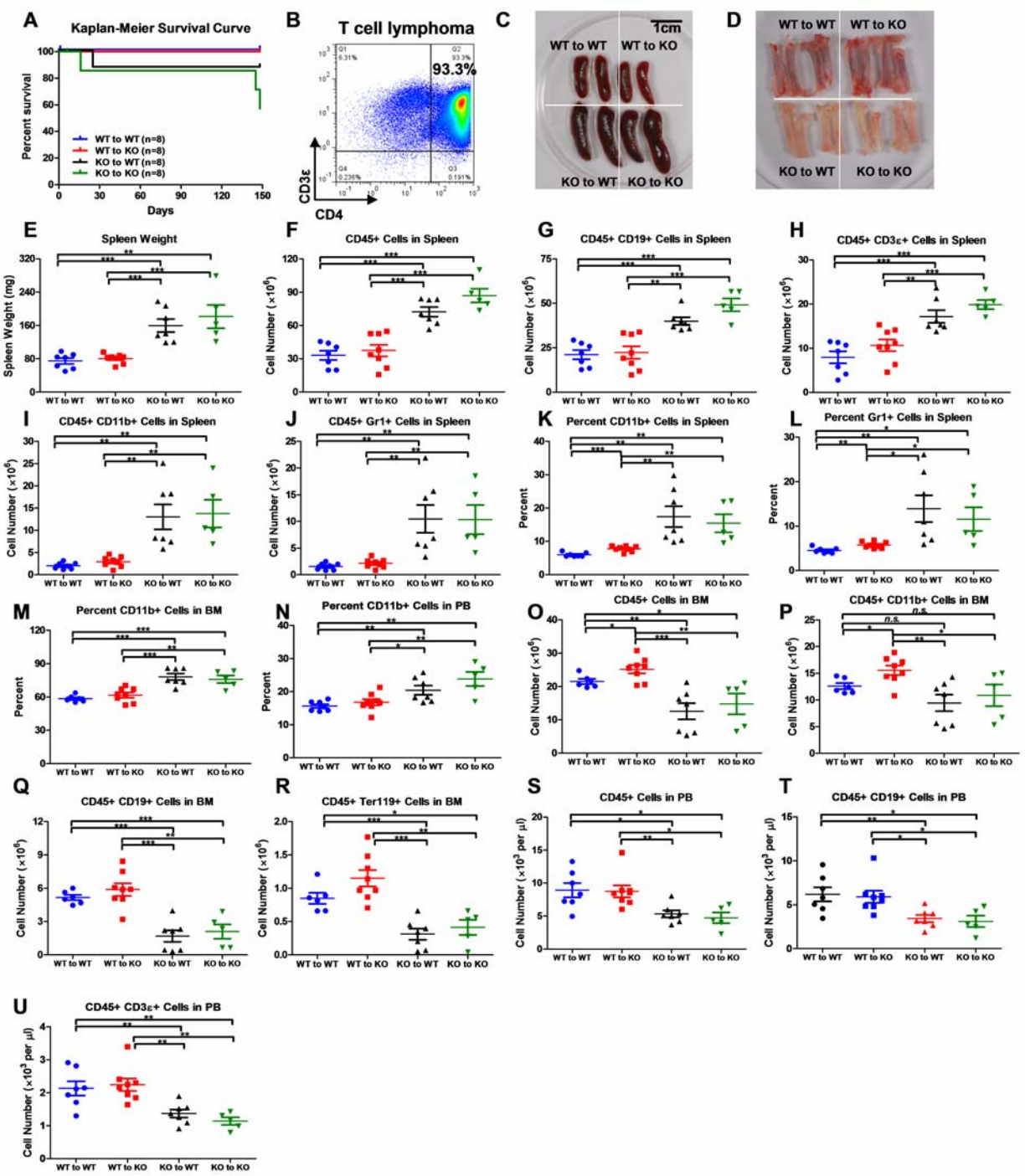

Figure S3. Hematopoetic-intrinsic and –extrinsic contribution to hematopoietic defects (related to Figure 3).

A-U. The same reciprocal BM transplant experiment as Fig 3A-J.

A. Kaplan-Meier survival curve of the four transplant groups (WT to WT, WT to KO, KO to WT and KO to KO). B. FACS plot of a CD4+ T-cell lymphoma from thymus of a moribund KO to KO mouse. Representative photographs of spleens (C) and bone marrows (D). E. Spleen weights.

Quantification of total number of CD45+ (F), CD19+ (G), CD3ε+ (H), CD11b+ (I) and Gr1+ (J) cells in spleen, percentage of CD11b+ (K) and Gr1+ (L) cells in spleen, percentage of CD11b+ cells in BM (M), percentage of CD11b+ cells in PB, number of CD45+ (O), CD11b+ (P), CD19+ (Q), Ter119+ (R) cells in BM and number of CD45+(S), CD19+ (T), and CD3ε+ (U) cells in PB by FACS.

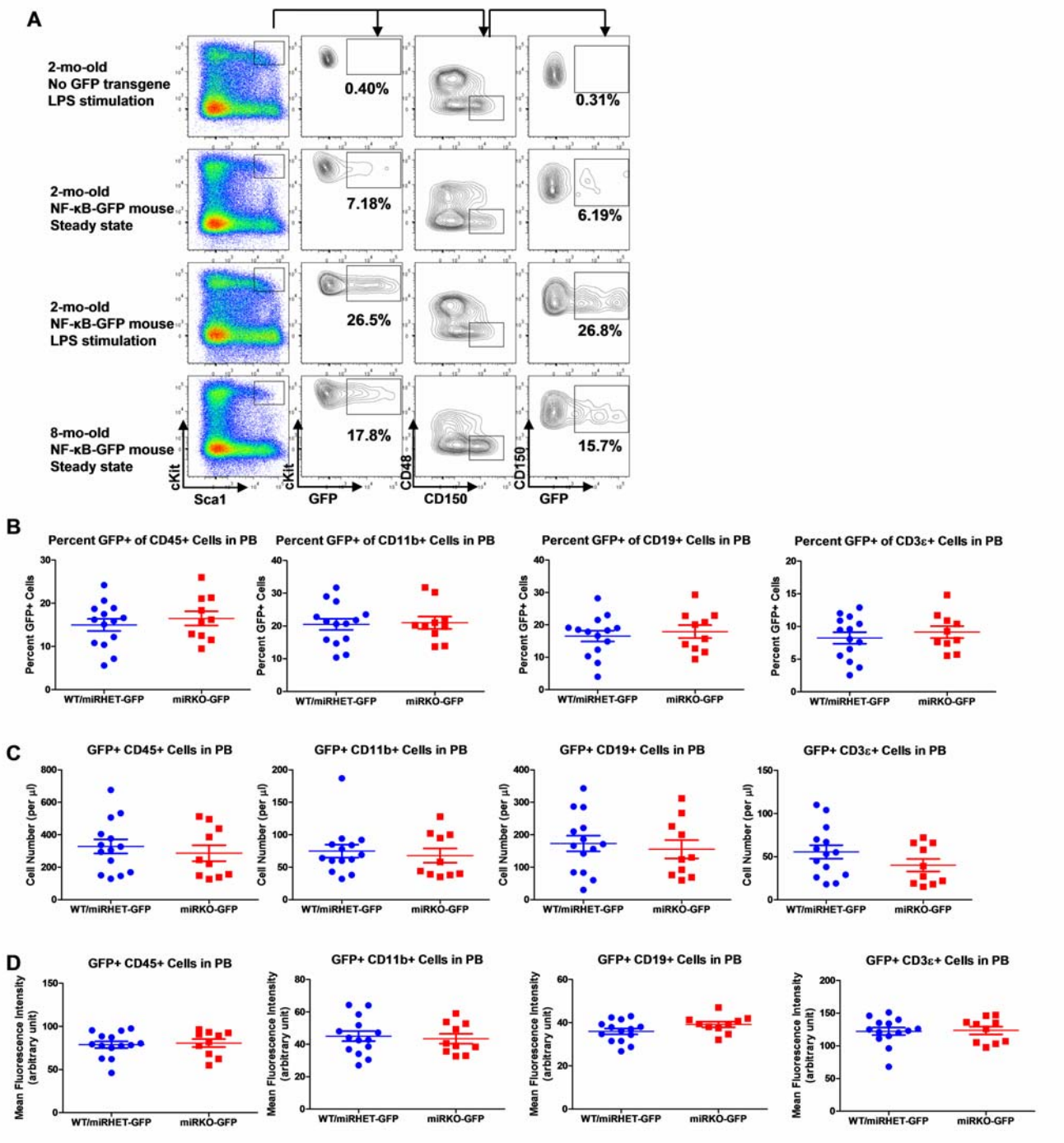

Figure S4. NF-κB activity in HSPCs and peripheral blood of NF-κB-GFP reporter mice (related to Figure 5).
A. Regular WT mice and WT NF-κB-GFP reporter mice were challenged with one dose of LPS intraperitoneally (2mg LPS/kg body weight). GFP+ cells in various lineages were quantified by FACS six hours after injection. Representative FACS plots of 2-month-old regular WT mouse (without NF-κB-GFP transgene) with LPS stimulation, 2-month-old WT NF-κB-GFP reporter mouse at basal state, 2-month-old WT NF-κB-GFP reporter mouse with LPS stimulation, and 8-month-old WT NF-κB-GFP reporter mouse at basal state. Percent of GFP+ cells in LSK cells and HSCs were shown. B. Basal level of percent (B), number (C) and mean fluorescence intensity (MFI) (D) of GFP+ cells in various lineages in peripheral blood (PB) of 2-month-old WT (WT-GFP), miR-146a+/- (miRHET-GFP), and miR-146a-/- (miRKO-GFP) NF-κB-GFP reporter mice were quantified by FACS.

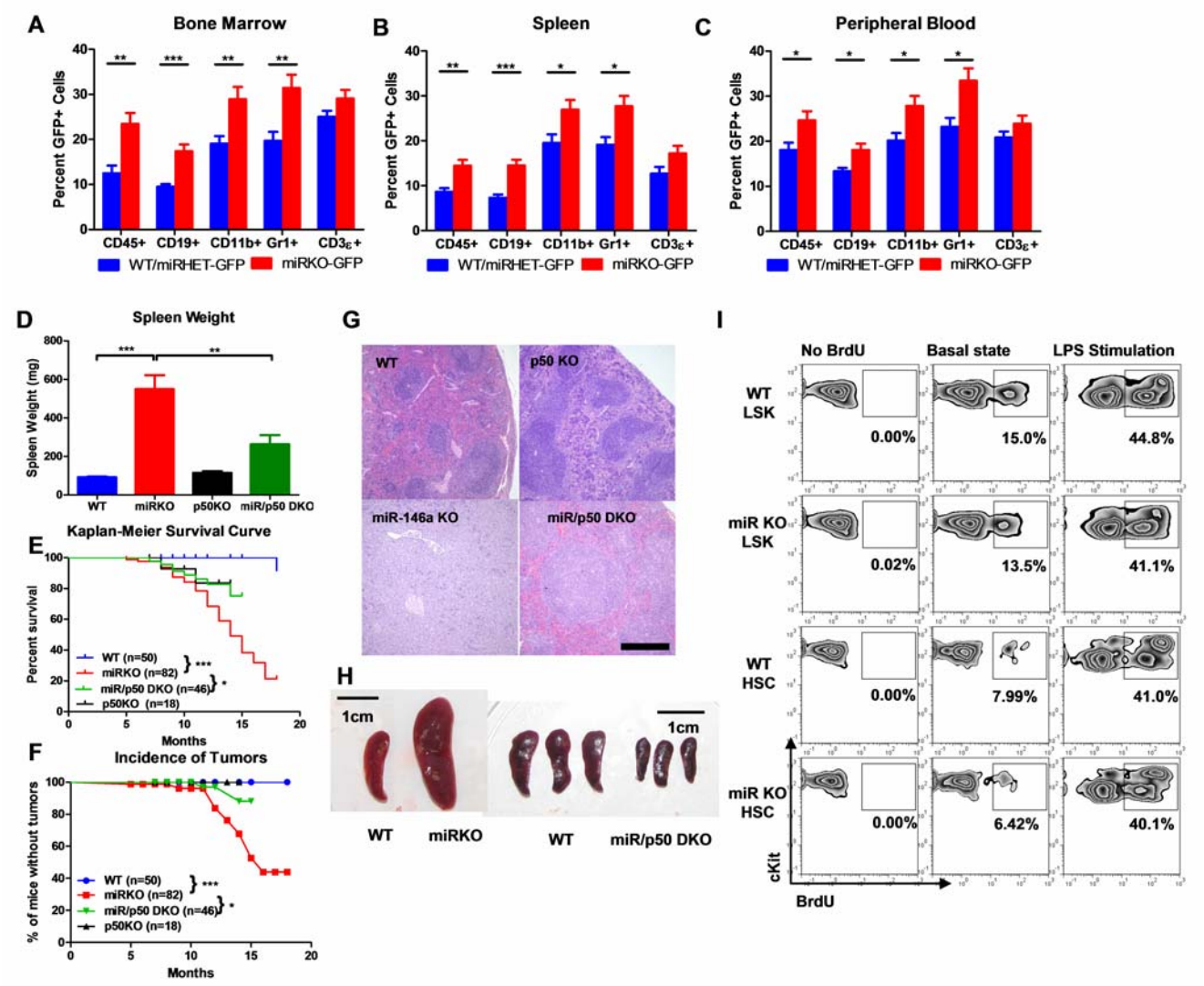

Figure S5. NF-κB regulates HSC proliferation and differentiation during chronic inflammation. (related to Figure 5).
A-C (related to Figure 5A-C). 8-week-old WT (WT-GFP), miR-146a+/- (miRHET-GFP), and miR-146a-/- (miRKO-GFP) NF-κB-GFP reporter mice were subjected to repeated intraperitoneal LPS stimulation (3mg LPS/kg of body weight every other day) for one week. Percent of GFP+ cells in various lineages were quantified by FACS. Quantification of GFP+ cells in various lineages, including CD45+, CD19+, CD11b+, Gr1+ and CD3ε+, in bone marrow (A), spleen (B) and peripheral blood (C).
D-H (related to Figure 5J-M). Age-and-sex-matched WT, miR-146a KO (miR KO), p50 KO and miR-146a-/-p50-/- (miR/p50 DKO) mice were allowed to age to up to 18 months. Mice were harvested as they became moribund or at the end of the experiment. Spleen weight (D), Kaplan-Meier survival curve (E) and incidence of tumors (F). G. Representative images of spleen histology (H&E staining) from 12-month-old female WT, miR KO, p50 KO and miR/p50 DKO mice. Spleen from a miR-146a KO mouse with myeloid sarcoma was shown. Scale bar, 400 μm. H. Representative photographs of spleens from Rag2-/-γC-/- mice transplanted with WT, miR KO, or miR/p50 DKO spleen cells. Scale bar, 1 cm.
I (related to Figure 5F-J). 8-week-old WT and miR-146a KO (miR KO) mice were challenged with one dose of LPS (2mg LPS/kg of body weight) intraperitoneally for 12 hours. 1 mg of BrdU was injected intraperitoneally. BrdU+ HSPCs were quantified by FACS. Representative FACS plots of BrdU+ LSK cells and LSK CD150+CD48- HSCs in bone marrow of WT and miR KO mice. No BrdU, no BrdU injection; Basal state, no LPS injection; LPS stimulation, BrdU and LPS injection.

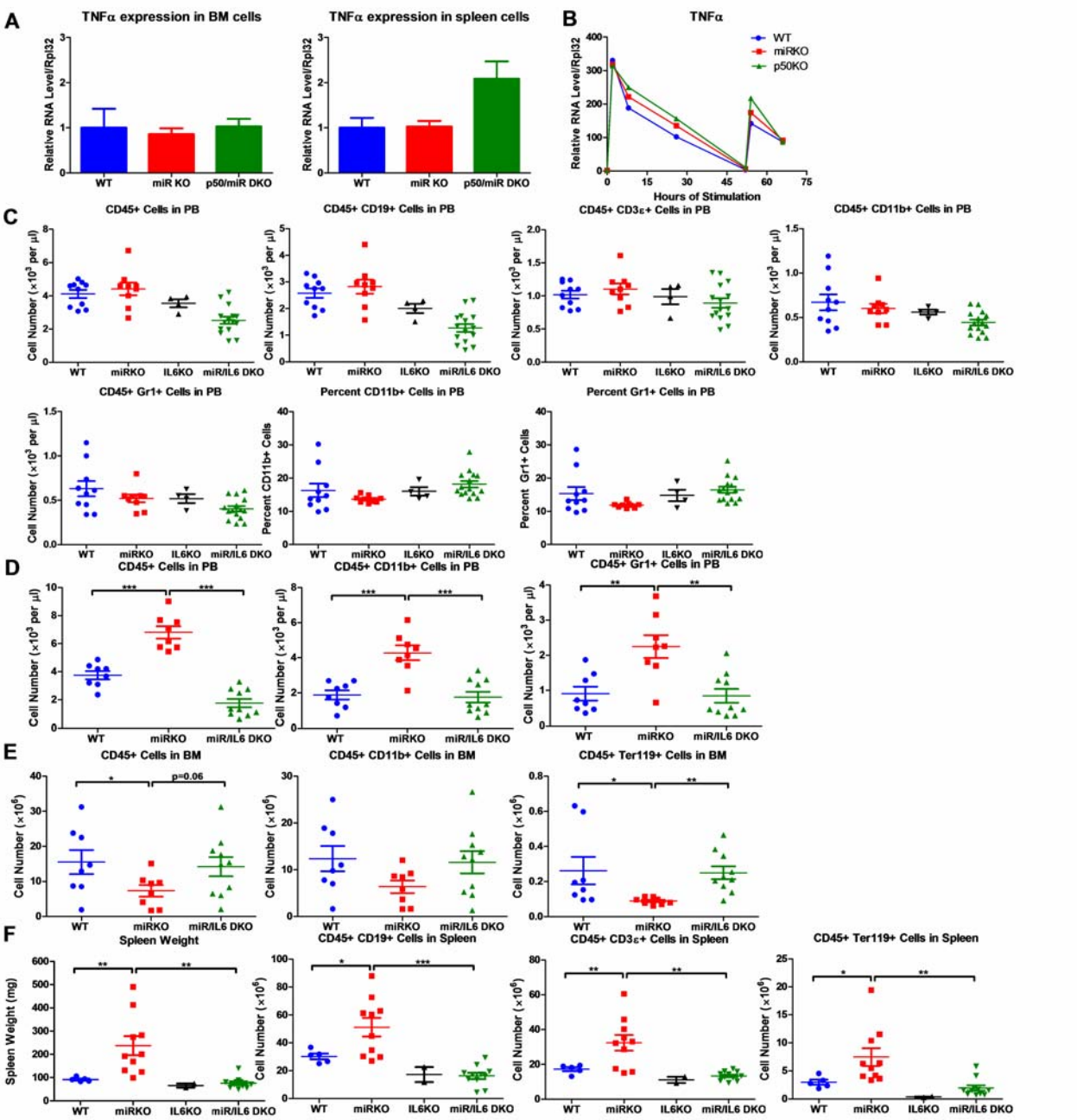

Figure S6. NF-κB-regulated pro-inflammatory cytokine IL-6 is an important driver of HSC depletion and myeloproliferation (related to Figure 6). A (related to Figure 6A, B). Gene expression of TNFα in BM cells (A) and spleen cells (B) of aging wildtype (WT), miR-146a-/- (miRKO), and miR-146a-/- p50-/- (miR/p50 DKO) mice measured by RT-qPCR. All mice are age-and-sex matched 6-10 month-old female mice. B (related to Figure 6C). Gene expression of TNFα in bone marrow-derived macrophages (BMMs) stimulated *in vitro* with LPS (100 ng/ml) measured by RT-qPCR. First stimulation with LPS was given at 0 hour and re-stimulation at 48 hours. BMMs are generated from 8-week-old WT, miR KO, and p50 KO mice. C (related to Figure 6G-I). Unperturbed 2-month-old WT, miR KO, p50 KO and miR/IL6 DKO mice were bled for FACS analysis. Quantification of total number and percent of various cell lineages in peripheral blood under steady state.
D-E (related to Figure 6G). 2-month-old WT, miR KO, and miR/IL6 DKO mice after repeated intraperitoneal injection of LPS (3mg LPS/kg body weight on Day 1, 3, 5 and 7) and mice were harvested on Day 8. D. Quantification of total number of CD45+, CD45+CD11b+ and CD45+Gr1+ cells in peripheral blood (PB). E. Quantification of total number of CD45+, CD45+CD11b+ and CD45+Ter119+ cells in bone marrow (BM). F (related to Figure 6H-J). Age-and-sex-matched WT, miR KO, IL6 KO and miR/IL6 DKO mice were allowed to age to 6-7 months before harvested for FACS analysis. Quantification of spleen weight and total number of CD45+CD19+, CD45+CD3ε+ and CD45+Ter119+ cells in spleen.

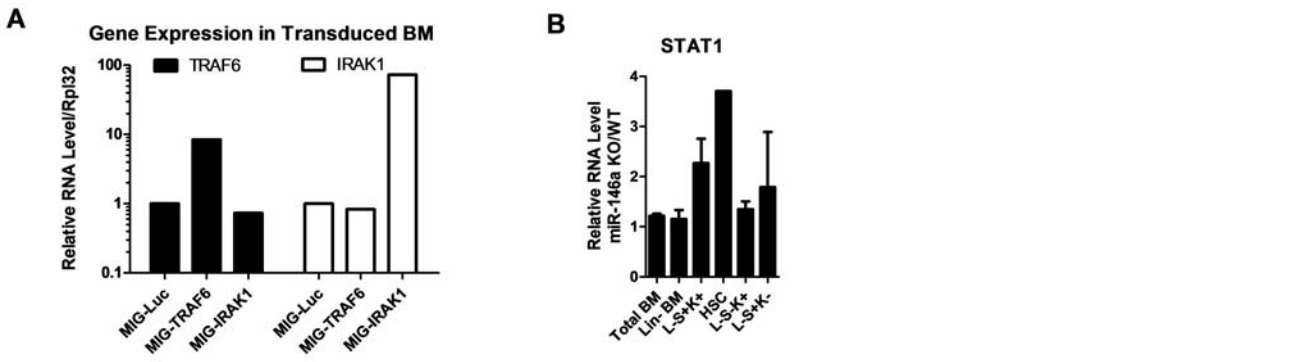

Figure S7. A. (Related to Figure 7D). Expression of TRAF6 and IRAK1 in BM HSPCs tranduced with pMIG-Luc, pMIG-TRAF6, or pMIG-IRAK viruses (~50% GFP+). B. (Related to Figure 7C). Gene expression of STAT1 in various BM HSPC lineages from 2-month-old miR-146a KO and WT mice. Fold change of miR-146a KO over WT cells was graphed.

DISCUSSION

In this study, we have shown that a single microRNA, miR-146a, is a critical regulator of HSC homeostasis following chronic exposure of mice to LPS or during the aging process. Mice lacking miR-146a develop a series of defects that can be accelerated by multiple LPS treatments. Extrapolating from this observation, we suggest that the natural exposure of miR-146a KO mice to bacteria and other infectious agents may be the cause of the 'spontaneous' deterioration of HSC function (bone marrow failure), excessive myelopoiesis and tumor formation that is observed in these animals. It could well be that the excess myelopoiesis seen in normal mice as they age is a consequence of the same process [111-112]. One obvious test of these notions, to examine HSC function in germ free mice, is not feasible because of the many secondary consequences of completely ablating the normal microbiota and will require more subtle approaches. The remarkable circumstance that a single microRNA plays such a crucial role in this process has allowed us to uncover it.

Because of the existence of mice lacking miR-146a we were able to use mouse genetics to elucidate the pathway by which miR-146a functions. Consistent with data from studies of the function of this microRNA in other cell types, in HSCs it acts to control NF-κB. We could see NF-κB activated in cells from LPS-treated mice and could show that deletion of the NF-κB subunit p50 ameliorated the symptoms evident in the miR-146a KO mice. The exact locus of its action appears to be modulation of TRAF6 expression because overproduction of TRAF6 caused symptoms similar to those seen in the KO. The other validated target of miR-146a, IRAK1, did not appear very involved in the pathology we studied here because it was not consistently elevated in the miR-146a KO and its overproduction did not produce much symptomatology. NF-κB activates many genes but we found that IL-6 is a very important mediator of the pathology of the miR-146a KO. This suggests the following pathway of action of miR-146a: infections or other perturbations activate NF-κB in HSCs through TRAF6 and

other signal transducers; the basal and NF-κB-enhanced levels of miR-146a then limit the amount of TRAF6, allowing the system to quickly return to basal NF-κB activity when the danger has passed; the transient NF-κB activation causes a transient increase in IL-6 and the IL-6 acts on the stem and progenitor cells causing them to transiently differentiate into myeloid cells. Lacking miR-146a, the action of NF-κB is extended, the production of IL-6 is exaggerated, the myelopoietic stress on the HSPCs is extended and the over time the pathological symptoms of continual myelopoiesis, bone marrow failure and cancer emerge. This may be a pathway in humans that leads to myelodysplastic syndrome.

The function of individual miRNAs in the most primitive hematopoietic stem cells is relatively unexplored, except in the case of miR-125 family, which is enriched in the long-term HSCs and can positively regulate HSC number and long-term HSC output [14,113]. In this study, we added miR-146a to the list of genes that regulate HSC homeostasis during chronic inflammation and aging. The function of miR-146a in this context seems to be through the regulation of TRAF6, a validated target of miR-146a in macrophages/monocytes and T cells [19-20]. Overexpression of miR-155 also causes pathological myelopoiesis similarly to that caused by deletion of miR-146a. MiR-155 appears to act by inhibiting the negative-acting phosphatase SHIP 1 [70]. Enforced expression of TRAF6 in HSPCs results in cell death and/or engraftment failure and rapid bone marrow failure, a finding consistent with a previous study [37]. The same study also showed that overexpression of TRAF6 in HSPCs induced IL-6 production, which was responsible for some key features of 5q- syndrome, a subtype of MDS. It is worth noting that the level of TRAF6 expression in transduced HSPCs is about 10-fold higher than that observed in miR-146a-deficient HSCs, and thus the phenotype of enforced TRAF6 overexpression in HSPCs is more rapid and dramatic, precluding a careful analysis of HSC function and activity. It will be interesting to develop a system to modulate the level of TRAF6 overexpression in a more controlled

manner for HSC analysis and to characterize the effects of downregulating TRAF6 genetically or by RNA interference in miR-146a-deficient HSCs. In addition to TRAF6 and IRAK1, STAT1 and RelB have been identified as direct targets of miR-146a in regulatory T cells and Ly6C^{hi} monocytes, respectively [17,43]. Recent studies have provided strong evidence for roles of both IFNα and IFNγ in regulating HSC quiescence and proliferation [99,101]. As a downstream transcription factor of both types of interferons, one might speculate that increased STAT1 may also be contributing to miR-146a-deficiency-induced HSC proliferation and exhaustion. Our preliminary analysis has shown upregulation of STAT1 mRNA in miR-146a-deficient HSCs (Fig S7B). A recent study has also suggested a role of non-canonical NF-κB activators RelB and NF-κB2 in regulating HSC self-renewal [114]. Whether RelB also contributes to the HSC defect in the context of miR-146a-deficiency remains to be determined.

Under stress-free conditions, NF-κB is not essential for HSC function [102]. However, we have demonstrated that NF-κB is activated in HSCs during inflammatory stimulation and physiological aging. More importantly, in the absence of miR-146a, uncontrolled NF-κB activation in the setting of chronic inflammation during long-term aging results in diminished HSC longevity and quality and exaggerated myeloid differentiation, ultimately leading to pathological development of HSC exhaustion and myeloproliferative neoplasms. The excessive HSC proliferation and myeloid differentiation can be accelerated in young miR-146a-deficient mice by repeated inflammatory stimulation with bacterial components. Given the multitude of mechanisms involved in downregulating NF-κB activity [67,115], these results highlight the critical, non-redundant role of miR-146a in the negative regulation of NF-κB activity during chronic inflammation. In this way, miR-146a acts as a guardian of the functional capabilities and longevity of murine hematopoietic stem cells.

In an effort to further characterize the effects downstream of NF-κB activation in the absence of miR-146a, we identified IL-6 as one of the culprit NF-κB-reponsive genes. Among its pleiotropic functions, IL-6 is a strong stimulator of HSPC proliferation. In addition, IL-6 and its downstream transcription factor STAT3 are both important regulators of emergency granulopoiesis [116-117]. IL-6 can activate NF-κB, forming a positive feed-forward loop, and act through STAT3 to activate additional genes involved in cell cycle regulation, proliferation and anti-apoptosis, either directly on HSPCs and myeloid cancer cells or indirectly by contributing to the general pro-inflammatory and pro-proliferative environment. This signaling pathway involving NF-κB/IL-6/STAT3 has been demonstrated to be important in the pathogenesis of various epithelial cancers associated with inflammation, especially gastrointestinal cancer and breast cancer [106,118-119]. Interestingly, a recent report shows that chronic myelogenous leukemia (CML) driven by the classic Bcr-Abl oncogenic fusion protein can be attenuated by genetic deletion of IL-6 [120]. It will be interesting to identify the genes regulated by NF-κB and STATs that are directly responsible for activating the proliferation and differentiation programs within HSPCs and for driving myeloid oncogenesis.

This study has also identified an important role of dysregulated lymphocytes in driving HSC abnormality and myeloproliferative disease in our model, suggesting that autoreactive lymphocytes can provide extrinsic stimulus to diseases like bone marrow failure and myeloproliferative neoplasms/myelodysplastic syndromes in genetically susceptible hosts. Importantly, systemic autoimmunity has long been observed in some MDS patients [121]. In addition, given the importance of IL-6, a known regulator of CD4 T cell differentiation towards either T_h17 or T_{reg} cells, it will be interesting to determine whether overproduction of IL-6 contributes to abnormal hematopoiesis by altering the ratio of CD4 T cell subsets. Defining the precise role of various lymphocyte subsets,

including T_h1, T_h2, T_h17 and T_{reg} cells, using lineage-specific miR-146a knockout mouse may provide further insight into how different cell types influence physiologic and pathologic hematopoiesis.

This study provides an insight into the function of miR-146a and NF-κB in regulating HSC proliferation and differentiation under the influence of physiological stressors. In addition, this study also has several other important implications. First, it provides direct evidence that prolonged and uncontrolled inflammation-driven hematopoiesis can ultimately exhaust the HSC pool and lead to myeloid malignancies in genetically susceptible hosts, according nicely with some recent large scale epidemiological studies showing that chronic immune stimulation from past infection or autoimmunity increases the risk of developing myeloid malignancies, including AML, MDS, and myeloproliferative neoplasms (MPN) [122-124]. This study provides a possible molecular basis for these intriguing epidemiological observations and offers a unique experimental system to further explore the cellular and molecular pathways by which infection and autoimmunity can trigger myeloid malignancies; it may also provide a way to test potential therapeutic interventions. Second, miR-146a-deficient mice represent an excellent model to understand the pathogenesis of MDS, a hematopoietic malignancy of older adults (median age of 70 years) [125] that has consistently shown reduced expression of miR-146a. Lastly, it suggests that chronic inflammation may be a potential cause of the age-related decline in HSC function. Therapeutically, given that many of the cellular and molecular components are important in driving the overall pathology, inhibition of p50 subunit of NF-κB, hyperactivated lymphocytes, IL-6 overproduction, and TRAF6 represent multiple opportunities for therapeutic intervention to disrupt the pathogenic process generating myeloid malignancies, and combinatorial inhibition may have even greater therapeutic impact.

EXPERIMENTAL PROCEDURES

Mice. All mice were on a C57BL/6 genetic background and housed under specific pathogen-free condition at the California Institute of Technology. All double knockout mice were made by crossing single knockout mice. Experiments with mice were approved by the institutional Animal Care and Use Committee of the California Institute of Technology. Mouse harvest, tumor analysis, and tumor transplant into Rag2-/-γC-/- mice were performed as described [44]. For *in vivo* and *in vitro* stimulation, *E. coli* 055:B5 LPS (Sigma) was used.

Cell Culture and Bone Marrow Dervied Macrophages (BMMs). Total bone marrow cells from wildtype, miR-146a$^{-/-}$, or p50$^{-/-}$ mice were lysed with red blood cell lysis buffer (Biolegend) and were cultured in DMEM supplemented with 10% (vol/vol) Fetal Bovine Serum (Cellgro), penicillin and streptomycin, and M-CSF (20ng/ml) for 6 days. On Day 7, BMMs were stimulated with *E. coli* 055:B5 LPS (100ng/ml) for 0, 2, 8, and 24 hours. At 24 hours, BMMs were washed with phosphate buffered saline (PBS) and taken off LPS stimulation for 24 hours. At 48 hours, BMMs were re-stimulated with 100ng/ml LPS for additional 16 hours.

Flow Cytometry and Sorting. Spleen, bone marrow, and peripheral blood cells were lysed with red blood cell lysis buffer (Biolegend). Fluorophore- or biotin-conjugated antibodies against CD45, CD3ε, CD4, CD8, CD11b, Gr1, B220, CD19, Ter119, NK1.1, cKit, Sca1, CD48, CD150, EPCR, Ki-67 (Biolegend or eBioscience) were used for staining. BrdU staining was performed with BrdU staining kit from BD Biosciences. Cells were analyzed on a MACSQuant9 or MACSQuant10 Analyzer (Miltenyi) for both percentage and cell number. Data analysis was performed with FloJo software (TreeStar). Hematopoietic stem and progenitor cell sorting was performed by first depleting lineage^{+} bone marrow cells with magnetic beads (Miltenyi) and then stained with indicated antibodies before sorted on a FACSAria machine (BD).

Quantitative RT-PCR and ELISA. Total RNA was extracted with TRIzol reagent (Invitrogen) from spleen or bone marrow cells after red blood cell lysis. cDNA was synthesized using iScript cDNA synthesis kit (Bio-Rad) followed by SYBR Green-based quantatitive PCR (Quantas). Rpl32 was used as the normalization gene. MiRNA detection was performed with Taqman RT-qPCR probes (Life Technologies). Sno202 was used as the normalization gene. Specific cytokines, including IL-6 and TNFα, were measured in cell culture medium or mouse serum by ELISA according to manufacturer's protocol (eBioscience).

Histopathology. Organs were fixed in 10% neutral-buffered formalin immediately after necropsy. After fixation, organs was embedded in paraffin and processed for hematoxylin and eosin (H&E) staining. The histolopathological analysis was performed by a board-certified hematopathologist.

Statistical Analysis. All figures were graphed as mean ± standard error of the mean (SEM). Student T-test and Kaplan-Meier survival analysis were performed using GraphPad Prism software. * denotes $p<0.05$, ** denotes $p<0.01$, *** denotes $p<0.001$.

REFERENCES

1. Lee, R.C., Feinbaum, R.L. & Ambros, V. The C. elegans heterochronic gene lin-4 encodes small RNAs with antisense complementarity to lin-14. *Cell* **75**, 843-854 (1993).
2. Wightman, B., Ha, I. & Ruvkun, G. Posttranscriptional regulation of the heterochronic gene lin-14 by lin-4 mediates temporal pattern formation in C. elegans. *Cell* **75**, 855-862 (1993).
3. O'Connell, R.M., Rao, D.S., Chaudhuri, A.A. & Baltimore, D. Physiological and pathological roles for microRNAs in the immune system. *Nat Rev Immunol* **10**, 111-122 (2010).
4. Baltimore, D., Boldin, M.P., O'Connell, R.M., Rao, D.S. & Taganov, K.D. MicroRNAs: new regulators of immune cell development and function. *Nat Immunol* **9**, 839-845 (2008).
5. Cifuentes, D.*, et al.* A novel miRNA processing pathway independent of Dicer requires Argonaute2 catalytic activity. *Science* **328**, 1694-1698 (2010).
6. Cheloufi, S., Dos Santos, C.O., Chong, M.M. & Hannon, G.J. A dicer-independent miRNA biogenesis pathway that requires Ago catalysis. *Nature* **465**, 584-589 (2010).
7. Czech, B. & Hannon, G.J. Small RNA sorting: matchmaking for Argonautes. *Nat Rev Genet* **12**, 19-31 (2011).
8. Bartel, D.P. MicroRNAs: target recognition and regulatory functions. *Cell* **136**, 215-233 (2009).
9. Guo, H., Ingolia, N.T., Weissman, J.S. & Bartel, D.P. Mammalian microRNAs predominantly act to decrease target mRNA levels. *Nature* **466**, 835-840 (2010).
10. Baek, D.*, et al.* The impact of microRNAs on protein output. *Nature* **455**, 64-71 (2008).
11. Lal, A.*, et al.* miR-24 Inhibits cell proliferation by targeting E2F2, MYC, and other cell-cycle genes via binding to "seedless" 3'UTR microRNA recognition elements. *Mol Cell* **35**, 610-625 (2009).
12. Vasudevan, S., Tong, Y. & Steitz, J.A. Switching from repression to activation: microRNAs can up-regulate translation. *Science* **318**, 1931-1934 (2007).
13. O'Carroll, D.*, et al.* A Slicer-independent role for Argonaute 2 in hematopoiesis and the microRNA pathway. *Genes Dev* **21**, 1999-2004 (2007).
14. Guo, S.*, et al.* MicroRNA miR-125a controls hematopoietic stem cell number. *Proc Natl Acad Sci U S A* **107**, 14229-14234 (2010).
15. O'Connell, R.M.*, et al.* Sustained expression of microRNA-155 in hematopoietic stem cells causes a myeloproliferative disorder. *J Exp Med* **205**, 585-594 (2008).
16. Taganov, K.D., Boldin, M.P., Chang, K.J. & Baltimore, D. NF-kappaB-dependent induction of microRNA miR-146, an inhibitor targeted to signaling proteins of innate immune responses. *Proc Natl Acad Sci U S A* **103**, 12481-12486 (2006).
17. Etzrodt, M.*, et al.* Regulation of monocyte functional heterogeneity by miR-146a and Relb. *Cell Rep* **1**, 317-324 (2012).
18. Jurkin, J.*, et al.* miR-146a is differentially expressed by myeloid dendritic cell subsets and desensitizes cells to TLR2-dependent activation. *J Immunol* **184**, 4955-4965 (2010).
19. Boldin, M.P.*, et al.* miR-146a is a significant brake on autoimmunity, myeloproliferation, and cancer in mice. *J Exp Med* **208**, 1189-1201 (2011).
20. Yang, L.*, et al.* miR-146a controls the resolution of T cell responses in mice. *J Exp Med* **209**, 1655-1670 (2012).

21. Starczynowski, D.T., *et al.* MicroRNA-146a disrupts hematopoietic differentiation and survival. *Exp Hematol* **39**, 167-178 e164 (2011).
22. Hou, J., *et al.* MicroRNA-146a feedback inhibits RIG-I-dependent Type I IFN production in macrophages by targeting TRAF6, IRAK1, and IRAK2. *J Immunol* **183**, 2150-2158 (2009).
23. Monk, C.E., Hutvagner, G. & Arthur, J.S. Regulation of miRNA transcription in macrophages in response to Candida albicans. *PLoS One* **5**, e13669 (2010).
24. Cameron, J.E., *et al.* Epstein-Barr virus latent membrane protein 1 induces cellular MicroRNA miR-146a, a modulator of lymphocyte signaling pathways. *J Virol* **82**, 1946-1958 (2008).
25. Ghani, S., *et al.* Macrophage development from HSCs requires PU.1-coordinated microRNA expression. *Blood* **118**, 2275-2284 (2011).
26. Curtale, G., *et al.* An emerging player in the adaptive immune response: microRNA-146a is a modulator of IL-2 expression and activation-induced cell death in T lymphocytes. *Blood* **115**, 265-273 (2010).
27. Labbaye, C., *et al.* A three-step pathway comprising PLZF/miR-146a/CXCR4 controls megakaryopoiesis. *Nat Cell Biol* **10**, 788-801 (2008).
28. Chang, T.C., *et al.* Widespread microRNA repression by Myc contributes to tumorigenesis. *Nat Genet* **40**, 43-50 (2008).
29. Dai, R., *et al.* Suppression of LPS-induced Interferon-gamma and nitric oxide in splenic lymphocytes by select estrogen-regulated microRNAs: a novel mechanism of immune modulation. *Blood* **112**, 4591-4597 (2008).
30. Xia, H., *et al.* microRNA-146b inhibits glioma cell migration and invasion by targeting MMPs. *Brain Res* **1269**, 158-165 (2009).
31. Chou, C.K., *et al.* miR-146b is highly expressed in adult papillary thyroid carcinomas with high risk features including extrathyroidal invasion and the BRAF(V600E) mutation. *Thyroid* **20**, 489-494 (2010).
32. Geraldo, M.V., Yamashita, A.S. & Kimura, E.T. MicroRNA miR-146b-5p regulates signal transduction of TGF-beta by repressing SMAD4 in thyroid cancer. *Oncogene* **31**, 1910-1922 (2012).
33. Katakowski, M., *et al.* MiR-146b-5p suppresses EGFR expression and reduces in vitro migration and invasion of glioma. *Cancer Invest* **28**, 1024-1030 (2010).
34. Man, Y.G., *et al.* Aberrant expression of chromogranin A, miR-146a, and miR-146b-5p in prostate structures with focally disrupted basal cell layers: an early sign of invasion and hormone-refractory cancer? *Cancer Genomics Proteomics* **8**, 235-244 (2011).
35. Perry, M.M., Williams, A.E., Tsitsiou, E., Larner-Svensson, H.M. & Lindsay, M.A. Divergent intracellular pathways regulate interleukin-1beta-induced miR-146a and miR-146b expression and chemokine release in human alveolar epithelial cells. *FEBS Lett* **583**, 3349-3355 (2009).
36. Boldin, M.P. & Baltimore, D. MicroRNAs, new effectors and regulators of NF-kappaB. *Immunol Rev* **246**, 205-220 (2012).
37. Starczynowski, D.T., *et al.* Identification of miR-145 and miR-146a as mediators of the 5q-syndrome phenotype. *Nat Med* **16**, 49-58 (2010).
38. Taganov, K.D., Boldin, M.P. & Baltimore, D. MicroRNAs and immunity: tiny players in a big field. *Immunity* **26**, 133-137 (2007).

39. Nahid, M.A., Pauley, K.M., Satoh, M. & Chan, E.K. miR-146a is critical for endotoxin-induced tolerance: IMPLICATION IN INNATE IMMUNITY. *J Biol Chem* **284**, 34590-34599 (2009).
40. Nahid, M.A., Satoh, M. & Chan, E.K. Mechanistic role of microRNA-146a in endotoxin-induced differential cross-regulation of TLR signaling. *J Immunol* **186**, 1723-1734 (2011).
41. El Gazzar, M., Church, A., Liu, T. & McCall, C.E. MicroRNA-146a regulates both transcription silencing and translation disruption of TNF-alpha during TLR4-induced gene reprogramming. *J Leukoc Biol* **90**, 509-519 (2011).
42. Tang, Y.*, et al.* MicroRNA-146A contributes to abnormal activation of the type I interferon pathway in human lupus by targeting the key signaling proteins. *Arthritis Rheum* **60**, 1065-1075 (2009).
43. Lu, L.F.*, et al.* Function of miR-146a in controlling Treg cell-mediated regulation of Th1 responses. *Cell* **142**, 914-929 (2010).
44. Zhao, J.L.*, et al.* NF-kappaB dysregulation in microRNA-146a-deficient mice drives the development of myeloid malignancies. *Proc Natl Acad Sci U S A* **108**, 9184-9189 (2011).
45. Opalinska, J.B.*, et al.* MicroRNA expression in maturing murine megakaryocytes. *Blood* **116**, e128-138 (2010).
46. Chassin, C.*, et al.* miR-146a mediates protective innate immune tolerance in the neonate intestine. *Cell Host Microbe* **8**, 358-368 (2010).
47. Perry, M.M.*, et al.* Rapid changes in microRNA-146a expression negatively regulate the IL-1beta-induced inflammatory response in human lung alveolar epithelial cells. *J Immunol* **180**, 5689-5698 (2008).
48. Lofgren, S.E.*, et al.* Genetic association of miRNA-146a with systemic lupus erythematosus in Europeans through decreased expression of the gene. *Genes Immun* **13**, 268-274 (2012).
49. Luo, X.*, et al.* A functional variant in microRNA-146a promoter modulates its expression and confers disease risk for systemic lupus erythematosus. *PLoS Genet* **7**, e1002128 (2011).
50. Chan, E.K., Satoh, M. & Pauley, K.M. Contrast in aberrant microRNA expression in systemic lupus erythematosus and rheumatoid arthritis: is microRNA-146 all we need? *Arthritis Rheum* **60**, 912-915 (2009).
51. Abou-Zeid, A., Saad, M. & Soliman, E. MicroRNA 146a expression in rheumatoid arthritis: association with tumor necrosis factor-alpha and disease activity. *Genet Test Mol Biomarkers* **15**, 807-812 (2011).
52. Nakasa, T.*, et al.* Expression of microRNA-146 in rheumatoid arthritis synovial tissue. *Arthritis Rheum* **58**, 1284-1292 (2008).
53. Yamasaki, K.*, et al.* Expression of MicroRNA-146a in osteoarthritis cartilage. *Arthritis Rheum* **60**, 1035-1041 (2009).
54. Korn, T., Bettelli, E., Oukka, M. & Kuchroo, V.K. IL-17 and Th17 Cells. *Annu Rev Immunol* **27**, 485-517 (2009).
55. Chen, T.*, et al.* MicroRNA-146a regulates the maturation process and pro-inflammatory cytokine secretion by targeting CD40L in oxLDL-stimulated dendritic cells. *FEBS Lett* **585**, 567-573 (2011).
56. Yang, K.*, et al.* MiR-146a inhibits oxidized low-density lipoprotein-induced lipid accumulation and inflammatory response via targeting toll-like receptor 4. *FEBS Lett* **585**, 854-860 (2011).

57. Bejar, R., Levine, R. & Ebert, B.L. Unraveling the molecular pathophysiology of myelodysplastic syndromes. *J Clin Oncol* **29**, 504-515 (2011).
58. Rhyasen, G.W. & Starczynowski, D.T. Deregulation of microRNAs in myelodysplastic syndrome. *Leukemia* **26**, 13-22 (2012).
59. O'Connell, R.M., Rao, D.S. & Baltimore, D. microRNA regulation of inflammatory responses. *Annu Rev Immunol* **30**, 295-312 (2012).
60. Votavova, H., *et al.* Differential expression of microRNAs in CD34+ cells of 5q-syndrome. *Journal of hematology & oncology* **4**, 1 (2011).
61. Garzon, R., *et al.* MicroRNA signatures associated with cytogenetics and prognosis in acute myeloid leukemia. *Blood* **111**, 3183-3189 (2008).
62. Wang, Y., *et al.* MicroRNAs expression signatures are associated with lineage and survival in acute leukemias. *Blood Cells Mol Dis* **44**, 191-197 (2010).
63. Paik, J.H., *et al.* MicroRNA-146a downregulates NFkappaB activity via targeting TRAF6 and functions as a tumor suppressor having strong prognostic implications in NK/T cell lymphoma. *Clin Cancer Res* **17**, 4761-4771 (2011).
64. O'Connell, R.M. & Baltimore, D. MicroRNAs and hematopoietic cell development. *Curr Top Dev Biol* **99**, 145-174 (2012).
65. O'Connell, R.M., Zhao, J.L. & Rao, D.S. MicroRNA function in myeloid biology. *Blood* **118**, 2960-2969 (2011).
66. Baltimore, D. NF-kappaB is 25. *Nat Immunol* **12**, 683-685 (2011).
67. Liew, F.Y., Xu, D., Brint, E.K. & O'Neill, L.A. Negative regulation of toll-like receptor-mediated immune responses. *Nat Rev Immunol* **5**, 446-458 (2005).
68. Ben-Neriah, Y. & Karin, M. Inflammation meets cancer, with NF-kappaB as the matchmaker. *Nat Immunol* **12**, 715-723 (2011).
69. O'Connell, R.M., Taganov, K.D., Boldin, M.P., Cheng, G. & Baltimore, D. MicroRNA-155 is induced during the macrophage inflammatory response. *Proc Natl Acad Sci U S A* **104**, 1604-1609 (2007).
70. O'Connell, R.M., Chaudhuri, A.A., Rao, D.S. & Baltimore, D. Inositol phosphatase SHIP1 is a primary target of miR-155. *Proc Natl Acad Sci U S A* **106**, 7113-7118 (2009).
71. Androulidaki, A., *et al.* The kinase Akt1 controls macrophage response to lipopolysaccharide by regulating microRNAs. *Immunity* **31**, 220-231 (2009).
72. Tili, E., *et al.* Modulation of miR-155 and miR-125b levels following lipopolysaccharide/TNF-alpha stimulation and their possible roles in regulating the response to endotoxin shock. *J Immunol* **179**, 5082-5089 (2007).
73. Rodriguez, A., *et al.* Requirement of bic/microRNA-155 for normal immune function. *Science* **316**, 608-611 (2007).
74. Thai, T.H., *et al.* Regulation of the germinal center response by microRNA-155. *Science* **316**, 604-608 (2007).
75. O'Connell, R.M., *et al.* MicroRNA-155 promotes autoimmune inflammation by enhancing inflammatory T cell development. *Immunity* **33**, 607-619 (2010).
76. Huffaker, T.B., *et al.* Epistasis between microRNAs 155 and 146a during T cell-mediated antitumor immunity. *Cell Rep* **2**, 1697-1709 (2012).
77. Costinean, S., *et al.* Pre-B cell proliferation and lymphoblastic leukemia/high-grade lymphoma in E(mu)-miR155 transgenic mice. *Proc Natl Acad Sci U S A* **103**, 7024-7029 (2006).

78. Xiao, C. & Rajewsky, K. MicroRNA control in the immune system: basic principles. *Cell* **136**, 26-36 (2009).
79. Calin, G.A. & Croce, C.M. MicroRNA signatures in human cancers. *Nat Rev Cancer* **6**, 857-866 (2006).
80. Grivennikov, S.I., Greten, F.R. & Karin, M. Immunity, inflammation, and cancer. *Cell* **140**, 883-899 (2010).
81. Braun, T., *et al.* Targeting NF-kappaB in hematologic malignancies. *Cell Death Differ* **13**, 748-758 (2006).
82. Shen, H.M. & Tergaonkar, V. NFkappaB signaling in carcinogenesis and as a potential molecular target for cancer therapy. *Apoptosis* **14**, 348-363 (2009).
83. Williams, A.E., Perry, M.M., Moschos, S.A., Larner-Svensson, H.M. & Lindsay, M.A. Role of miRNA-146a in the regulation of the innate immune response and cancer. *Biochem Soc Trans* **36**, 1211-1215 (2008).
84. Boldin, M.P., *et al.* miR-146a is a significant brake on autoimmunity, myeloproliferation and cancer in mice. *J Exp Med* (In press).
85. Kogan, S.C., *et al.* Bethesda proposals for classification of nonlymphoid hematopoietic neoplasms in mice. *Blood* **100**, 238-245 (2002).
86. Gerondakis, S., *et al.* Unravelling the complexities of the NF-kappaB signalling pathway using mouse knockout and transgenic models. *Oncogene* **25**, 6781-6799 (2006).
87. Sha, W.C., Liou, H.C., Tuomanen, E.I. & Baltimore, D. Targeted disruption of the p50 subunit of NF-kappa B leads to multifocal defects in immune responses. *Cell* **80**, 321-330 (1995).
88. Cao, Z., Xiong, J., Takeuchi, M., Kurama, T. & Goeddel, D.V. TRAF6 is a signal transducer for interleukin-1. *Nature* **383**, 443-446 (1996).
89. Hartupee, J., Li, X. & Hamilton, T. Interleukin 1alpha-induced NFkappaB activation and chemokine mRNA stabilization diverge at IRAK1. *J Biol Chem* **283**, 15689-15693 (2008).
90. Hoffmann, A., Leung, T.H. & Baltimore, D. Genetic analysis of NF-kappaB/Rel transcription factors defines functional specificities. *EMBO J* **22**, 5530-5539 (2003).
91. Ishikawa, H., *et al.* Chronic inflammation and susceptibility to bacterial infections in mice lacking the polypeptide (p)105 precursor (NF-kappaB1) but expressing p50. *J Exp Med* **187**, 985-996 (1998).
92. Beg, A.A., Sha, W.C., Bronson, R.T. & Baltimore, D. Constitutive NF-kappa B activation, enhanced granulopoiesis, and neonatal lethality in I kappa B alpha-deficient mice. *Genes Dev* **9**, 2736-2746 (1995).
93. Cilloni, D., Martinelli, G., Messa, F., Baccarani, M. & Saglio, G. Nuclear factor kB as a target for new drug development in myeloid malignancies. *Haematologica* **92**, 1224-1229 (2007).
94. Braun, T., *et al.* NF-kappaB constitutes a potential therapeutic target in high-risk myelodysplastic syndrome. *Blood* **107**, 1156-1165 (2006).
95. Rao, D.S., *et al.* MicroRNA-34a perturbs B lymphocyte development by repressing the forkhead box transcription factor Foxp1. *Immunity* **33**, 48-59 (2010).
96. Seita, J. & Weissman, I.L. Hematopoietic stem cell: self-renewal versus differentiation. *Wiley Interdiscip Rev Syst Biol Med* **2**, 640-653 (2010).
97. King, K.Y. & Goodell, M.A. Inflammatory modulation of HSCs: viewing the HSC as a foundation for the immune response. *Nat Rev Immunol* **11**, 685-692 (2011).

98. Nagai, Y., *et al.* Toll-like receptors on hematopoietic progenitor cells stimulate innate immune system replenishment. *Immunity* **24**, 801-812 (2006).
99. Baldridge, M.T., King, K.Y., Boles, N.C., Weksberg, D.C. & Goodell, M.A. Quiescent haematopoietic stem cells are activated by IFN-gamma in response to chronic infection. *Nature* **465**, 793-797 (2010).
100. Esplin, B.L., *et al.* Chronic exposure to a TLR ligand injures hematopoietic stem cells. *J Immunol* **186**, 5367-5375 (2011).
101. Essers, M.A., *et al.* IFNalpha activates dormant haematopoietic stem cells in vivo. *Nature* **458**, 904-908 (2009).
102. Gerondakis, S., *et al.* NF-kappaB subunit specificity in hemopoiesis. *Immunol Rev* **246**, 272-285 (2012).
103. Lee, E.G., *et al.* Failure to regulate TNF-induced NF-kappaB and cell death responses in A20-deficient mice. *Science* **289**, 2350-2354 (2000).
104. Magness, S.T., *et al.* In vivo pattern of lipopolysaccharide and anti-CD3-induced NF-kappa B activation using a novel gene-targeted enhanced GFP reporter gene mouse. *J Immunol* **173**, 1561-1570 (2004).
105. Lippert, E., *et al.* Gnotobiotic IL-10; NF-kappaB mice develop rapid and severe colitis following Campylobacter jejuni infection. *PLoS One* **4**, e7413 (2009).
106. Naugler, W.E. & Karin, M. The wolf in sheep's clothing: the role of interleukin-6 in immunity, inflammation and cancer. *Trends Mol Med* **14**, 109-119 (2008).
107. Hawley, R.G., Fong, A.Z., Burns, B.F. & Hawley, T.S. Transplantable myeloproliferative disease induced in mice by an interleukin 6 retrovirus. *J Exp Med* **176**, 1149-1163 (1992).
108. Brandt, S.J., Bodine, D.M., Dunbar, C.E. & Nienhuis, A.W. Dysregulated interleukin 6 expression produces a syndrome resembling Castleman's disease in mice. *J Clin Invest* **86**, 592-599 (1990).
109. Nahid, M.A., Satoh, M. & Chan, E.K. MicroRNA in TLR signaling and endotoxin tolerance. *Cell Mol Immunol* **8**, 388-403 (2011).
110. Nimer, S.D. MDS: a stem cell disorder--but what exactly is wrong with the primitive hematopoietic cells in this disease? *Hematology Am Soc Hematol Educ Program*, 43-51 (2008).
111. Beerman, I., Maloney, W.J., Weissmann, I.L. & Rossi, D.J. Stem cells and the aging hematopoietic system. *Curr Opin Immunol* **22**, 500-506 (2010).
112. Salminen, A., *et al.* Activation of innate immunity system during aging: NF-kB signaling is the molecular culprit of inflamm-aging. *Ageing Res Rev* **7**, 83-105 (2008).
113. O'Connell, R.M., *et al.* MicroRNAs enriched in hematopoietic stem cells differentially regulate long-term hematopoietic output. *Proc Natl Acad Sci U S A* **107**, 14235-14240 (2010).
114. Zhao, C., *et al.* Noncanonical NF-kappaB signaling regulates hematopoietic stem cell self-renewal and microenvironment interactions. *Stem Cells* **30**, 709-718 (2012).
115. Ruland, J. Return to homeostasis: downregulation of NF-kappaB responses. *Nat Immunol* **12**, 709-714 (2011).
116. Zhang, P., *et al.* Upregulation of interleukin 6 and granulocyte colony-stimulating factor receptors by transcription factor CCAAT enhancer binding protein alpha (C/EBP alpha) is critical for granulopoiesis. *J Exp Med* **188**, 1173-1184 (1998).
117. Zhang, H., *et al.* STAT3 controls myeloid progenitor growth during emergency granulopoiesis. *Blood* **116**, 2462-2471 (2010).

118. Iliopoulos, D., Hirsch, H.A. & Struhl, K. An epigenetic switch involving NF-kappaB, Lin28, Let-7 MicroRNA, and IL6 links inflammation to cell transformation. *Cell* **139**, 693-706 (2009).
119. Grivennikov, S., *et al.* IL-6 and Stat3 are required for survival of intestinal epithelial cells and development of colitis-associated cancer. *Cancer Cell* **15**, 103-113 (2009).
120. Reynaud, D., *et al.* IL-6 controls leukemic multipotent progenitor cell fate and contributes to chronic myelogenous leukemia development. *Cancer Cell* **20**, 661-673 (2011).
121. Nimer, S.D. Myelodysplastic syndromes. *Blood* **111**, 4841-4851 (2008).
122. Anderson, L.A., *et al.* Risks of myeloid malignancies in patients with autoimmune conditions. *Br J Cancer* **100**, 822-828 (2009).
123. Hasselbalch, H.C. Perspectives on chronic inflammation in essential thrombocythemia, polycythemia vera, and myelofibrosis: is chronic inflammation a trigger and driver of clonal evolution and development of accelerated atherosclerosis and second cancer? *Blood* **119**, 3219-3225 (2012).
124. Kristinsson, S.Y., *et al.* Chronic immune stimulation might act as a trigger for the development of acute myeloid leukemia or myelodysplastic syndromes. *J Clin Oncol* **29**, 2897-2903 (2011).
125. Sekeres, M.A., *et al.* Characteristics of US patients with myelodysplastic syndromes: results of six cross-sectional physician surveys. *J Natl Cancer Inst* **100**, 1542-1551 (2008).

LIST OF PUBLICATIONS

1. **Zhao, J.L.*,** Ma, C*. Diloreto, R., O'Connell, R.M., Heath, J.R., Baltimore, D. Functional heterogeneity among apparently undifferentiated hematopoietic stem and progneitor cells. In review.

2. **Zhao, J.L.**, Rao, D.S., O'Connell, R.M., Baltimore, D. MicroRNA-146a acts as a guardian of the quality and longevity of hematopoietic stem cells. In review.

3. Cheng, H.S., Sivachandran, N., Lau, A., Boudreau, E., **Zhao, J.L.**, Baltimore, D., Delgado-Olguin, P., Cybulsky, M.I., Fish, J.E. MicroRNA-146 represses endothelial activation by inhibiting transcriptional and post-transcriptional pro-inflammatory pathways. In review.

4. So, A.*, **Zhao, J.L.***, Baltimore, D. (2013). The Yin and Yang of microRNAs: Leukemia and Immunity. Immunol Rev. *253*(1):129-45.

5. Huffaker, T.B., Hu, R., Runtsch, M.C., Bake, E., Chen, X., **Zhao, J**., Round, J.L., Baltimore, D., and O'Connell, R.M. (2012). Epistasis between microRNAs 155 and 146a during T cell-mediated antitumor immunity. Cell Rep *2*, 1697-1709.

6. Yang, L., Boldin, M.P., Yu, Y., Liu, C.S., Ea, C.K., Ramakrishnan, P., Taganov, K.D., **Zhao, J.L.**, and Baltimore, D. (2012). miR-146a controls the resolution of T cell responses in mice. J Exp Med *209*, 1655-1670.

7. Etzrodt, M., Cortez-Retamozo, V., Newton, A., **Zhao, J.**, Ng, A., Wildgruber, M., Romero, P., Wurdinger, T., Xavier, R., Geissmann, F., *et al.* (2012). Regulation of monocyte functional heterogeneity by miR-146a and Relb. Cell Rep *1*, 317-324.

8. O'Connell, R.M.*, **Zhao, J.L.*,** and Rao, D.S. (2011). MicroRNA function in myeloid biology. Blood *118*, 2960-2969.

9. **Zhao, J.L**.*, Rao, D.S.*, Boldin, M.P., Taganov, K.D., O'Connell, R.M., and Baltimore, D. (2011). NF-kappaB dysregulation in microRNA-146a-deficient mice drives the development of myeloid malignancies. Proc Natl Acad Sci U S A *108*, 9184-9189.

10. Boldin, M.P., Taganov, K.D., Rao, D.S., Yang, L., **Zhao, J.L**., Kalwani, M., Garcia-Flores, Y., Luong, M., Devrekanli, A., Xu, J., *et al.* (2011). miR-146a is a significant brake on autoimmunity, myeloproliferation, and cancer in mice. J Exp Med *208*, 1189-1201.